0008-7114

Caryologia

2024
Vol. 77 - n. 3

International Journal of Cytology, Cytosystematics and Cytogenetics

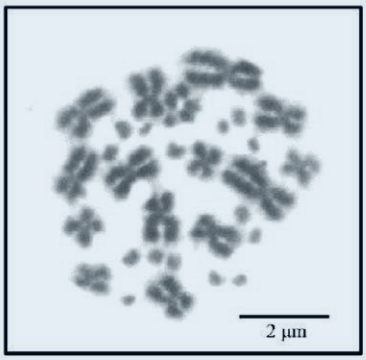

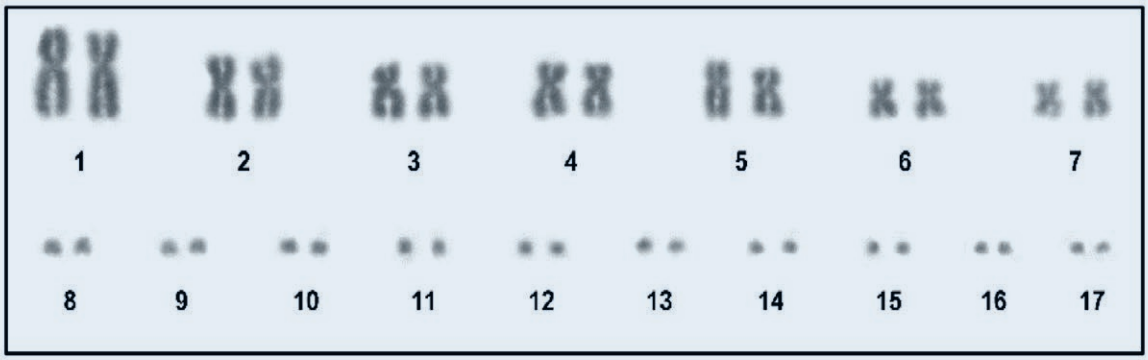

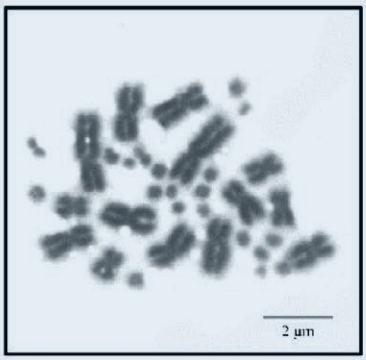

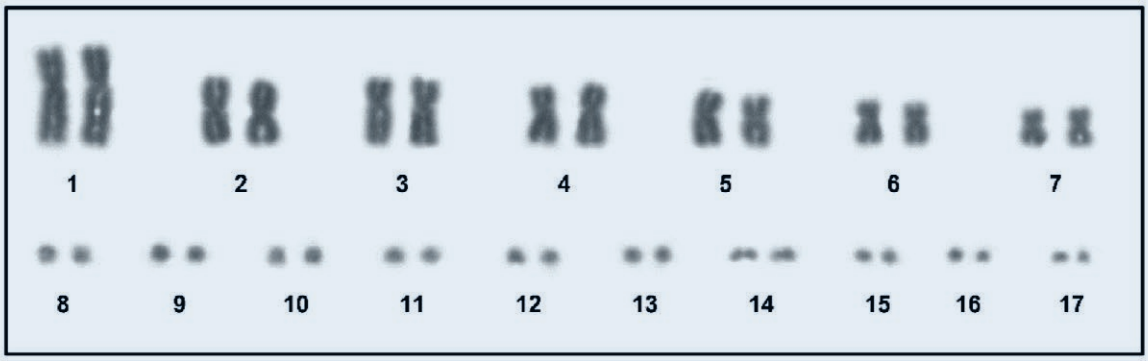

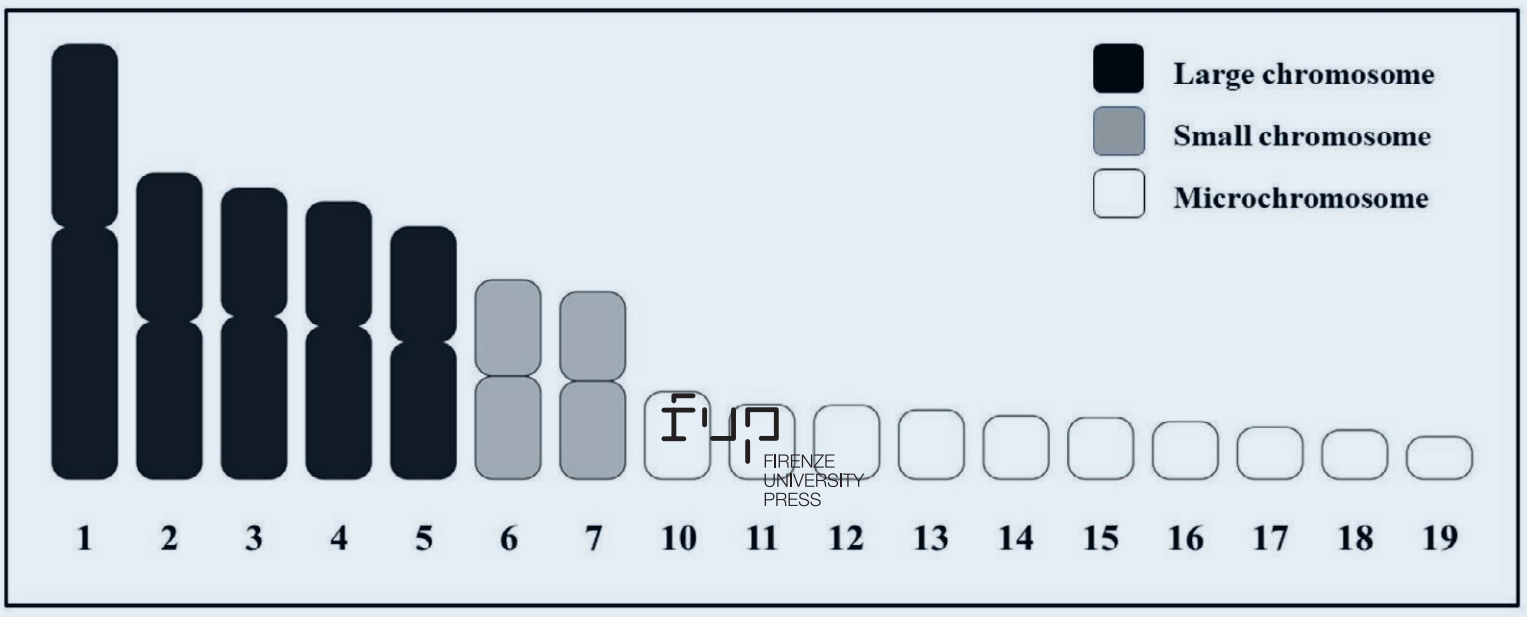

FIRENZE UNIVERSITY PRESS

Caryologia. International Journal of Cytology, Cytosystematics and Cytogenetics
Caryologia is devoted to the publication of original papers, and occasionally of reviews, about plant, animal and human karyological, cytological, cytogenetic, embryological and ultrastructural studies. Articles about the structure, the organization and the biological events relating to DNA and chromatin organization in eukaryotic cells are considered. *Caryologia* has a strong tradition in plant and animal cytosystematics and in cytotoxicology. Bioinformatics articles may be considered, but only if they have an emphasis on the relationship between the nucleus and cytoplasm and/or the structural organization of the eukaryotic cell.

Cover: figure from the article inside by Praween Supanuam et al. The genome of the southern short-horned tree dragon *Acanthosaura meridiona* Trivalairat, Sumontha, Kunya & Chaingkul, 2022 (Squamata, Draconinae) was analyzed using classical and molecular techniques to identify and study its chromosomal and repetitive elements.

Caryologia

International Journal of Cytology, Cytosystematics and Cytogenetics

Volume 77, Issue 3 - 2024

Firenze University Press

***Caryologia*. International Journal of Cytology, Cytosystematics and Cytogenetics**
https://riviste.fupress.net/index.php/caryologia
ISSN 0008-7114 (print) | ISSN 2165-5391 (online)

Direttore Responsabile: **Alessio Papini**

Published by Firenze University Press

Firenze University Press
Università degli Studi di Firenze
via Cittadella, 7, 50144 Firenze, Italy
www.fupress.com

Caryologia
International Journal of Cytology, Cytosystematics and Cytogenetics

Firenze University Press
https://riviste.fupress.net/index.php/caryologia

OPEN ACCESS

Citation: Supanuam, P., Jantarat, S., Kraiprom, T., Buathip, S., Jumrusthanasan, S., Kaewsri, S., Donbundit, N., Buasriyot, P., Thongnetr, W., Phimphan, S., & Tanomtong, A. (2024). The genome of the southern short-horned tree dragon *Acanthosaura meridiona* Trivalairat, Sumontha, Kunya & Chaingkul, 2022 (Squamata, Draconinae) was analyzed using classical and molecular techniques to identify and study its chromosomal and repetitive elements. *Caryologia* 77(3): 3-10. doi: 10.36253/caryologia-2961

Received: Sep 12, 2024

Accepted: Nov 1, 2024

Published: March 25, 2025

Data Availability Statement: All relevant data are within the paper and its Supporting Information files.

Competing Interests: The Author(s) declare(s) no conflict of interest.

ORCID
PS: 0000-0002-2979-9245
SJ: 0009-0006-0376-0808
TK: 0009-0004-7741-7151
PB: 0000-0003-0821-7629
WT: 0009-0000-2598-3144
SP: 0000-0002-4781-1009
AT: 0009-0007-3424-2971

The genome of the southern short-horned tree dragon *Acanthosaura meridiona* Trivalairat, Sumontha, Kunya & Chaingkul, 2022 (Squamata, Draconinae) was analyzed using classical and molecular techniques to identify and study its chromosomal and repetitive elements

Praween Supanuam[A], Sittisak Jantarat[B,*], Thaintip Kraiprom[B], Somsak Buathip[B], Sarun Jumrusthanasan[C], Sarawut Kaewsri[C], Nattasuda Donbundit[D], Phichaya Buasriyot[E], Weera Thongnetr[F], Sumalee Phimphan[G], Alongklod Tanomtong[D]

[a]Biology Program, Faculty of Science, Ubon Ratchathani Rajabhat University, Ubon Ratchathani, Thailand; [b]Program of Biology, Department of Science, Faculty of Science and Technology, Prince of Songkla University, Pattani Campus, Thailand; [c]Biology Program, Faculty of Science, Buriram Rajabhat University, Buriram, Thailand; [d]Department of Biology, Faculty of Science, Khon Kaen University, Khon Kaen, Thailand; [e]Department of Health Sciences, Faculty of Science and Technology, Rajamangala University of Technology Suvarnabhumi, Nonthaburi, Thailand; [f]Division of Biology, Department of Science, Faculty of Science and Technology, Rajamangala University of Technology Krungthep, Bangkok, Thailand; [g]Biology Program, Faculty of Science and Technology, Phetchabun Rajabhat University, Phetchabun, Thailand.
*Corresponding author: sitthisak.j@psu.ac.th

Abstract. The cytogenetics of the southern short-horned tree dragon (*Acanthosaura meridiona*) are not reported yet. This study describes the karyotype of *Acanthosaura meridiona* Trivalairat, Sumontha, Kunya & Chaingkul, 2022 from southern Thailand. We using Giemsa staining, Ag-NOR banding, and fluorescence in situ hybridization (FISH) techniques using microsatellites $d(CA)_{15}$, $d(TA)_{15}$, $d(CGG)_{10}$, and $d(CAA)_{10}$ probes to analyze the chromosome. The karyotype of the *A. meridiona* is 2n = 34 chromosomes (fundamental number of 46), of which 5 pairs were large metacentric chromosomes, 2 pairs small metacentric chromosomes, and 20 microchromosomes (chromosome formula: $2n=34=L^m_{10}+S^m_4+20mi$). There are no sex differences in karyotypes between males and females. The NORs loci were on pair 5 of the large metacentric macrochromosomes. The FISH technique showed $d(CA)_{15}$ and $d(CGG)_{10}$ repeats on specific regions microchromosomes, while signals of $d(TA)_{15}$ and $d(CAA)_{10}$ repeats interspersed on macro- and microchromosomes. This study is significant for enhances our comprehension of the evolutionary mechanism of agamid lizards and promotes the conservation of biodiversity in tropical rainforests.

Keywords: *Acanthosaura meridiona*, chromosome marker, fluorescence in situ hybridization (FISH), microsatellite pattern, Draconinae.

INTRODUCTION

The agamid lizards belonging to the genus *Acanthosaura* Gray, 1831, possess spinose scales with spines on heads and above eyes, along with a prominent spiky crest down their spine (Grismer 2011). All of these species are active during the day and live in trees of Southeast Asia's forested areas, including Myanmar, Thailand, Cambodia, Laos, Vietnam, Yunnan, the Indochinese and Thai-Malay Peninsula, Sumatra, and the Anambas and Natunus Archipelagos (Ananjeva et al. 2008; Manthey 2008; Grismer 2011). The genus *Acanthosaura* currently contains 20 species (Ananjeva et al. 2020; Liu et al. 2020; Trivalairat et al. 2022; Liu et al. 2022; Uetz and Hallermann. 2024).

Currently, there are seven species of *Acanthosaura* in Thailand, namely, *A. armata, A. aurantiacrista, A. cardamomensis, A. crucigera, A. lepidogaster, A. meridiona*, and *A. phuketensis* (Uetz and Hallermann. 2024). *Acanthosaura meridiona* is present in Trang Province, Krabi Province, Nakhon Si Tammarat Province, Songkhla Province, Surat Thani Province, Satun Province, Thailand. *Acanthosaura meridiona* is similar to *A. crucigera* and was previously regarded as an identical species. Wood et al. (2010) found that the southern population of *A. crucigera* exhibited different characteristics that were not present in the true *A. crucigera* population from western Thailand. Nevertheless, *A.* cf. *crucigera* from the southern population has undergone separation into *A. meridiona* (Trivalairat et al. 2022), with the Phuket mountain range acts as a barrier separating the two species. *Acanthosaura* is possible that the extent of variety within this genus is still underestimated. Therefore, cytogenetic research on agamid lizards must achieve greater precision in species differentiation.

Information about karyotypes in *Acanthosaura* only concerns one report in *A. armata* with conventional technique. The karyotypes of Draconinae vary from 2n=32 to 2n=46, with both macrochromosomes and microchromosomes, and absence of sex chromosomes (Ota and Hikida 1989; Sharma and Nakhasi 1980; Li et al. 1981; Ota 1988; Solleder and Schmid 1988; Kritpetcharat et al. 1999; Diong et al. 2000; Ota et al. 2002; Singh and Banerjee 2004; Zongyun et al. 2004; Patawang et al. 2015).

This study looks at the cytogenetic points of view that constitute useful tools of genetic sex chromosome systems, different evolutionary lineages and to delineate evolutionary trends in a great number of taxa (Mezzasalma et al. 2021 and Mezzasalma et al. 2024). This paper first describes *Acanthosaura meridiona*'s chromosomal features, using conventional staining, Ag-NOR banding, and fluorescence in situ hybridization techniques.

MATERIALS AND METHODS

Five adult male and five female specimens of barred gliding lizard (*Acanthosaura meridiona*) were collected from Ban Wang Sai, Mae Wat subdistrict, Than To District, in Yala Province, Thailand. The agamid lizards were transferred to the laboratory and identified according to the morphological criteria (Chan-Ard et al. 2015; Das 2015). Experiments were performed in accordance with ethical protocols, as approved by the Ethics Committee of Prince of Songkla, Pattani Campus (Ref.AI001/2024).

Chromosomes were directly prepared *in vivo* (Patawang et al. 2018) as follows. Metaphasic and meiotic chromosomes were obtained from bone marrow and testis, according the colchicine-hypotonic-fixation-air drying technique (provide references). The chromosomes were stained with 20% Giemsa's for 30 minutes, Ag-NOR staining was conducted according to Howell and Black (1980). Chromosomal checks were performed on mitotic metaphase cells under light microscope.

FISH experiments were performed with microsatellite sequences, specifically $(TA)_{15}$, $(CA)_{15}$, $(CAA)_{10}$, and $(CGG)_{10}$ using high stringency conditions (Yano et al. 2017). The sequences were directly labeled by Cy3 at the 5'end (Sigma, St. Louis, MO, USA) as described by Kubat et al. (2008). FISH was performed under stringent conditions and hybridization in a moist chamber at 37 °C overnight (Sassi et al. 2023). Chromosomes were counterstained with 4',6-Diamidino-2-phenylindole dihydrochloride (DAPI, 1.2 μg/ml) mounted in antifade solution (Vector, Burlingame, CA, USA,) (Aiumsumang et al. 2021; Patawang et al. 2022; Prasopsin et al. 2022; Thongnetr et al. 2022a).

At least 20 metaphase spreads per individual were analyzed to confirm the diploid number, karyotype structure, NORs and FISH data. Chromosomes were classified according to centromere position as metacentric (m), submetacentric (sm), acrocentric (a), and telocentric (t) (Turpin and Lejeune 1965). For the chromosomal arm number (NF; fundamental number); m, sm and a were scored as bi-armed while t as mono-armed. The microchromosomes are chromosomes that are 5 times less long than the largest pair of chromosomes (Patawang et al. 2016; 2017; 2018).

RESULTS AND DISCUSSION

Mitotic chromosome features from Giemsa staining

Agamidae includes 585 species, of which 94 have been karyologically investigated (Mezzasalma et al. 2024). Karyotypes are discontinuous with a variable chromosome number of macro- and/or micro-chromo-

Table 1. Mean length of short arm chromosome (Ls), length of long arm chromosome (Ll), length of total chromosomes (LT), relative length (RL), centromeric index (CI), and standard deviation (SD) from 20 metaphases of male and female of the southern short-horned tree dragon (*Acanthosaura meridiona*) 2n=34.

Chro. Pair	Ls (μm)	Ll (μm)	LT (μm)	RL±SD.	CI±SD.	Chro.	
						Size	Type
1	2.022	2.772	4.794	0.165±0.014	0.575±0.029	Large	metacentric
2	1.634	1.736	3.371	0.117±0.006	0.517±0.021	Large	metacentric
3	1.411	1.794	3.205	0.110±0.007	0.556±0.031	Large	metacentric
4	1.371	1.684	3.055	0.106±0.005	0.551±0.026	Large	metacentric
5*	1.270	1.509	2.779	0.096±0.004	0.543±0.025	Large	metacentric
6	1.059	1.136	2.195	0.076±0.003	0.516±0.021	Small	metacentric
7	0.982	1.082	2.064	0.071±0.004	0.524±0.022	Small	metacentric
8	0.000	0.813	0.813	0.029±0.002	1.000±0.000	microchromosome	
9	0.000	0.762	0.762	0.027±0.003	1.000±0.000	microchromosome	
10	0.000	0.761	0.761	0.027±0.005	1.000±0.000	microchromosome	
11	0.000	0.762	0.762	0.027±0.003	1.000±0.000	microchromosome	
12	0.000	0.699	0.699	0.024±0.003	1.000±0.000	microchromosome	
13	0.000	0.679	0.679	0.024±0.003	1.000±0.000	microchromosome	
14	0.000	0.632	0.632	0.022±0.002	1.000±0.000	microchromosome	
15	0.000	0.573	0.573	0.020±0.003	1.000±0.000	microchromosome	
16	0.000	0.540	0.540	0.019±0.003	1.000±0.000	microchromosome	
17	0.000	0.469	0.469	0.016±0.003	1.000±0.000	microchromosome	

* = NORs bearing chromosomes, Chro. = Chromosome.

somes, namely macrochromosomes ranging from 10 to 28, and microchromosomes from 0 to 24 (Mezzasalma et al. 2024). In Draconinae, based on 21 species reports, karyotypes range from 2n=32- to 46 (Table 2). However, so far the present study first reports the karyotype of *Acanthosaura meridiona*, loci of NORs, and by Fluorescence in situ hybridization the distribution of $(TA)_{15}$, $(CA)_{15}$, $(CAA)_{10}$, and $(CGG)_{10}$ microsatellites.

The results revealed that the chromosome number of *A. meridiona* was 34 (14 macrochromosomes, and 20 microchromosomes). The karyotype comprised ten large metacentric chromosomes, four small metacentric chromosomes, and 20 microchromosomes (Table 1 and Figure 1). This result differs with from that of *A. armatus* of 2n=32 with 12 metacentric macrochromosomes, 20 microchromosomes. The fundamental number (NF) of *A. meridiona* and *A. armatus* was 46 and 44, respectively. It is possible that the different macrochromosome numbers may have been caused by an event of tandem fusion and centromere deletion involving the chromosome number and NF variation. A similar process of autonomous reduction in total chromosomal number through autosome translocation has been reported in other lizard families, including Anguidae, Scincidae, Iguanidae, Gekkonidae, and Phrynosomatidae (Adegoke and Ejere 1991; Trifonov et al. 2015).

There is no evidence of differentiated sex chromosomes in this species which agreeable with all species of Draconinae (Ota and Hikida 1989; Sharma and Nakhasi 1980; Li et al. 1981; Ota 1988; Solleder and Schmid 1988; Kritpetcharat et al. 1999; Diong et al. 2000; Ota et al. 2002; Singh and Banerjee 2004; Zongyun et al. 2004; Patawang et al. 2015). Squamates exhibit a considerable degree of variability in their chromosome sex determination systems. Various families exhibit diverse sex-chromosome systems, which can be either simple or multiple, and include either male (XX/XY) or female (ZZ/ZW) heterogamety. These systems encompass all hypothesized stages of heterogametic sex chromosomes, including homomorphic and pseudo-autosomal to heteromorphic and completely heterochromatic chromosomes (Alam et al. 2018 and Mezzasalma et al. 2021).

Nucleolar organizer region from Ag-NOR banding

Ag-NOR banding, a species-specific marker, primarily identifies karyotypes. Silver staining, on the other hand, only detects the nucleolar organizer areas that are actively involved in transcription (Silva et al. 2008). The improvement of the Ag-NOR staining method has been very important in comparing NOR variation because it

Table 2. Comparative chromosome studies of subfamily Draconinae.

Species	2n	Karyotype	NOR	Locality	References
Acanthosaura armata	32	12m+20mi	-	Malaysia	Ota et al. (2002)
A. meridiona	34	14m+20mi	5qter	Thailand	This study
Bronchocela cristatella	34	14m+20mi	-	Singapore	Ota et al. (2002)
	34	12m/sm+22mi	2qter	Asia	Solleder and Schmid (1988)
Calotes emma alticristatus	34	12m/sm+22mi	2qter	Asia	Solleder and Schmid (1988)
	34	12m/sm+22mi	-	Thailand	Kritpetcharat et al. (1999)
	34	12m+22mi	-	Malaysia	Ota et al. (2002)
	34	-	-	India	Singh and Banerjee (2004)
C. jerdoni	34	12m/sm+22mi	-	India	Sharma and Nakhasi (1980)
	34	-	-	India	Singh and Banerjee (2004)
C. mystaceus	34	12m/sm+22mi	2qter	Asia	Solleder and Schmid (1988)
	34	12m/sm+22mi	-	Thailand	Kritpetcharat et al. (1999)
	34	-	-	India	Singh and Banerjee (2004)
	34	10m+2m+22mi	2qter	Thailand	Patawang et al. (2015)
C. versicolor	34	12m/sm+22mi	2qter	Asia	Solleder and Schmid (1988)
	34	12m/sm+22mi	-	Thailand	Kritpetcharat et al. (1999)
	34	12m+22mi		Singapore	Ota et al. (2002)
	34	12m/sm+22mi	2qter	Thailand	Patawang et al. (2015)
C. vultuosus	32, 34	-	-	India	Singh and Banerjee (2004)
	34	12m/sm+22mi	-	India	Sharma and Nakhasi (1980)
Draco cornutus	34	16m+18mi	-		
D. haematopogon	34	16m+18mi	-	Malaysia	Ota and Hikida (1989)
D. quinquefasciatus	34	16m+18mi	-		
Diploderma splendidum	34	12m+22mi	-	China	Zongyun et al. (2004)
D. swinhonis	36	10bi+26a	-	Central Taiwan	Ota (1988)
	40	6bi+34a	-	Central Taiwan	
	46	46a	-	Northern Taiwan	
Gonocephalus chamaeleontinus	42	22m+20mi	-		
G. liogaster	42	22m+20mi	-		
G. bellii	42	22m+20mi	-	Malaysia	Diong et al. (2000)
G. grandis	42	22m+20mi	-		
G. robinsonii	32	12m+20mi	-		
Japalura variegata	34	-	-	India	Singh and Banerjee (2004)
J. varcoae	34	12m+22mi	-	China	Li et al. (1981)
Ptyctolaemus gularis	34	12m/sm+22mi	-	India	Sharma and Nakhasi (1980)

Note: 2n: diploid chromosome number, m: metracentric, sm: submetracentric, a: acrocentric, bi: biarms, mi: microchromosome, and qter: long arm of chromosome.

lets us find the metaphase chromosomal locations that are linked to NOR. The present study, the chromosome markers of *A. meridiona* observable NORs on the telomeric region of large metacentric macrochromosome pair 5th (Figure 2). Similarly, the previous report of NOR position in Draconinae was located on telomeric region of q-arm in 4 species of *Calotes* consisting of *C. cristatellus*, *C. emma*, *C. mystaceus*, and *C. versicolor* (Solleder and Schmid 1988; Patawang et al. 2015). However, findings from both traditional and molecular cytogenetics suggest that the location of NOR loci on microchromosomes is usually thought of as an ancestral trait in most families and genera (Mezzasalma et al. 2021; Waters et al. 2021; Deakin and Ezaz 2019).

Microsatellite pattern

Microsatellites, also known as simple sequence repeats (SSRs), are short DNA sequences consisting of

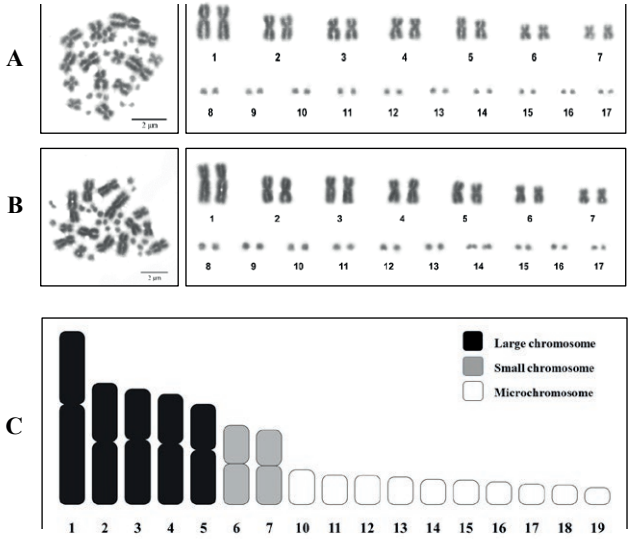

Figure 1. Metaphase plates and standardized karyotypes of male (A.), female (B.) and Idiogram (C.) of the southern short-horned tree dragon, *Acanthosaura meridiona*, 2n=34 by conventional staining.

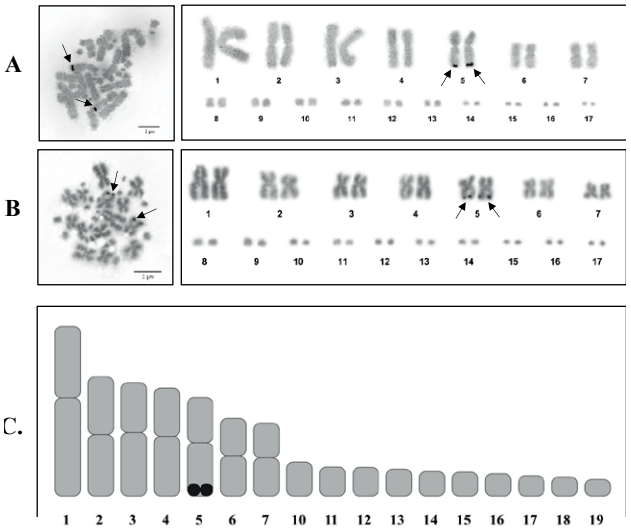

Figure 2. Metaphase plates and standardized karyotypes of male (A.), female (B.) and Idiogram (C.) of the southern short-horned tree dragon, *Acanthosaura meridiona*, 2n=34 by Ag-NOR banding, arrows indicate NORs.

1–6 base pairs. They are distinguished by the presence of repetitive units, which can range from 4 to 40 repeats in a sequence (Tautz and Renz 1984; Ellegren 2004; Chistiakov et al. 2006). They appear either dispersed or clustered in euchromatin and heterochromatin regions, widely distributed across eukaryotic genomes. They show

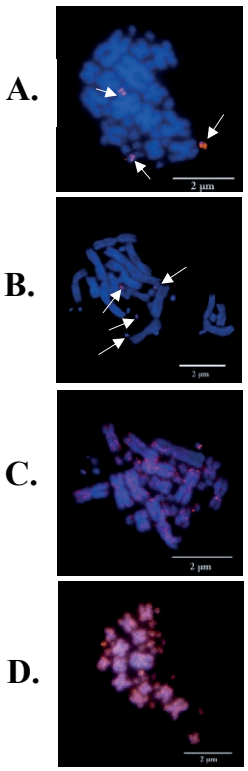

Figure 3. Metaphase plates and hybridization patterns with microsatellite probes d(CA)$_{15}$ (A.), d(CGG)$_{10}$ (B.), d(TA)$_{15}$ (C.), and d(CAA)$_{10}$ (D.) (red signals) on metaphase plates of the southern short-horned tree dragon, *Acanthosaura meridiona*, 2n=34, chromosomes were counterstained with DAPI (blue).

Table 3. The hybridization patterns with microsatellite probes d(CA)$_{15}$, d(CGG)$_{10}$, d(TA)$_{15}$, and d(CAA)$_{10}$ of the southern short-horned tree dragon (*Acanthosaura meridiona*).

Probe	Signal
d(CA)$_{15}$	Pair 13 & 15
d(CGG)$_{10}$	Pair 15 & 16
d(TA)$_{15}$	Throughout genome (weak)
d(CAA)$_{10}$	Throughout genome (strong)

a significant variation in the number of copies of genetic material (Ellegren 2004). Microsatellite repeat patterns of *A. meridiona* indicated the presence of specific regions on microchromosomes, including pair 13 and 15 with d(CA)$_{15}$ repeats, and pair 15 and 16 with d(CGG)$_{10}$ repeats. While d(TA)$_{15}$ and d(CAA)$_{10}$, showed cumulative signals dispersed throughout the chromosomes (Table 3, Figure 3). The microsatellite loci exhibited a significant level of evolutionary advancement. Thus, it is common for many species to have diverse patterns of repeated sequences. Most of them and scattered them

across the genome (Thongnetr et al. 2019; 2022a; 2022b; Khawporntip et al. 2024). However, in certain species, they may localize into specific regions (Srikulnath et al. 2009; Alam et al. 2021). Interestingly, signals of the $d(CA)_{15}$ probe specifically is on a chromosome of pair 13, a finding that is unclear and remains unexplained. This suggests that using Fluorescence in situ Hybridisation (FISH), the process of mapping cDNA or BAC clones to the chromosomes of southern short-horned tree dragon has successfully addressed certain constraints (O'Meally et al. 2009; Alföldi et al. 2011; Srikulnath et al. 2015; Young et al. 2013; Deakin et al. 2016; Badenhorst et al. 2015). By integrating data from several species, one can obtain intra-sequence information that enhances our understanding of the evolution of chromosome in lizards.

In conclusion, we first present the karyotype, NORs and microsatellite $d(CA)_{15}$, $d(TA)_{15}$, $d(CGG)_{10}$, and $d(CAA)_{10}$ patterns on the chromosomes of the southern short-horned tree dragon. *Acanthosaura meridiona* has 2n=34 chromosomes (14 macrochromosomes, and 20 microchromosomes), NF=46. The karyotype consisting of 5 pairs of large metacentric chromosomes, 2 pairs of large metacentric chromosomes, and 20 microchromosomes. NORs were located on the telomeric region of large metacentric macrochromosome pair 5^{th}. Microsatellite repeat patterns indicated the presence of specific regions on microchromosomes, including pair 13 and 15 with $d(CA)_{15}$ repeats, and pair 15 and 16 with $d(CGG)_{10}$ repeats. While $d(TA)_{15}$ and $d(CAA)_{10}$, showed cumulative signals dispersed throughout the chromosomes. This study is valuable for improving our understanding of the evolutionary process of agamid lizards and advocating for biodiversity protection in tropical rainforests. Moreover, we suggest that more species be studied using cytogenetics and that techniques be investigated further to gain a deeper understanding of chromosomal diversity and evolution within this genus.

ACKONOWLEDGEMENT

This research was supported by National Science, Research and Innovation Fund (NSRF) and Prince of Songkla University (Ref. No. SAT6701179S).

REFERENCES

Adegoke JA, Ejere VC. 1991. Description of the chromosomes of three lizard species belonging to the genus *Mabuya* (Scincidae, Reptilia). Caryologia. 44:333–342.

Aiumsumang S. Phimphan S. Suwannapoom C, Chaiyasan P, Supiwong W, Tanomtong A. 2021. A comparative chromosome study on five Minnow fishes (Cyprinidae, Cypriniformes) in Thailand. Caryologia 74(1):89-96.

Alam SM, Sarre SD, Georges A, Ezaz T. 2021. Karyotype Characterisation of two Australian dragon lizards (Squamata: Agamidae: Amphibolurinae) reveals subtle chromosomal rearrangements between related species with similar karyotypes. Cytogenet Genome Res. 160(10):610-624.

Alam SM, Sarre SD, Gleeson D, Georges A, Ezaz T. 2018. Did lizards follow unique pathways in sex chromosome evolution? Genes. 9(239).

Alföldi J, Di Palma F, Grabherr M, Williams C, Kong L, Mauceli E, Russell P, Lowe CB, Glor RE, Jaffe JD, and et al. 2011. The genome of the green anole lizard and a comparative analysis with birds and mammals. Nature. 477:587–591.

Ananjeva NB, Ermakov OA, Nguyen SN, Nguyen TT, Murphy RW, Lukonina SA, Orlov NL. 2020. A new species of *Acanthosaura* Gray, 1831 (Squamata: Agamidae) from central highlands, Vietnam. Russ J Herpetol. 27(4):217–230.

Ananjeva NB, Orlov NL, Kalyabina-Hauf SA. 2008. Species of Acanthosaura Gray, 1831 (Agamidae: Sauria, Reptilia) of Vietnam: results of Molecular and Morphological study. Biol Bull. 35(2):178 –186.

Badenhorst D, Hillier LW, Literman R, Montiel EE, Radhakrishnan S, Shen Y, Minx P, Janes DE, Warren WC, Edwards SV, and et al. 2015. Physical mapping and refinement of the painted turtle genome (*Chrysemys picta*) inform amniote genome evolution and challenge turtle-bird chromosomal conservation. Genome Biol Evol. 7:2038–2050.

Chistiakov DA, Hellemans B, Volckaert FAM. 2006. Microsatellites and their genomic distribution, evolution, function and applications: a review with special reference to fish genetics. Aquaculture. 255:1–29. doi: 10.1016/j.aquaculture.2005.11.031.

Chan-Ard T, Nabhitabhata J, Parr JW. 2015. A field guide to the reptiles of Thailand. NY: Oxford University Press.

Das I. 2015. Field guide to the reptiles of South-East Asia. London: Bloomsbury Publishing.

Deakin JE, Edwards MJ, Patel H, O'Meally D, Lian J, Stenhouse R, Ryan S, Livernois AM, Azad B, Holleley CE, and et al. 2016. Anchoring genome sequence to chromosomes of the central bearded dragon (*Pogona vitticeps*) enables reconstruction of ancestral squamate macrochromosomes and identifies sequence content of the Z chromosome. BMC Genomics. 17(447).

Deakin JE, Ezaz T. 2019. Understanding the evolution of reptile chromosomes through applications of combined cytogenetics and genomics approaches. Cytogenet. Genome Res. 157:7–20. doi: 10.1159/000495974.

Diong CH, Low MH, Tan EC, Yong HS, Hikida T, Ota H. 2000. On the Monophyly of the Agamid Genus *Gonocephalus* Kaup, 1825 (Reptilia: Squamata) A Chromosomal Perspective. Curr. Herpetol. 19(2):71-79.

Ellegren H. 2004. Microsatellites: simple sequences with complex evolution. Nat Rev Genet. 5:435–445. doi: 10.1038/nrg1348.

Grismer LL. 2011. Lizards of Peninsular Malaysia, Singapore and their Adjacent Archipelagos, Edition Chimaira, Frankfürt am Main.

Howell WM, Black DA. 1980. Controlled silver-staining of nucleolus organizer regions with a protective colloidal developer: a 1-step method. Experientia. 36: 1014-1015.

Khawporntip W, Jantarat S, Supanuam P, Buatip S, Kraiprom T, Donbundit N, Thongnetr W, Tanomtong A. 2024. First Molecular Cytogenetics Report of Blue-headed Flying Lizard (*Draco volans*) outside Protected Area of Hala-bala Forest at Than To District, Yala Province, Thailand. Burapha Science Journal, 29(2), 782–792.

Kritpetcharat O, Kritpetcharat C, Luangpirom A, Watcharanon P. 1999. Karyotype of four Agamidae species from the Phu Phan national park in Thailand. Sci. Asia, 25(4):185-188.

Kubat Z, Hobza R, Vyskot B, Kejnovsky E. 2008. Microsatellite accumulation in the Y chromosome of *Silene latifolia*. Genome 51:350–356.

Li Shu-shen, Wang Ying-xiang, Wang Rui-fang, Li Chong-yun, Liu Guang-zuo. 1981. A Karyotypical Study of *Japalura varcoae* (Boulenger). Zoological Research, 2(3): 223-228.

Liu S, Hou M, Mo MZ, Rao DQ. 2020. A new species of the genus *Acanthosaura* (Squamata, Agamidae) from Yunnan, China, with comments on its conservation status. ZooKeys. 959:113–135.

Liu S, Rao D, Hou M, Orlov NL, Ananjeva NB, Zhang D. 2022. Two new species of *Acanthosaura* Gray, 1831 (Reptilia: Agamidae) from Yunnan province, China Russ J Herpetol. 29(2): 93–109. doi: 10.30906/1026-2296-2022-29-2-93-109.

Manthey U. 2008. Agamid Lizards of Southern Asia-Agamen des südlichen Asien-Draconinae 1. Terralog. Vol. 7a, Edition Chimaira, Frankfürt am Main.

Mezzasalma M, Guarino FM, Odierna G. 2021. Lizards as Model Organisms of Sex Chromosome Evolution: What We Really Know from a Systematic Distribution of Available Data? Genes. 12(1341).

Mezzasalma M, Macirella R, Odierna G, Brunelli E. 2024. Karyotype Diversification and Chromosome Rearrangements in Squamate Reptiles. Genes. 15(371). doi: org/10.3390/genes15030371.

O'Meally D, Miller H, Patel HR, Graves JA, Ezaz T. 2009. The first cytogenetic map of the tuatara, *Sphenodon punctatus*. Cytogenet Genome Res. 127:213–23.

Ota, H. 1988. Karyotypic differentiation in an agamid lizard, *Japalura swinhonis swinhonis*. Experientia, 44(1):66-68.

Ota H, Hikida T. 1989. Karyotypes of three species of the genus *Draco* (Agamidae: Lacertilia) from Sabah, Malaysia. Japan J. Herpetol. 13(1):1-6.

Ota H, Diong CH, Tan EC, Yong HS. 2002. Karyotypes of four agamid lizards from Southeast Asia. Curr. Herpetol. 21(1):35-41.

Patawang I, Pinthong K, Thongnetr W, Sornnok S, Kaewmad P, Tanomtong A. 2018. Additional description of karyotype and meiotic features of *Takydromus sexlineatus* (Squamata, Lacertidae) from Northeastern Thailand. The Nucleus 61(2):163-169.

Patawang I, Prasopsin S, Suwannapoom C, Tanomtong A, Keawmad P, Thongnetr W. 2022. Chromosomal description of three *Dixonius* (Squamata, Gekkonidae) from Thailand. Caryologia 75(2):101-108.

Patawang I, Tanomtong A, Chuaynkern Y, Chuaynkern C, Duengkae P. 2015. Karyotype homology between *Calotes versicolor* and *C. mystaceus* (Squamata, Agamidae) from northeastern Thailand. The Nucleus 58(2):117-123.

Patawang I, Tanomtong A, Getlekha N, Phimphan S, Pinthong K, Neeratanaphan L. 2017. Standardized karyotype and idiogram of Bengal monitor lizard, *Varanus bengalensis* (Squamata, Varanidae). Cytologia 82(1):75-82.

Patawang I, Tanomtong A, Kaewmad P, Chuaynkern Y, Duengkae P. 2016. New record on karyological analysis and first study of NOR localization of parthenogenetic brahminy blind snake, Ramphotyphlops braminus (Squamata, Typhlopidae) in Thailand. The Nucleus 59(1): 61-66.

Prasopsin S., Muanglen,N, Ditcharoen S, Suwannapoom C, Tanomtong A, Thongnetr W. 2022. First Report on Classical and Molecular Cytogenetics of Doi Inthanon Benttoed Gecko, *Cyrtodactylus inthanon* Kunya et al., 2015 Squamata: Gekkonidae) in Thailand. Caryologia 75(2):109-117.

Sassi FMC, Toma GA, Cioffi MB. 2023. "FISH—In fish chromosomes," in Cytogenetics and molecular cytogenetics. Editor T. Liehr (Boca Raton, FL: CRC Press), 281–296.

Sharma GP, Nakhasi U. 1980. Karyotypic homology and evolution of the Agamid lizards. Cytologia, 45(1-2): 211-219.

Silva M, Pereira HS, Bento M, Santos AP, Shaw P, Delgado M, Neves N, Viegas W. 2008. Interplay of ribosomal DNA *loci* in nucleolar dominance: dominant NORs are upregulated by chromatin dynamics in the wheatrye system. PLoS ONE. 3. doi: 10.1371/journal.pone.0003824.

Singh AK, Banerjee R. 2004. Chromosomal diversity of Indian mammals, amphibians and reptiles. Rec. zool. Surv. India 102(3-4):127-138.

Solleder E, Schmid M. 1988. Cytogenetic studies on Sauria (Reptilia). I. Mitotic chromosomes of the Agamidae. Amphibia-reptilia 9(3):301-310.

Srikulnath K, Matsubara K, Uno Y, Thongpan A, Suputtitada S, Apisitwanich S, Matsuda Y, Nishida C. 2009. Karyological characterization of the butterfly lizard (*Leiolepis reevesii rubritaeniata*, Agamidae, Squamata) by molecular cytogenetic approach. Cytogenet Genome Res, 125(3):213-223.

Srikulnath K, Uno Y, Nishida C, Ota H, Matsuda Y. 2015. Karyotype reorganization in the Hokou gecko (*Gekko hokouensis*, Gekkonidae): the process of microchromosome disappearance in Gekkota. PLoS One. doi: 10.1371/journal.pone.0134829.

Tautz D, Renz M.1984. Simple sequences are ubiquitous repetitive components of eukaryotic genomes. Nucleic Acids Res. 25:4127–4138. doi: 10.1093/nar/12.10.4127.

Thongnetr W, Aiumsumang S, Tanomtong A, Phimphan S. 2022a. Classical chromosome features and microsatellites repeat in *Gekko petricolus* (Reptilia, Gekkonidae) from Thailand. Caryologia 75(2):81-88.

Thongnetr W, Prasopsin S, Aiumsumang S, Ditcharoen S, Tanomtong A, Wongchantra P, Bunnaen W, Phimphan S. 2022b. First report of chromosome and karyological analysis of *Gekko nutaphandi* (Gekkonidae, Squamata) from Thailand: Neo-diploid chromosome number in genus *Gekko*. Caryologia 75(4): 103-109. doi: 10.36253/caryologia-1875.

Thongnetr W, Tanomtong A, Prasopsin S, Maneechot N, Pinthong K, Patawang I. 2019. Cytogenetic study of the Bent-toed Gecko (Reptilia, Gekkonidae) in Thailand; I: Chromosomal classical features and NORs characterization of *Cyrtodactylus kunyai* and *C. interdigitalis*. Caryologia 72(1): 23-28. doi: 10.13128/cayologia-248.

Trifonov VA, Paoletti A, Barucchi VC, Kalinina T, O'Brien PCM, Ferguson-Smith MA Giovannotti M. 2015. Comparative Chromosome Painting and NOR Distribution Suggest a Complex Hybrid Origin of Triploid *Lepidodactylus lugubris* (Gekkonidae). PLoS ONE. 10. doi: doi.org/10.1371/journal.pone.0132380.

Trivalairat P, Sumontha M, Kunya K, Chiangkul K. 2022. *Acanthosaura meridiona* sp. nov. (Squamata: Agamidae), a new short-horned lizard from southern Thailand. Herpetological Journal. 32, 34-50. doi: 10.33256/32.1.3450.

Turpin R, Lejeune J. 1965. Les chromosomes humains (caryotype normal et variations pathologiques). Paris: Gauthier-Villars. [in France]

Uetz P, Hallermann J. The Reptile Database. 1995-2024. [accessed 2024 Aug 15]. http://www.reptile-database.org/

Waters PD, Patel HR, Ruiz-Herrera A, Álvarez-González L, Lister NC, Simakov O, Ezaz T, Kaur P, Frere C, Grutzner F, and et al. 2021. Microchromosomes are building blocks of bird, reptile, and mammal chromosomes. Proc. Natl. Acad. Sci. USA. 118(45). doi: 10.1073/pnas.2112494118.

Wood PL Jr, Grismer LL, Grismer JL, Neang T, Chav T. Holden J. 2010. A new cryptic species of *Acanthosaura* Gray, 1831 (Squamata: Agamidae) from Thailand and Cambodia. Zootaxa 2488, 22 – 38.

Yano CF, Bertollo LA, Ezaz T, Trifonov V, Sember A, Liehr T. 2017. Highly conserved Z and molecularly diverged W chromosomes in the fish genus *Triportheus* (Characiformes, Triportheidae). Heredity 118, 276–283. doi: 10.1038/hdy.2016.83

Young MJ, O'Meally D, Sarre SD, Georges A, Ezaz T. 2013. Molecular cytogenetic map of the central bearded dragon, Pogona vitticeps (Squamata: Agamidae). Chromosome Res. 21: 361–374. doi: 10.1007/s10577-013-9362-z.

Zongyun L, Mingqin G, Lu W, Ming C, Xiuqin W. 2004. Studies on spermary chromosomes and its meiosis of *Japalura splendida* Barbour and Dunn, 1919. Sichuan Dongwu. Sichuan J. Zool. 23(3):281-284.

Caryologia
International Journal of Cytology, Cytosystematics and Cytogenetics

Firenze University Press
https://riviste.fupress.net/index.php/caryologia

OPEN ACCESS

Citation: Fairoj, S. A., Ghosh, U. K., Islam, M. M., Jahan, K., Anamika, Siddiqui, S., Alshaharani, M. O., Siddiqua, A. & Yassin, H. M. (2024). Amelioration strategy of saline stress in wheat with salicylic acid: a review. *Caryologia* 77(3): 11-25. doi: 10.36253/caryologia-2812

Received: Jun 7, 2024

Accepted: Oct 16, 2024

Published: March 25, 2025

Data Availability Statement: All relevant data are within the paper and its Supporting Information files.

Competing Interests: The Author(s) declare(s) no conflict of interest.

ORCID
MI: 0000-0001-7588-6414

Amelioration strategy of saline stress in wheat with salicylic acid: a review

Syeda Afia Fairoj[1,†], Uttam Kumar Ghosh[1,†], Md. Moshiul Islam[1,*], Khurshida Jahan[1], Anamika[1], Sazada Siddiqui[2], Mohammed O. Alshaharani[2], Ayesha Siddiqua[3], Habab Merghani Yassin[2]

[1] *Department of Agronomy, Bangabandhu Sheikh Mujibur Rahman Agricultural University, Gazipur-1706, Bangladesh*
[2] *Department of Biology, College of Science, King Khalid University, Abha-61413, Saudi Arabia*
[3] *Department of Clinical Pharmacy, King Khalid University, Abha-61413, Saudi Arabia*
* Corresponding author. E-mail: moshiul@bsmrau.edu.bd
[†]These authors contributed equally to this work

Abstract. Salinity, an adverse abiotic stress, is lowering the productivity of agricultural crops including wheat worldwide. It creates obstacles in normal crop growth and development. Salinity is affecting the morpho-physiology and productivity of wheat. It is also responsible for inducing oxidative, osmotic and ionic stress (high Na^+/K^+ ratio), while decreasing the K^+ concentrations in plants. Many insights indicate a positive relationship between salicylic acid application and improvement of the morpho-physiological attributes and productivity of wheat both in saline and non-saline conditions. Salinity-induced morphological and physiological alterations have resulted in a drastic decline in wheat yields globally. Morpho-physiological parameters and yield contributing parameters are correlated with each other. Salinity stress reduces the shoot length, shoot fresh mass, root length, root fresh mass, leaf area, leaf fresh weight, number of tillers, shoot dry mass, root dry mass, leaf dry weight, chlorophyll contents (SPAD), leaf relative water content, stomatal conductance, photosynthetic rate, transpiration, CO_2 assimilation rate, internal CO_2 concentration, spikelets per spike, grain weight per spike, number of grains per spike grain yield, straw yield, biological yield, harvest index in wheat. It also induces autophagy and programmed cell death in wheat. Application of salicylic acid on saline stressed wheat significantly improves all the aforementioned parameters along with maintaining lower Na^+ concentrations and a Na^+/K^+ ratio. Furthermore, salicylic acid alleviates the detrimental effects of salt stress ultimately promoting salt tolerance in wheat. Hence, this paper aims to provide a comprehensive review of major research advances on amelioration of salinity on morpho-physiology and productivity of wheat by the application of salicylic acid.

Keywords: salt stress, wheat, salicylic acid, morpho-physiology, productivity, autophagy.

INTRODUCTION

Rapid global climate change has increased the frequency and severity of abiotic stresses on plants (Ghosh et al., 2022; Fairoj et al., 2023; Austin and

Ballaré, 2023; Mao et al., 2023). Throughout their life cycle, plants are frequently subjected to a variety of abiotic stresses that disrupt cellular membrane and developmental processes (Fadiji et al., 2023; Jing et al., 2023). Salinity is a major abiotic stress that reduces the productivity of agricultural crops including wheat worldwide (Corti et al., 2023a; Jing et al., 2023). Wheat (*Triticum aestivum* L.) is a major cereal crop which is used as staple food by approximately one third people of the world (Fairoj et al., 2023).

Salinity causes osmotic stress and ionic stress which affects plant growth and development (Mariyam et al., 2023; Rostampour et al., 2023; Sóti et al., 2023). Osmotic stress is caused mainly by Na^+ and Cl^- in the soil solution which reduces the availability of water to roots (Naz et al., 2023a; Soni et al., 2023; Wang et al., 2023). When plant roots uptake Na^+ and/or Cl^- and these ions accumulated to pernicious levels in leaves, ion toxicity occurs (Hayat et al., 2022; Saeed et al., 2023). Ion imbalances and nutrient deficiency occur due to salinity (Naz et al., 2023b). Salinity reduces the growth of plant through osmotic effects; declines the ability of plants to take up water and this causes reduction in growth (Abrar et al., 2022; Zarbakhsh and Shahsavar, 2023). Thus, reduced water uptake is the common feedback of plants subjected to salinity stress (Masarmi et al., 2023; Tammam et al., 2023). Lower water status in plant body slows the rate of cell division and expansion mainly through a loss of turgor (Ahmad et al., 2023; Ullah et al., 2023). It affects almost every aspect of the morphology both external and internal physiology of plants and significantly reduces the yield. High salinity in soil badly affects the quality and quantity of crop production (Khan et al., 2023; Thampi et al., 2023) by inhibiting seeds germination, seedlings growth and developmental phases due to cumulative influences of higher osmotic potential and toxicity of specific ions (Hadjadj et al., 2023; Sarkar et al., 2023). Salinity restricts the growth and production by affecting physiological processes, including modification of ion balance, mineral nutrition, water status, stomatal behavior and photosynthetic efficiency (Iftikhar et al., 2023; Kumar et al., 2023) and oxidative damage due to manufacture of higher levels of reactive oxygen species (ROS), variations in the antioxidant enzymes (Loudari et al., 2023; Mangal et al., 2023; Singh et al., 2023). Salinity stress has been shown to increase chromosomal abnormalities, MDA, and proline buildup, impair the ascorbate-glutathione (AsA-GSH) cycle function, and cause programmed cell death (PCD) (Fedoreyeva et al., 2022; Prajapati et al., 2023). Various strategies have been evolved by plants to adapt to hostile surroundings (Blonder et al., 2023; Liu et al., 2023). To address salinity hassle, application of salicylic acid to wheat might be an effective strategy. Salicylic acid is phenolic in nature that is held by plants (Esmaeili et al., 2023; Rubio-Rodríguez et al., 2023). It has been allowed as an endogenous regulator in plants after discovering that it is involved in many plant physiological processes like photosynthesis, transpiration, nutrient uptake, chlorophyll synthesis, protein synthesis and transport (Arif et al., 2023; Azeem et al., 2023a; Pirasteh-Anosheh et al., 2023). SA induces changes in leaf anatomy and chloroplast structure and mitigates the antagonistic impact of salinity (Aazami et al., 2023; Sharma et al., 2023). A large number of studies advocate that salicylic acid treatment significantly increased quantities of endogenous salicylic acid, enhanced the antioxidant enzymes and contents of non-enzymatic compounds, improved the ratio of potassium to sodium and increased the plant growth resulting in the improved abiotic tolerance (Feng et al., 2023; Jalili et al., 2023; Pai and Sharma, 2023; Youssef et al., 2023). However, the influence of salicylic acid is mainly dependent on the concentration, plant species and application type (Ben Youssef et al., 2023; Elhindi et al., 2023). It is a cell reinforcement compound which controls plant development (Kaya et al., 2023; Virág et al., 2023). Exogenous application of salicylic acid has impact on stomatal conclusion and increases plant dry biomass (shoot and root) in wheat (Abdi et al., 2022; Iqbal et al., 2022; Fairoj et al., 2023).

Salicylic acid helps to induce abiotic stress tolerance by by scavenging ROS, enhancing RWC, gas exchange activities and photosynthetic pigments, maintaining lower Na^+ concentrations and a Na^+/K^+ ratio, maintaining cell turgor, protecting cell structures and maintaining ion homeostasis (Ali et al., 2023; Arikan et al., 2023; Hussain et al., 2023; Omidi et al., 2022; Shaukat et al., 2022). The production of wheat, which is Bangladesh's second most important cereal crop, is inadequate in the country's coastal regions. The nation still produces a lot less wheat each year than is needed. Incorporating wheat into the current farming pattern on the saline soil could prove to be a worthwhile endeavor in utilizing these lands to address the food and nutritional deficit of Bangladesh's rapidly growing population. The understanding of changes in physiological processes controlled by salicylic acid and NaCl may offer a foundation for improving wheat plant yield in regions severely impacted by salt stress. Thus, the primary goal of this review is to assess the advantageous effects of salicylic acid on the morpho-physiology and productivity of wheat grown in saline environments.

EFFECTS OF SALICYLIC ACID ON MORPHOLOGICAL TRAITS

Reduction in plant height by salt stress is a common phenomenon for different crops (Ali et al., 2022; Kumar et al., 2022). Salinity had negative effect on the rate of photosynthesis, enzymatic activity level of carbohydrates and growth hormones that resulted in reduced plant height (Hu et al., 2022; Yan et al., 2022). Biswas et al. (2019) reported that the reduction in plant height was probably resulted from a slow growth caused by osmotic stress imposed by high concentration of salts in the rooting zone.

Khanam et al. (2018) analysed the growth and yield returns of two rice cultivars, BR55 and BR43 under salt stress and reported that plant height, total tiller, leaf number, leaf area decreased significantly with the increasing levels of NaCl. High salt stress may create obstacles in root and shoot elongation and reduce fresh and dry weight in plant by decreasing of osmotic potential (Azeem et al., 2023b; Trușcă et al., 2023). The cell wall thickening and inhabitation of cell elongation are the most common effects which results in reduction in growth and development of shoot and root under saline condition (Dabravolski and Isayenkov, 2023; Liu et al., 2022). Dry matter production and number of green leaves per plant were reduced with the increasing salinity due to inhibition of the formation of leaf primordia under salt stress (Fairoj et al., 2023; Mariyam et al., 2023). It has been reported that leaf number per plant was reduced by salinity and the effect was alleviated by SA treatment. SA treatment increased leaf number per plant in wheat (Abdi et al., 2022; Fan et al., 2022).

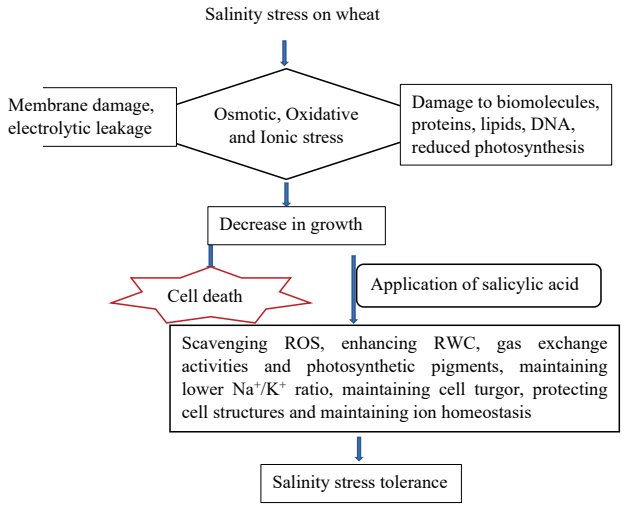

Figure 1. Schematic representation of salinity stress effects on wheat and tolerance to it.

Suhaib et al. (2018) performed an experiment with two wheat cultivars (Faisalabad- 2008 and Punjab-2011) with two levels of salicylic acid (0.25 mM and 0.50 mM) under two salt levels (75 mM and 150 mM). Salt stress had negative impact on shoot length of wheat plant. The results are agreed with the findings of Corti et al. (2023b) and observed that leaf area and shoot surface area were reduced in saline situation in *Eruca sativa*. Suhaib et al. (2018) observed significant enhancement in shoot length, root length, number of tillers when salicylic acid was applied (Figure 2a, 2b, 2c).

Ghafiyehsanj et al. (2013) evaluated the influence of salicylic acid on some biochemical characteristics of wheat under saline stress and reported that salinity significantly reduced the plant growth but application of salicylic acid improved the growth by increasing root length. Abdel-Lattif et al. (2019) conducted two field experiments to evaluate the response of using different concentrations of salicylic acid viz. zero (control), 100 and 200 mg L^{-1} in three wheat varieties, Gemmeiza7, Sakha 93 and Giza168 under salt stress.. They reported that spraying wheat with 100mg L^{-1} of salicylic acid significantly increased the plant height, plant dry weight, plant fresh weight of all varieties (Gemmeiza7, Sakha 93 and Giza168) compared with control. They concluded that, exogenously applied SA increased the salinity tolerance of wheat, particularly by reducing the negative effects of salts.

Cornelia et al. (2010) evaluated the effect of Salicylic acid on salinity treated wheat. They used following treatment combinations, control (C) 12 hour soaked in water and germinated in water; sample 1 (S_1) 12 hour soaked in water and germinated in 200 mM NaCl solution; sample 2 (S_2) 12 hour soaked in 0.1 mM SA solution and germinated in 200 mM NaCl solution; sample 3 (S_3) 12 hour soaked in 0.05mM SA solution and germinated in 200 mM NaCl solution (Table 1). The salt treatment significantly reduced plant height, leaf area, leaf fresh weight, leaf dry weight. The negative effect of salt stress was reduced for both concentration of SA solution but maximum enhancements in plant height, leaf area, leaf fresh weight, leaf dry weight were recorded in case of treatments with 0.1 mM SA solution.

Turkyilmaz (2012) had also studied the consequence of SA application under salinity stress. He reported that, plant height, dry weight per plant of wheat was reduced by salinity, and the effect was alleviated by SA treatment. SA treatment significantly increased plant height, dry weight per plant of wheat. The results are in agreement with Fairoj et al. (2023).

Loutfy et al. (2020) concluded that during combined interaction of 0.5 mM SA and 150 mM NaCl treatment

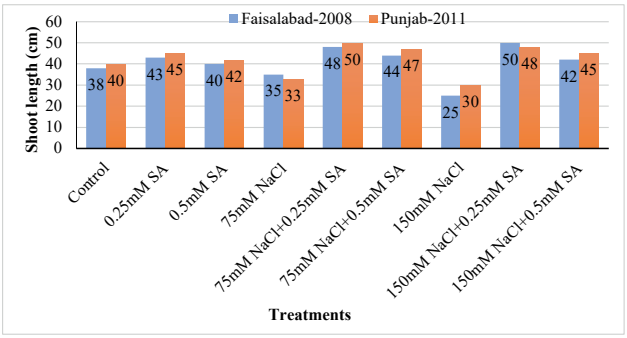

Figure 2a. Mitigation of salt stress on shoot length of wheat through the application of salicylic acid. (Source: Modified from Suhaib et al., 2018).

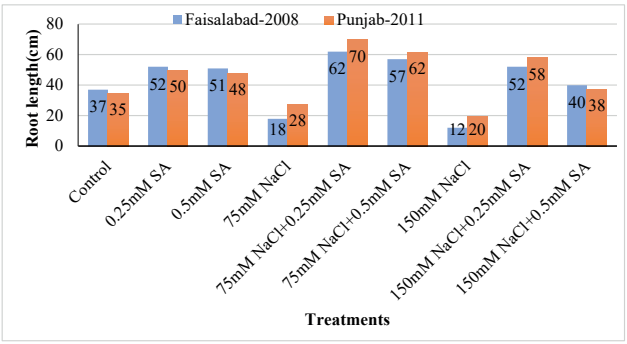

Figure 2b. Mitigation of salt stress on root length of wheat through the application of salicylic acid. Source: (Modified from Suhaib et al., 2018).

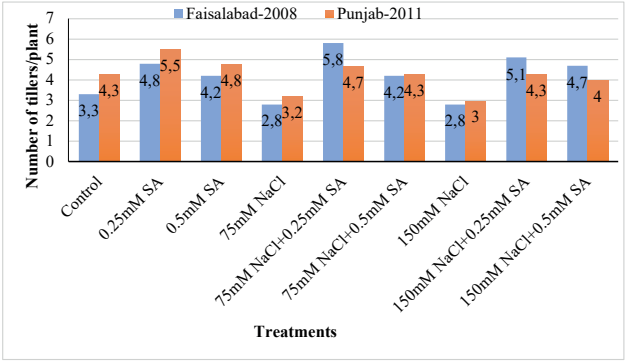

Figure 2c. Mitigation of salt stress on number of tillers of wheat through the application of salicylic acid. Source: (Modified from Suhaib et al., 2018).

root fresh mass, root dry mass shoot dry mass, root dry mass were increased in both Gemaza-1 and Sakha-69 wheat variety than 150 mM NaCl treatment (Figure 3a, 3b, 3c, 3d). Desoky and Merwad (2015) evaluated the

Table 1. Salicylic acid mitigates the effects of salinity on leaf area, leaf fresh weight and leaf dry weight of wheat.

Treatment	Leaf area (cm^2)	Leaf fresh weight (g)	Leaf dry weight (g)
Control	7.14	0.082	0.0092
150mM NaCl	5.23	0.058	0.0053
150mM NaCl+ 0.05mM SA	6.25	0.065	0.0054
150mM Nacl+0.1mM SA	6.98	0.084	0.0114

Source: (Modified from Cornelia et al., 2010).

response of exogenous application of salicylic acid (SA) under NaCl stress on wheat plants (*Triticum aestivum* L.) to different levels of foliar spray of salicylic acids at a rate of 0.1% and 0.2 %. SA_1 was 0.1% and salinity levels were, 3 dSm^{-1}, 6 dSm^{-1}, 9 dSm^{-1}. They concluded that NaCl treatment significantly reduced the plant height, dry weight per plant and the effect was alleviated by SA treatment.

Afzal et al. (2006) assessed the mitigation of salinity stress by hormonal priming with abscisic acid (ABA), salicylic acid and ascorbic acid in spring wheat. Seeds primed with 50 ppm ascorbic acid and 50 ppm SA significantly increased root length, shoot length, root dry weight, root fresh weight, shoot fresh weight and shoot dry weight. Fardus et al. (2018) examined to evaluate salicylic acid-induced improvement in germination and growth parameters of wheat under salinity stress. . Five salinity levels recorded as control, 50 mM, 100 Mm, 150 mM and 200 mM of NaCl were imposed on salinity tolerant and salinity sensitive (variety of wheat namely, BARI Gom 25 and BARI Gom 21. They reported that, plant height, length of shoot, length of root, tiller number per hill, fresh weight per plant, dry weight per plant, fresh weight of root per seedling, dry weight of root per seedling, fresh weight of shoot per seedling, dry weight of shoot per seedling was reduced by salinity and the negative effect of salt stress was alleviated by SA treatment.

EFFECTS OF SALICYLIC ACID ON PHYSIOLOGICAL TRAITS

Salicylic acid is a plant hormone which plays diverse physiological roles in plants, including growth, flower induction, nutrient absorption, stomatal closure, ethylene biosynthesis and photosynthesis (Desire and Arslan, 2021; Jangra et al., 2023). The response of plants to salinity is the reduction of total chlorophyll and carotenoids contents in leaves of reported by most of the studies. Plants that are grown under saline stress, photosynthetic

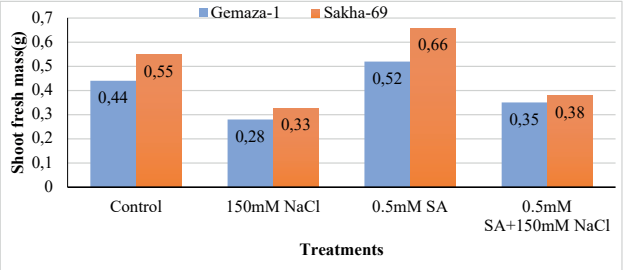

Figure 3a. Mitigation of salt stress effects on shoot fresh mass of two wheat cultivars through the application of salicylic acid. Source: (Modified from Loutfy et al., 2020).

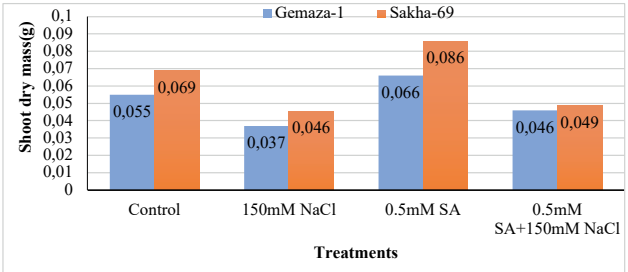

Figure 3b. Mitigation of salt stress effects on shoot dry mass of two wheat cultivars through the application of salicylic acid. Source: (Modified from Loutfy et al., 2020).

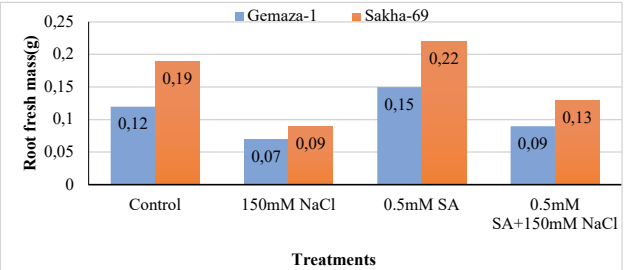

Figure 3c. Mitigation of salt stress effects on root fresh mass of two wheat cultivars through the application of salicylic acid. Source: (Modified from Loutfy et al., 2020)

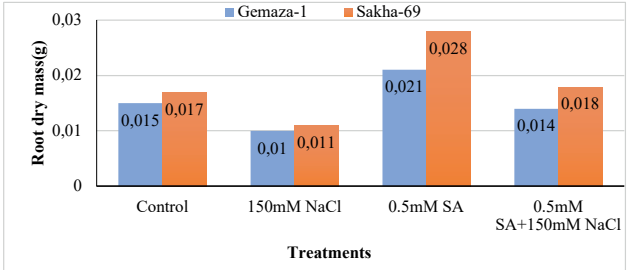

Figure 3d. Mitigation of salt stress effects on root dry mass of two wheat cultivars through the application of salicylic acid. Source: (Modified from Loutfy et al., 2020).

activity reduces resulting in reduced plant growth, leaf area, chlorophyll content and chlorophyll fluorescence (Mousavi et al., 2022; Song et al., 2019). It has been observed that under the influence of salinity the photosynthetic pigments greatly decreased due to chlorophyll a, b and carotenoids reduced significantly in saline stressed plants (Askari et al., 2023; Singh et al., 2022).

Turan et al. (2007) investigated variations in chlorophyll concentrations and growth of wheat plants (*Triticum aestivum* L. cv: Cakmak-79) which were grown under salinity stress in greenhouse conditions. They found that the normal growth and development of plants were disturbed by salt stress. The increased amount of NaCl applied to soil resulted in lower chlorophyll content. Hossain et al. (2006) performed an experiment with two wheat varieties namely Aghrani and Kanchan that were exposed to to 50, 100 and 150 mM NaCl till their maturity. They found decreasing trends of chlorophyll content with increasing salinity levels in both variety. Biswas et al. (2019) reported that longer the exposure to salinity stress higher the decreases the SPAD value. It has been reported by the pre-treatment of salicylic acid as a foliar spray mitigated the salt stress impact on the total chlorophyll (SPAD) pigment content of wheat seedling leaves (Hafez, 2016; Noreen et al., 2019).

Suhaib et al. (2018) evaluated the response of two wheat cultivars (Faisalabad-2008 and Punjab-2011), with two levels of salicylic acid (0.25 mM and 0.50 mM) under two salt levels (75 mM and 150 mM). Salt stress had negative impact on chlorophyll content and $Na^{+/}K^{+}$ ratio of wheat plant under both levels of salt stress whereas, 0.25 mM salicylic acid was more effective than 50 mM salicylic acid. Chlorophyll content significantly increased with the application of salicylic acid. They reported that the maximum chlorophyll content per plant was observed in 0.25 mM SA under 75 mM NaCl (Figure 4). The salinity treatments significantly increased the Na^{+}/K^{+} ratio in wheat plants. The maximum Na^{+}/K^{+} ratio was observed under 150 mM NaCl treatment and in Punjab-2011. But salicylic acid remarkably reduced the sodium uptake by the plantsand increased uptake of K^{+}. As a result, Na^{+}/K^{+} ratio was decreased for using salicylic acid (Figure 5).

Biswas et al. (2019) concluded that, chlorophyll content of wheat was reduced by salinity and the effect was alleviated by SA treatment. Loutfy et al. (2020) reported the response of 2 wheat cultivars (Gemaza-1 and Sakha-69) under four different treatments i.e. (i) Control (ii) 150 mM NaCl (iii) 0.5 mM SA, and (iv) 0.5 mM SA and 150 mM NaCl. They reported that, with the pres-

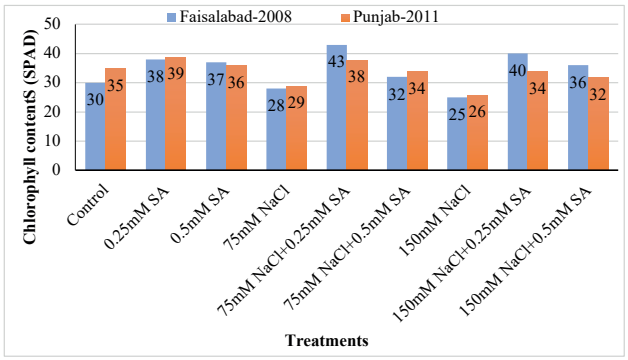

Figure 4. Salicylic acid mitigates the salinity effects on chlorophyll contents (SPAD value) of wheat. Source: (Modified from Suhaib et al., 2018)

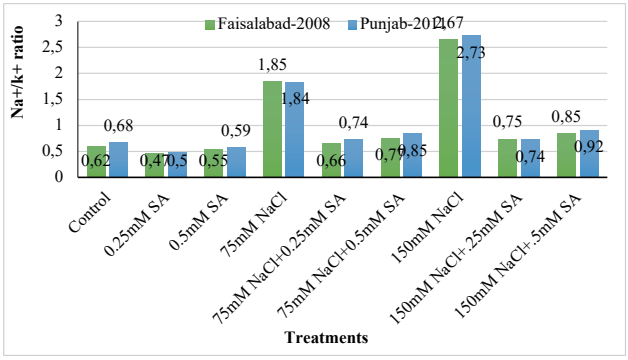

Figure 5. Salicylic acid mitigates the salinity effects on Na^{+}/K^{+} ratio of wheat. Source: (Modified from Suhaib et al., 2018)

ence of 150 mM NaCl, SA significantly recovered chlorophyll content of wheat. Salt stress caused a reduction of 16–24% in PPC in Gemaza-1 and 12–18% reduction in Sakha-69.SA increased PPCs in both cultivars, by 10–20% for carotenoid or Chlorophyll a, but only 2–4% for Chlorophyll b. SA also recovered the reduced PPCs, near to control levels for carotenoid (99–98%), or to 90–96% and 85–91% of control for Chlorophyll a and Chlorophyll b, respectively. They also reported that leaf relative water content was lowest under 150mM NaCl treatment but addition of 0.5mM SA increased leaf relative water content of wheat under both saline and non-saline condition in both Gemaza-1and Sakha-69.

Cornelia et al. (2010) evaluated the effect of SA on salinity treated wheat following treatment combinations, control (C) – 12 h soaked in water and germinated in water; sample 1 (S_1) – 12 h soaked in water and germinated in 200 mM NaCl solution; sample 2 (S_2) – 12 h soaked in 0.1 mM SA solution and germinated in 200 mM NaCl solution; sample 3 (S_3) – 12 h soaked in

Table 2. Effect of salicylic acid (SA) on leaf relative water content, stomatal conductance and photosynthetic rate of wheat plant under salt stress.

Treatment	Leaf relative water content (%)	Stomatal conductance rate (mol $m^{-2}s^{-1}$)	Photosynthetic rate (µmol CO_2 m^{-2} s^{-1})
Control	81.9	0.08	2.33
150 mM NaCl	67.9	0.04	1.29
150 mM NaCl+.05 mM SA	74.9	0.06	1.35
150 mM Nacl+.1 mM SA	82.9	0.07	2.17

Source: (Modified from Cornelia et al., 2010).

0.05mM SA solution and germinated in 200 mM NaCl solution. They found that salicylic acid application increased the content of assimilatory pigments as compared with salt stressed samples. The effect of the salicylic acid solutions treatment was contingent on the concentration which was used. The content of chlorophyll an increased non-significantly after seeds presoaking in 0.05 mM SA solution. Chlorophyll a and chlorophyll b contents increased very significantly than salt stressed when treated with 0.1 mM SA solution. Cornelia et al. (2010) also reported that maximum leaf relative water content, stomatal conductance, photosynthetic rate was observed in addition of 0.1 mM SA with the presence of 150 mM NaCl treatment (Table 2).

Silva et al. (2020) conducted an experiment where the treatments consisted of five levels of electrical conductivity of supplied water - ECw (0.8, 1.6, 2.4,3.2 and 4.0 dS m-1) and four concentrations of salicylic acid (0, 1.2, 2.4 and 3.6 mM). They reported that SA treatment mitigated salts tress and increased stomatal conductance, transpiration, CO_2 assimilation rate, internal CO_2 concentration of salinity treated soursop (*Annona muricata* L.). Methenni et al. (2018), analysing the influence of salicylic acid (0, 0.5 and 1.0 mM) and salt stress (0 and 200 mM of NaCl) on olive plants *(Olea europaea* L.) confirmed that 1.0 mM salicylic acid upgraded increments in CO_2 assimilation rate and stomatal conductance.

Khan et al. (2019) investigated the feasible influence of foliar and soil-applied SA and bagasse compost (BC) introduction on wheat (*Triticum aestivum* L.) grown under saline condition (EC 14 dSm^{-1}). They reported that the artificially developed salinity significantly reduced chlorophyll content of wheat plants but application of SA significantly increased chlorophyll content of salinity treated wheat.

The advantageous effect of salicylic acid on CO_2 assimilation rate, confirmed in plants subjected to concentrations of up to 1.4 mM, may be related to the ability of salicylic acid to promote enzymatic and photo-

synthetic activities, while also maintaining the balance between the manufacture and elimination of reactive oxygen species (Batista et al., 2019). Morad et al. (2013) evaluated the effect of salt stress and salicylic acid application on growth and yield component traits of wheat where they concluded that foliar application of salicylic acid stimulated the growth of wheat plants via the enhancement of the biosynthesis of photosynthetic pigments; increased relative water content and thus salicylic acid promoted wheat growth.

Salinity stress has been shown to increase chromosomal abnormalities, MDA, and trigger autophagy, as well as programmed cell death (PCD) (Fedoreyeva et al., 2022; Liu et al., 2009; Ma et al., 2024; Prajapati et al., 2023; Tabur et al., 2021; Tabur et al., 2022).

PCD is a series of processes that occur in different tissue cells that are intended to die but have a specific positive effect related to the function of the cell, the tissue itself, or the whole organism (Kabbage et al., 2017). It has been observed that this process can occur in a variety of highly specialized tissues depending on their developmental stage, such as tapetum cells during lysis, prior to pollen release, abnormal megaspore death during megasporogenesis in angiosperms by forming antipodal cells or nucellus dissolution during gametophyte formation (Hanaoka et al., 2002; Reggiori et al., 2005; Thumm et al., 1994; Tsukada and Ohsumi, 1993; Xie and Klionsky, 2007).

Autophagy is a protein degradation process in which cells recycle cytoplasmic contents when subjected to environmental stress conditions or during certain stages of development. Upon the induction of autophagy, a double membrane autophagosome forms around cytoplasmic components and delivers them to the vacuole or lysosome for degradation. In plants, autophagy has been shown previously to be induced during abiotic stresses including nutrient starvation and oxidative stress (Liu et al., 2009). Although autophagy appears to be implicated in plant responses to abiotic stresses, its exact involvement has yet to be revealed. Salt and osmotic stress can enhance ROS generation and cause protein damage, and a possible hypothesis is that autophagy aids in the degradation of oxidized proteins during salt and osmotic stress (Pilot et al., 2004).

Fedoreyeva et al. (2022) conducted an experiment and found that in control wheat roots, the Carboxy-H2DFFDA marker detects ROS only in the apical part of the root cap, whereas under salt stress, Carboxy-H2DFFDA accumulates in cells of different root zones, indicating an increase in ROS content and the activation of oxidative stress and cellular damage. Thus, the buildup of the ROS fluorescent marker Carboxy-H2DFFDA in root cells in response to salt indicates that ROS homeostasis was disrupted in these cells and root tissues, potentially leading to PCD.

Liu et al. (2009) stated that autophagy is induced in high salt and osmotic stress conditions, which coincides with an increase in the expression of the *Arabidopsis thaliana* autophagy-related gene *AtATG18a*. Autophagy-defective *RNAi-AtATG18a* plants are more sensitive to salt and drought than wild-type plants, indicating that autophagy plays a role in stress responses. NADPH oxidase inhibitors prevent autophagy induction under nutritional restriction and salt stress, but not during osmotic stress, demonstrating that autophagy can be initiated via NADPH oxidase-dependent or -independent mechanisms.

An experiment was conducted by Tabur et al. (2021) to investigate the efficiency of salicylic acid (SA) on cytotoxicity and genotoxicity induced by salinity stress in the barley apical meristems and they found that salt stress caused a significant decrease in mitotic index of barley seeds depending on concentration increase, while the frequency of chromosomal abnormality increased. Similarly, it was discovered that the mitotic index value dropped with SA therapy alone, although chromosomal aberrations increased. However, when SA and varied salt concentrations were used concurrently, the greatest salt concentration performed better than low salt concentrations in reducing the mitodepressive effect of salt stress by boosting the mitotic index by about twofold (Table 3). In contrast, low salt levels in this application were more effective than high salt levels in mitigating the clastogenic effect of salt stress on chromosomal structure and behaviors. Thus, they suggested that SA's protective role against the cytotoxic effects of salinity stress is more effective at low salt concentrations.

The pretreatment process of seeds was performed by soaking 24 h in constant volumes of distilled water (control) or SA. Various concentrations of salt were added to germination medium. All data were evaluated as three replicates

EFFECTS OF SALICYLIC ACID ON YIELD CONTRIBUTING PARAMETERS AND YIELD

Salt stress decreased the grain yield through a reduction in various components like in grains spike^{-1}, thousand grain weight, grain yield plant^{-1} spike number and grain number in most of the genotypes under saline condition (Al-Khafaji and Al-Burki, 2021; EL Sabagh et al., 2021; Sen et al., 2022). Decrease of grain yield by salt stress has been reported by Shah et al. (2023) and Gandahi et al. (2020). Khan et al. (2019) examined to evalu-

Table 3. Mitotic index values and frequency of chromosome abnormalities in meristem cells of barley exposed to different NaCl concentrations after salicylic acid pretreatment.

Mitotic Index (%)			Chromosome Abnormalities (%)		
NaCl Concentration (M, mol/L)	Control	SA (1µM, micromolar)	NaCl Concentration (M, mol/L)	Control	SA (1µM, micromolar)
0.00 (Distilled water)	*6.92 ± 0.6^{d}	5.50 ± 0.3^{c}	0.00 (Distilled water)	*0.00 ± 0.0^{a}	1.06 ± 0.0^{a}
0.32	6.10 ± 0.2^{c}	3.55 ± 0.2^{a}	0.32	2.07 ± 0.1^{b}	1.77 ± 0.4^{b}
0.35	3.57 ± 0.2^{b}	3.47 ± 0.3^{a}	0.35	2.80 ± 0.0^{c}	2.71 ± 0.3^{c}
0.40	2.41 ± 0.3^{a}	4.68 ± 0.8^{b}	0.40	3.48 ± 0.5^{d}	3.73 ± 0.3^{d}

* ($P \leq 0.05$), ± Standard deviation Source: (Modified from Tabur et al., 2021).

ate the feasible effects of foliar and soil-applied SA (0.5 mM) and bagasse compost (BC) addition on wheat (*Triticum aestivum* L.) growth in saline soil (EC 14 dSm^{-1}). They concluded that artificially developed salinity significantly reduced length of spike, thousand grain weight of wheat plants while application of SA significantly increased spike length, thousand grain weight of salinity treated wheat.

Akher et al. (2013) conducted an experiment to observe the role of salicylic acid on alleviation of salt stress in wheat. Four different salinity levels and three different levels of salicylic acid (SA) was used to their experiment. They reported that salicylic acid (0.2 mmol SA and 0.4 mmol SA) had increased spikelets per spike, grains per spike, grain weight per spike, thousand grain weight, grain yield, straw yield, biological yield and harvest index under saline and non-saline condition (Figure 6 to 11). Under salt stress, the highest no of spikelets per spike, grains per spike, grain weight per spike, thousand grain weight, grain yield, straw yield, biological yield, harvest index was observed in case of application of 0.4 mmol SA with the presence of 2.8g NaCl /kg of soil.

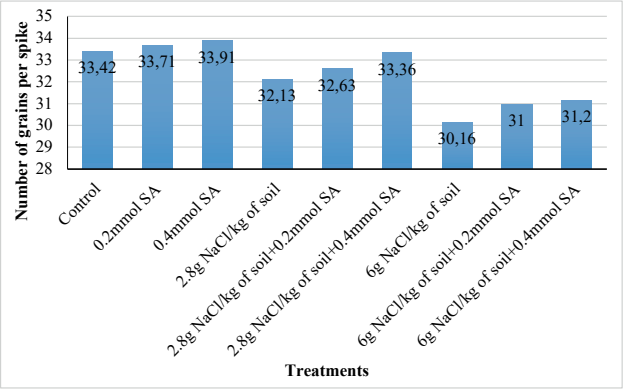

Figure 7. Amelioration of salinity stress on number of grains per spike of wheat through exogenous application of salicylic acid. Source: (Modified from Akher et al., 2018).

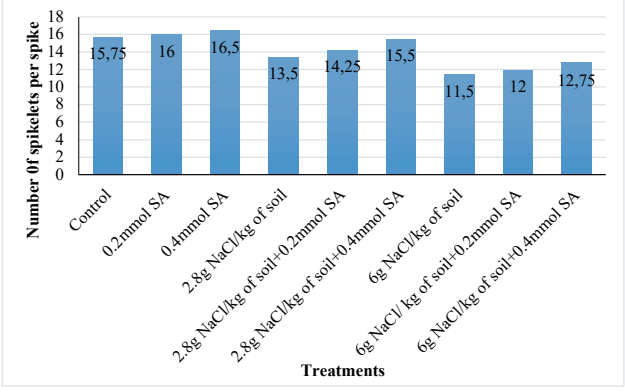

Figure 6. Amelioration of salinity stress on spikelets per spike of wheat through exogenous application of salicylic acid. Source: (Modified from Akher et al., 2018).

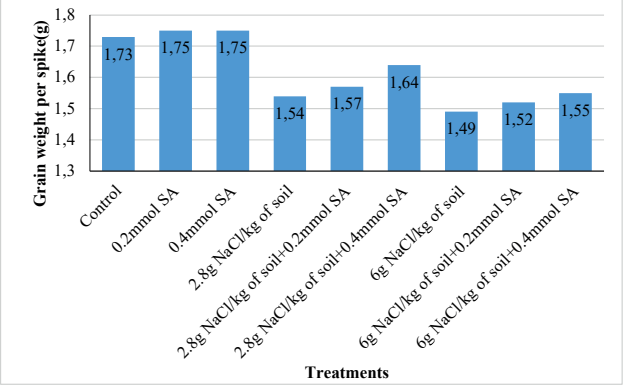

Figure 8. Amelioration of salinity stress on grain weight per spike of wheat through exogenous application of salicylic acid. (Modified from Akher et al., 2018).

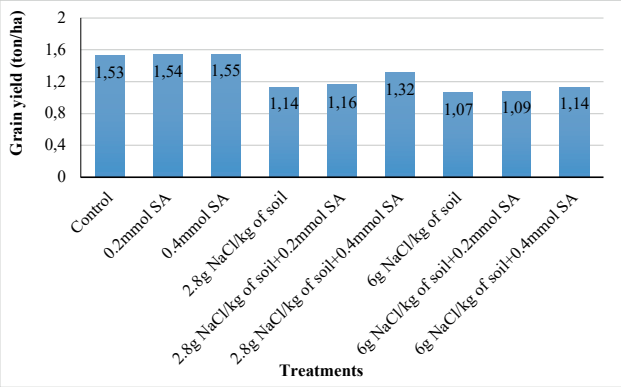

Figure 9. Combined effect of different levels of salinity and salicylic acid (SA) on grain yield of wheat. Source: (Akher et al., 2018).

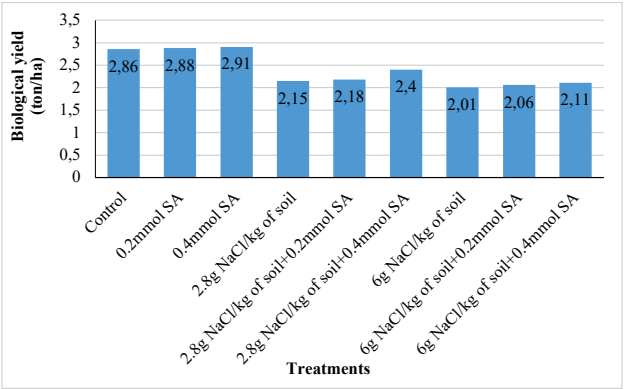

Figure 11. Combined effect of different levels of salinity and salicylic acid (SA) on biological yield of wheat. Source: (Akher et al., 2018).

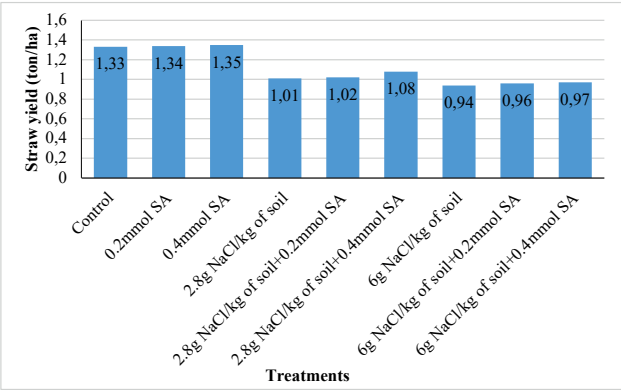

Figure 10. Combined effect of different levels of salinity and salicylic acid (SA) straw yield per plant of wheat. Source: (Akher et al., 2018).

Abdel-Lattif et al. (2019) conducted two field experiments to evaluate the response of using different concentrations of salicylic acid viz. control (zero), 100 mg L^{-1} and 200 mg L^{-1} in three wheat varieties, Gemmeiza7, Sakha 93 and Giza168 under salt stress. They reported that spraying the wheat (*Triticum aestivum* L.) plants with salicylic acid in both concentrations (100 and 200 mg L^{-1}) improved number of spikes per plant, filled grains per spike, spike weight/plant, grain yield per plant, grain yield(ton/ha), 100 grain weight.

Desoky and Merwad (2015) examined the response of exogenous application of salicylic acid (SA) under NaCl stress on wheat plants (*Triticum aestivum* L.) to different levels of foliar spray of salicylic acid. They concluded that NaCl treatment significantly reduced the grain yield per plant, straw yield per plant, biological yield, 1000 grain weight, efficiency yield and the effect was alleviated by SA treatment. SA treatment increased grain yield per plant, straw yield per plant, biological yield, 1000 grain weight, efficiency yield.

Morad et al. (2013) evaluated the response of salinity stress and salicylic acid on growth and yield traits of two variety of wheat. Three levels of NaCl treatment (control, 4 dS/m and 8 dS/m) and salicylic acid. They reported that, minimum no of grains per spike, weight of grains per spike, spike length was observed under 8 dS/m salinity but SA application alleviated the salt stress effect and under saline stress the highest no of grains per spike, weight of grains per spike, spike length was observed in addition of SA with the presence of 4 dS/m NaCl.

CONCLUSION

This review highlighted the deleterious effects of salinity stress on the morpho-physiological parameters of wheat, including transpiration, photosynthetic rate, internal CO_2 concentration, shoot and root length, number of total tillers, leaf area, leaf fresh and dry weight, shoot fresh and dry mass, root fresh and dry mass, chromosomal structure and behaviors. However, it is also conspicuous that application of salicylic acid has a positive influences on improving those morpho-physiological parameters of wheat under saline condition by scavenging ROS, enhancing RWC, gas exchange activities and photosynthetic pigments, maintaining lower Na^+ concentrations and a Na^+/K^+ ratio, maintaining cell turgor, protecting cell structures and maintaining ion homeostasis, all of which ultimately lead to induce abiotic stress tolerance. Therefore, more comprehensive research is required to investigate endogenous salicylic acid production, as well as improve wheat morpho-physiology and ionic homeostasis, both of which are critical for future sustainable crop produc-

tivity. Furthermore, increased field research on wheat genotypes is necessary to effectively mitigate salt stress by the use of exogenous salicylic acid, but it also needs to be cost-effective.

ACKNOWLEDGMENTS

The authors extend their appreciation to the Deanship of Research and Graduate Studies at King Khalid University for funding this work Large Group Project under grant number RGP2/49/45.

REFERENCES

Aazami, M.A., Maleki, M., Rasouli, F. and Gohari, G., 2023. Protective effects of chitosan based salicylic acid nanocomposite (CS-SA NCs) in grape (Vitis vinifera cv.'Sultana') under salinity stress. *Scientific Reports*, *13*(1), p.883.

Abdel-Lattif, H.M., Abbas, M.S. and Taha, M.H., 2019. Effect of salicylic acid on productivity and chemical constituents of some wheat (Triticum aestivum L.) varieties grown under saline conditions. *JAPS: Journal of Animal & Plant Sciences*, *29*(4).

Abdi, N., Van Biljon, A., Steyn, C. and Labuschagne, M.T., 2022. Salicylic acid improves growth and physiological attributes and salt tolerance differentially in two bread wheat cultivars. *Plants*, *11*(14), p.1853.

Abrar, M.M., Sohail, M., Saqib, M., Akhtar, J., Abbas, G., Wahab, H.A., Mumtaz, M.Z., Mehmood, K., Memon, M.S., Sun, N. and Xu, M., 2022. Interactive salinity and water stress severely reduced the growth, stress tolerance, and physiological responses of guava (Psidium guajava L.). *Scientific Reports*, *12*(1), p.18952.

Afzal, I., Basra, S.M., Farooq, M. and Nawaz, A.A.M.I.R., 2006. Alleviation of salinity stress in spring wheat by hormonal priming with ABA, salicylic acid and ascorbic acid. *Int. J. Agric. Biol*, *8*(1), pp.23-28.

Ahmad, N., Irfan, A., Ahmad, H.R., Salma, H., Tahir, M., Tamimi, S.A., Sajid, Z., Liaquat, G., Nadeem, M., Ali, M. and Abbasi, G.H., 2023. Impact of Changing Abiotic Environment on Photosynthetic Adaptation in Plants. In *New Frontiers in Plant-Environment Interactions: Innovative Technologies and Developments* (pp. 385-423). Cham: Springer Nature Switzerland.

Akher, S.A., Sarker, M.N.I. and Naznin, S., 2018. Salt Stress Mitigation by Salicylic Acid in Wheat for Food Security in Coastal Area of Bangladesh. *Journal of Plant Stress Physiology*, *4*, pp.07-16.

Al-Khafaji, Z.H. and Al-Burki, F.R., 2021, November. Study of the effect of salt stress and kinetin and their interaction on the growth and yield of wheat (Triticum aestivum L.). In *IOP Conference Series: Earth and Environmental Science* (Vol. 923, No. 1, p. 012084). IOP Publishing.

Ali, E., Hussain, S., Jalal, F., Khan, M.A., Imtiaz, M., Said, F., Ismail, M., Khan, S., Ali, H.M., Hatamleh, A.A. and Al-Dosary, M.A., 2023. Salicylic acid-mitigates abiotic stress tolerance via altering defense mechanisms in Brassica napus (L.). *Frontiers in Plant Science*, *14*.

Ali, R., Gul, H., Hamayun, M., Rauf, M., Iqbal, A., Hussain, A. and Lee, I.J., 2022. Endophytic fungi controls the physicochemical status of maize crop under salt stress. *Pol. J. Environ. Stud*, *31*, pp.561-573.

Arif, Y., Singh, P., Mir, A.R., Alam, P. and Hayat, S., 2023. Insights into salicylic acid-mediated redox homeostasis, carbohydrate metabolism and secondary metabolite involvement in improvement of photosynthetic performance, enzyme activities, ionomics, and yield in different varieties of Abelmoschus esculentus. *Plant Physiology and Biochemistry*, *203*, p.108047.

Arikan, B., Yildiztugay, E. and Ozfidan-Konakci, C., 2023. Responses of salicylic acid encapsulation on growth, photosynthetic attributes and ROS scavenging system in Lactuca sativa exposed to polycyclic aromatic hydrocarbon pollution. *Plant Physiology and Biochemistry*, *203*, p.108026.

Askari, M., Hamid, N., Abideen, Z., Zulfiqar, F., Moosa, A., Nafees, M. and El-Keblawy, A., 2023. Exogenous melatonin application stimulates growth, photosynthetic pigments and antioxidant potential of white beans under salinity stress. *South African Journal of Botany*, *160*, pp.219-228.

Austin, A.T. and Ballaré, C.L., 2023. Attackers gain the upper hand over plants in the face of rapid global change. Current Biology, 33(11), pp.R611-R620.

Azeem, M., Sultana, R., Mahmood, A., Qasim, M., Siddiqui, Z.S., Mumtaz, S., Javed, T., Umar, M., Adnan, M.Y. and Siddiqui, M.H., 2023. Ascorbic and Salicylic Acids Vitalized Growth, Biochemical Responses, Antioxidant Enzymes, Photosynthetic Efficiency, and Ionic Regulation to Alleviate Salinity Stress in Sorghum bicolor. *Journal of Plant Growth Regulation*, pp.1-14.

Azeem, M., Pirjan, K., Qasim, M., Mahmood, A., Javed, T., Muhammad, H., Yang, S., Dong, R., Ali, B. and Rahimi, M., 2023b. Salinity stress improves antioxidant potential by modulating physio-biochemical responses in Moringa oleifera Lam. *Scientific Reports*, *13*(1), p.2895.

Batista, V.C.V., Pereira, I.M.C., de Oliveira Paula-Marinho, S., Canuto, K.M., Pereira, R.D.C.A., Rodrigues, T.H.S., de Menezes Daloso, D., Gomes-Filho, E. and de Carvalho, H.H., 2019. Salicylic acid modulates primary and volatile metabolites to alleviate salt stress-induced photosynthesis impairment on medicinal plant Egletes viscosa. *Environmental and Experimental Botany*, *167*, p.103870.

Ben Youssef, R., Boukari, N., Abdelly, C. and Jelali, N., 2023. Mitigation of salt stress and stimulation of growth by salicylic acid and calcium chloride seed priming in two barley species. *Plant Biosystems-An International Journal Dealing with all Aspects of Plant Biology*, pp.1-11.

Biswas, D., Mannan, M.A., Karim, M.A. and Miah, M.Y., 2019. Amelioration of salinity tolerance in foxtail millet by applying plant growth regulators. *Bangladesh Agronomy Journal*, *22*(2), pp.25-39.

Blonder, B.W., Aparecido, L.M.T., Hultine, K.R., Lombardozzi, D., Michaletz, S.T., Posch, B.C., Slot, M. and Winter, K., 2023. Plant water use theory should incorporate hypotheses about extreme environments, population ecology, and community ecology. *New Phytologist*, *238*(6), pp.2271-2283.

Cornelia, P., Petrus, A., Pop, L., Chis, A. and Bandici, G.E., 2010. Exogenous salicylic acid involvement on some physiological parameters amelioration in salt stressed wheat (Triticum aestivum) plantlets. *Analele Universitatii din Oradea, Fascicula: Protectia Mediului*, *15*, pp.160-165.

Corti, E., Falsini, S., Schiff, S., Tani, C., Gonnelli, C. and Papini, A., 2023a. Saline stress impairs lipid storage mobilization during germination in eruca sativa. *Plants*, *12*(2), p.366.

Corti, E., Falsini, S., Gonnelli, C., Pieraccini, G., Nako, B. and Papini, A., 2023b. Salt-Affected Rocket Plants as a Possible Source of Glucosinolates. *International Journal of Molecular Sciences*, *24*(6), p.5510.

Dabravolski, S.A. and Isayenkov, S.V., 2023. The regulation of plant cell wall organisation under salt stress. *Frontiers in Plant Science*, *14*, p.1118313.

Desire, M. and Arslan, H., 2021. The effect of salicylic acid on photosynthetic characteristics, growth attributes, and some antioxidant enzymes on parsley (petroselinum crispum L.) under salinity stress. *Gesunde Pflanzen*, *73*(4), pp.435-444.

Desoky, E.S.M. and Merwad, A.R.M., 2015. Improving the salinity tolerance in wheat plants using salicylic and ascorbic acids. *Journal of Agricultural Science*, *7*(10), p.203.

Elhindi, K.M., Almana, F.A. and Al-Yafrsi, M.A., 2023. Morpho-Biochemical Modification of Petunia to Saline Water and Salicylic Acid Applications. *Horticulturae*, *9*(11), p.1197.

EL Sabagh, A., Islam, M.S., Skalicky, M., Ali Raza, M., Singh, K., Anwar Hossain, M., Hossain, A., Mahboob, W., Iqbal, M.A., Ratnasekera, D. and Singhal, R.K., 2021. Salinity stress in wheat (Triticum aestivum L.) in the changing climate: Adaptation and management strategies. *Frontiers in Agronomy*, *3*, p.661932.

Esmaeili, S., Sharifi, M., Ghanati, F., Soltani, B.M., Samari, E. and Sagharyan, M., 2023. Exogenous melatonin induces phenolic compounds production in Linum album cells by altering nitric oxide and salicylic acid. *Scientific Reports*, *13*(1), p.4158.

Fadiji, A.E., Yadav, A.N., Santoyo, G. and Babalola, O.O., 2023. Understanding the plant-microbe interactions in environments exposed to abiotic stresses: An overview. *Microbiological Research*, p.127368.

Fairoj, S.A., Islam, M.M., Islam, M.A., Zaman, E., Momtaz, M.B., Hossain, M.S., Jahan, N.A., Shams, S.N.U., Urmi, T.A., Rasel, M.A. and Khan, M.A.R., 2023. Salicylic acid improves agro-morphology, yield and ion accumulation of two wheat (Triticum aestivum l.) genotypes by ameliorating the impact of salt stress. *Agronomy*, *13*(1), p.25.

Fan, Y., Lv, Z., Li, Y., Qin, B., Song, Q., Ma, L., Wu, Q., Zhang, W., Ma, S., Ma, C. and Huang, Z., 2022. Salicylic acid reduces wheat yield loss caused by high temperature stress by enhancing the photosynthetic performance of the flag leaves. *Agronomy*, *12*(6), p.1386.

Fardus, J., Matin, M.A., Hasanuzzaman, M. and Hossain, M.A., 2018. Salicylic acid-induced improvement in germination and growth parameters of wheat under salinity stress. *JAPS: Journal of Animal & Plant Sciences*, *28*(1).

Fedoreyeva, L.I., Lazareva, E.M., Shelepova, O.V., Baranova, E.N. and Kononenko, N.V., 2022. Salt-induced autophagy and programmed cell death in wheat. *Agronomy*, *12*(8), p.1909.

Feng, D., Gao, Q., Liu, J., Tang, J., Hua, Z. and Sun, X., 2023. Categories of exogenous substances and their effect on alleviation of plant salt stress. *European Journal of Agronomy*, *142*, p.126656.

Ghafiyehsanj, E., Dilmaghani, K. and Shoar, H.H., 2013. The effects of salicylic acid on some of biochemical characteristics of wheat (Triticum aestivum L.) under salinity stress. *Annals of Biological Research*, *4*(6), pp.242-248.

Gandahi, N., Baloch, A.W., Sarki, S.M., Lund, M.M. and Kandhro, M.N., 2020. Correlation Analysis Between Morphological, Physiological And Yield Traits Under

Salinity Stress Condition In Wheat (Triticum Aestivum L.) Genotypes. *Pakistan Journal of Agriculture, Agricultural Engineering and Veterinary Sciences*, *36*(2), pp.129-134.

Ghosh, U.K., Islam, M.N., Siddiqui, M.N., Cao, X. and Khan, M.A.R., 2022. Proline, a multifaceted signalling molecule in plant responses to abiotic stress: understanding the physiological mechanisms. Plant Biology, 24(2), pp.227-239.

Hadjadj, S., Mahdjoubi, S., Hidoub, Y., Bahaz, T., Ghedamsi, Z., Regagda, S., Arfa, Y. and El Hadj-Khelil, A.O., 2023. Comparative effects of NaCl and Na2SO4 on germination and early seedling stages of the halophyte Carthamus tinctorius L. *Journal of Applied Research on Medicinal and Aromatic Plants*, *35*, p.100463.

Hafez, E.M., 2016. Influence of salicylic acid on ion distribution, enzymatic activity and some agromorphological characteristics of wheat under salt-affected soil. *Egyptian Journal of agronomy*, *38*(3), pp.455-469.

Hanaoka, H., Noda, T., Shirano, Y., Kato, T., Hayashi, H., Shibata, D., Tabata, S. and Ohsumi, Y., 2002. Leaf senescence and starvation-induced chlorosis are accelerated by the disruption of an Arabidopsis autophagy gene. Plant Physiology, 129(3), pp.1181-1193.

Hayat, K., Zhou, Y., Menhas, S., Hayat, S., Aftab, T., Bundschuh, J. and Zhou, P., 2022. Salicylic acid confers salt tolerance in Giant Juncao through modulation of redox homeostasis, ionic flux, and bioactive compounds: an ionomics and metabolomic perspective of induced tolerance responses. *Journal of Plant Growth Regulation*, *41*(5), pp.1999-2019.

Hossain, A.A., Halim, M.A., Hossain, F. and Maher Niger, M.A., 2006. Effects of NaCl salinity on some physiological characters of wheat (Triticum aestivum L.). *Bangladesh J. Bot*, *35*(1), pp.9-15.

Hu, C.H., Zheng, Y., Tong, C.L. and Zhang, D.J., 2022. Effects of exogenous melatonin on plant growth, root hormones and photosynthetic characteristics of trifoliate orange subjected to salt stress. *Plant Growth Regulation*, *97*(3), pp.551-558.

Hussain, S., Hafeez, M.B., Azam, R., Mehmood, K., Aziz, M., Ercisli, S., Javed, T., Raza, A., Zahra, N., Hussain, S. and Ren, X., 2023. Deciphering the role of phytohormones and osmolytes in plant tolerance against salt stress: Implications, possible cross-talk, and prospects. *Journal of Plant Growth Regulation*, pp.1-22.

Iftikhar, I., Shahbaz, M. and Wahid, M.A., 2023. Potential role of foliage applied strigolactone (GR24) on photosynthetic pigments, gas exchange attributes, mineral nutrients and yield components of Zea mays (L.) under saline regimes. *Gesunde Pflanzen*, *75*(3), pp.577-591.

Iqbal, M.S., Zahoor, M., Akbar, M., Ahmad, K.S., Hussain, S.A., Munir, S., Ali, M.A., Arshad, N., Masood, H., Zafar, S. and Ahmad, T., 2022. Alleviating the deleterious effects of salt stress on wheat (Triticum aestivum L.) By foliar application of gibberellic acid and salicylic acid. *Applied Ecology & Environmental Research*, *20*(1).

Jalili, I., Ebadi, A., Askari, M.A., KalatehJari, S. and Aazami, M.A., 2023. Foliar application of putrescine, salicylic acid, and ascorbic acid mitigates frost stress damage in Vitis vinifera cv. 'Giziluzum'. *BMC Plant Biology*, *23*(1), pp.1-15.

Jangra, M., Devi, S. and Kumar, N., 2023. Impact of Foliar Application of Salicylic Acid on Physiological Performance of Sorghum (Sorghum bicolor L.) under Salt Stress. *Agricultural Research Journal*, *9*(2).

Jing, H., Wilkinson, E.G., Sageman-Furnas, K. and Strader, L.C., 2023. Auxin and abiotic stress responses. *Journal of Experimental Botany*, p.erad325.

Kabbage, M., Kessens, R., Bartholomay, L.C. and Williams, B., 2017. The life and death of a plant cell. Annual Review of Plant Biology, 68(1), pp.375-404.

Kaya, C., Ugurlar, F., Ashraf, M. and Ahmad, P., 2023. Salicylic acid interacts with other plant growth regulators and signal molecules in response to stressful environments in plants. *Plant Physiology and Biochemistry*.

Khan, I., Ali, S.M., Chattha, M.U., Barbanti, L., Calone, R., Mahmood, A., Albishi, T.S., Hassan, M.U. and Qari, S.H., 2023. Neem and Castor Oil–Coated Urea Mitigates Salinity Effects in Wheat by Improving Physiological Responses and Plant Homeostasis. *Journal of Soil Science and Plant Nutrition*, pp.1-17.

Khan, M.I., Shoukat, M.A., Cheema, S.A., Ali, S., Azam, M., Rizwan, M., Qadri, R. and Al-Wabel, M.I., 2019. Foliar-and soil-applied salicylic acid and bagasse compost addition to soil reduced deleterious effects of salinity on wheat. *Arabian Journal of Geosciences*, *12*, pp.1-9.

Khanam, T., Akhtar, N., Halim, M.A. and Hossain, F., 2018. Effect of irrigation salinity on the growth and yield of two Aus rice cultivars of Bangladesh. *Jahangirnagar University Journal of Biological Sciences*, *7*(2), pp.1-12.

Kumar, A., Dhansu, P. and Mann, A. eds., 2023. *Salinity and Drought Tolerance in Plants: Physiological Perspectives*. Springer Nature.

Kumar, P., Choudhary, M., Halder, T., Prakash, N.R., Singh, V., V, V.T., Sheoran, S., Longmei, N., Rakshit, S. and Siddique, K.H., 2022. Salinity stress tolerance

and omics approaches: Revisiting the progress and achievements in major cereal crops. *Heredity*, *128*(6), pp.497-518.

Liu, Z., Zhao, M., Zhang, H., Ren, T., Liu, C. and He, N., 2023. Divergent response and adaptation of specific leaf area to environmental change at different spatio-temporal scales jointly improve plant survival. *Global Change Biology*, *29*(4), pp.1144-1159.

Liu, J., Shao, Y., Feng, X., Otie, V., Matsuura, A., Irshad, M., Zheng, Y. and An, P., 2022. Cell wall components and extensibility regulate root growth in Suaeda salsa and Spinacia oleracea under salinity. *Plants*, *11*(7), p.900.

Liu, Y., Xiong, Y. and Bassham, D.C., 2009. Autophagy is required for tolerance of drought and salt stress in plants. *Autophagy*, *5*(7), pp.954-963.

Loudari, A., Latique, S., Mayane, A., Colinet, G. and Oukarroum, A., 2023. Polyphosphate fertilizer impacts the enzymatic and non-enzymatic antioxidant capacity of wheat plants grown under salinity. *Scientific Reports*, *13*(1), p.11212.

Loutfy, N., Sakuma, Y., Gupta, D.K. and Inouhe, M., 2020. Modifications of water status, growth rate and antioxidant system in two wheat cultivars as affected by salinity stress and salicylic acid. *Journal of plant research*, *133*, pp.549-570.

Mao, H., Jiang, C., Tang, C., Nie, X., Du, L., Liu, Y., Cheng, P., Wu, Y., Liu, H., Kang, Z. and Wang, X., 2023. Wheat adaptation to environmental stresses under climate change: Molecular basis and genetic improvement. *Molecular Plant*.

Mangal, V., Lal, M.K., Tiwari, R.K., Altaf, M.A., Sood, S., Kumar, D., Bharadwaj, V., Singh, B., Singh, R.K. and Aftab, T., 2023. Molecular insights into the role of reactive oxygen, nitrogen and sulphur species in conferring salinity stress tolerance in plants. *Journal of Plant Growth Regulation*, *42*(2), pp.554-574.

Mariyam, S., Bhardwaj, R., Khan, N.A., Sahi, S.V. and Seth, C.S., 2023. Review on nitric oxide at the forefront of rapid systemic signaling in mitigation of salinity stress in plants: Crosstalk with calcium and hydrogen peroxide. *Plant Science*, p.111835.

Masarmi, A.G., Solouki, M., Fakheri, B., Kalaji, H.M., Mahgdingad, N., Golkari, S., Telesiński, A., Lamlom, S.F., Kociel, H. and Yousef, A.F., 2023. Comparing the salinity tolerance of twenty different wheat genotypes on the basis of their physiological and biochemical parameters under NaCl stress. *Plos one*, *18*(3), p.e0282606.

Methenni, K., Abdallah, M.B., Nouairi, I., Smaoui, A., Zarrouk, M. and Youssef, N.B., 2018. Salicylic acid and calcium pretreatments alleviate the toxic effect of salinity in the Oueslati olive variety. *Scientia Horticulturae*, *233*, pp.349-358.

Morad, M., Sara, S., Mohammad, D., Javad, R.M. and Majid, R., 2013. Effect of salicylic acid on alleviation of salt stress on growth and some physiological traits of wheat. *International Journal of Biosciences*, *3*(2), pp.20-27.

Mousavi, S.S., Karami, A. and Maggi, F., 2022. Photosynthesis and chlorophyll fluorescence of Iranian licorice (Glycyrrhiza glabra l.) accessions under salinity stress. *Frontiers in Plant Science*, *13*, p.984944.

Naz, M., Ghani, M.I., Atif, M.J., Raza, M.A., Bouzroud, S., Afzal, M.R., Riaz, M., Ali, M., Tariq, M. and Fan, X., 2023a. Sodium and Abiotic Stress Tolerance in Plants. *Beneficial Chemical Elements of Plants: Recent Developments and Future Prospects*, pp.307-330.

Naz, T., Iqbal, M.M., Akhtar, J. and Saqib, M., 2023b. Baseline hydroponic study for biofortification of bread wheat genotypes with iron and zinc under salinity: growth, ionic, physiological and biochemical adjustments. *Journal of Plant Nutrition*, *46*(5), pp.743-764.

Noreen, S., Shaheen, A., Shah, K.H. and Ammara, U., 2019. Effects of Aerial Application of Salicylic Acid on Growth, Pigment Concentration, Ions Uptake and Mitigation of Salinity Stress in Two Varieties of Wheat (Triticum aestivum L.). *Pakistan Journal of Life & Social Sciences*, *17*(2).

Omidi, M., Khandan-Mirkohi, A., Kafi, M., Zamani, Z., Ajdanian, L. and Babaei, M., 2022. Biochemical and molecular responses of Rosa damascena mill. cv. Kashan to salicylic acid under salinity stress. *BMC Plant Biology*, *22*(1), pp.1-20.

Pai, R. and Sharma, P.K., 2023. Exogenous supplementation of salicylic acid ameliorates salt-induced membrane leakage, ion homeostasis and oxidative damage in Sorghum seedlings. *Biologia*, pp.1-21.

Pilot, G., Stransky, H., Bushey, D.F., Pratelli, R., Ludewig, U., Wingate, V.P. and Frommer, W.B., 2004. Overexpression of GLUTAMINE DUMPER1 leads to hypersecretion of glutamine from hydathodes of Arabidopsis leaves. *The Plant Cell*, *16*(7), pp.1827-1840.

Pirasteh-Anosheh, H., Rahimpour, B., Mohammadi, H., Ranjbar, G. and Race, M., 2023. Induced salinity tolerance by salicylic acid through physiological manipulations. In *Phytohormones and Stress Responsive Secondary Metabolites* (pp. 99-109). Academic Press.

Prajapati, P., Gupta, P., Kharwar, R.N. and Seth, C.S., 2023. Nitric oxide mediated regulation of ascorbate-glutathione pathway alleviates mitotic aberrations and DNA damage in Allium cepa L. under salinity stress. International Journal of Phytoremediation, 25(4), pp.403-414.

Reggiori, F., Shintani, T., Chong, H., Nair, U. and Klionsky, D.J., 2005. Atg9 cycles between mitochondria and the pre-autophagosomal structure in yeasts. Autophagy, 1(2), pp.101-109.

Rostampour, P., Hamidian, M., Dehnavi, M.M. and Saeidimajd, G.A., 2023. Evaluation of osmoregulation and morpho-physiological responses of Borago officinalis under drought and salinity stress with equal osmotic potential. *Biochemical Systematics and Ecology*, *106*, p.104567.

Rubio-Rodríguez, E., Vera-Reyes, I., Rodríguez-Hernández, A.A., López-Laredo, A.R., Ramos-Valdivia, A.C. and Trejo-Tapia, G., 2023. Mixed elicitation with salicylic acid and hydrogen peroxide modulates the phenolic and iridoid pathways in Castilleja tenuiflora plants. *Planta*, *258*(1), p.20.

Saeed, S., Ullah, A., Ullah, S., Elshikh, M.S., Noor, J., Eldin, S.M., Zeng, F., Amin, F., Ali, M.A. and Ali, I., 2023. Salicylic acid and α-tocopherol ameliorate salinity impact on wheat. *ACS omega*, *8*(29), pp.26122-26135.

Sarkar, A.K., Oraon, S., Mondal, S. and Sadhukhan, S., 2023. Effect of salinity on seed germination and seedling growth of bullet cultivar of chilli (Capsicum annuum L.). *Brazilian Journal of Botany*, *46*(3), pp.513-525.

Sen, A., Islam, M.M., Zaman, E., Ghosh, U.K., Momtaz, M.B., Islam, M.A., Urmi, T.A., Mamun, M.A.A., Rahman, M.M., Kamal, M.Z.U. and Rahman, G.M., 2022. Agro-Morphological, Yield and Biochemical Responses of Selected Wheat (Triticum aestivum L.) Genotypes to Salt Stress. *Agronomy*, *12*(12), p.3027.

Shah, S.M.O., Jamal, Y. and Haq, I.U., 2023. Effect of Humic acid on Wheat (Triricum aestivum L.) under saline conditions. *Pure and Applied Biology (PAB)*, *13*(1), pp.93-100.

Sharma, A., Kohli, S.K., Khanna, K., Ramakrishnan, M., Kumar, V., Bhardwaj, R., Brestic, M., Skalicky, M., Landi, M. and Zheng, B., 2023. Salicylic acid: A phenolic molecule with multiple roles in salt-stressed plants. *Journal of Plant Growth Regulation*, pp.1-25.

Shaukat, K., Zahra, N., Hafeez, M.B., Naseer, R., Batool, A., Batool, H., Raza, A. and Wahid, A., 2022. Role of salicylic acid–induced abiotic stress tolerance and underlying mechanisms in plants. In *Emerging plant growth regulators in agriculture* (pp. 73-98). Academic Press.

Silva, A.A.R.D., Lima, G.S.D., Azevedo, C.A.V.D., Veloso, L.L.D.S.A. and Gheyi, H.R., 2020. Salicylic acid as an attenuator of salt stress in soursop. *Revista Caatinga*, *33*, pp.1092-1101.

Singh, A., Rajput, V.D., Sharma, R., Ghazaryan, K. and Minkina, T., 2023. Salinity stress and nanoparticles: Insights into antioxidative enzymatic resistance, signaling, and defense mechanisms. *Environmental Research*, p.116585.

Singh, P., Kumar, V., Sharma, J., Saini, S., Sharma, P., Kumar, S., Sinhmar, Y., Kumar, D. and Sharma, A., 2022. Silicon supplementation alleviates the salinity stress in wheat plants by enhancing the plant water status, photosynthetic pigments, proline content and antioxidant enzyme activities. *Plants*, *11*(19), p.2525.

Song, X., Zhou, G., Ma, B.L., Wu, W., Ahmad, I., Zhu, G., Yan, W. and Jiao, X., 2019. Nitrogen application improved photosynthetic productivity, chlorophyll fluorescence, yield and yield components of two oat genotypes under saline conditions. *Agronomy*, *9*(3), p.115.

Soni, P.G., Basak, N., Rai, A.K., Sundha, P., Chandra, P. and Yadav, R.K., 2023. Occurrence of salinity and drought stresses: status, impact, and management. In *Salinity and Drought Tolerance in Plants: Physiological Perspectives* (pp. 1-28). Singapore: Springer Nature Singapore.

Sóti, A., Ounoki, R., Kósa, A., Mysliwa-Kurdziel, B., Sárvári, É. and Solymosi, K., 2023. Ionic, not the osmotic component, is responsible for the salinity-induced inhibition of greening in etiolated wheat (Triticum aestivum L. cv. Mv Béres) leaves: a comparative study. *Planta*, *258*(5), pp.1-18.

Suhaib, M., Ahmad, I., Munir, M., Iqbal, M.B., Abuzar, M.K. and Ali, S., 2018. Salicylic acid induced physiological and ionic efficiency in wheat under salt stress. *Pakistan Journal of Agricultural Research*, *31*(1), pp.79-85.

Tabur, S., Bayraktar, N.B.K. and Özmen, S., 2022. L-Ascorbic acid modulates the cytotoxic and genotoxic effects of salinity in barley meristem cells by regulating mitotic activity and chromosomal aberrations. Caryologia, 75(3), pp.19-29.

Tabur, S., Avci, Z.D. and Özmen, S., 2021. Exogenous salicylic acid application against mitodepressive and clastogenic effects induced by salt stress in barley apical meristems. *Biologia*, *76*, pp.341-350.

Tammam, A.A., Rabei Abdel Moez Shehata, M., Pessarakli, M. and El-Aggan, W.H., 2023. Vermicompost and its role in alleviation of salt stress in plants–I. Impact of vermicompost on growth and nutrient uptake of salt-stressed plants. *Journal of Plant Nutrition*, *46*(7), pp.1446-1457.

Thampi, M., Dhanraj, N.D., Prasad, A., Ganga, G. and Jisha, M.S., 2023. Phosphorus Solubilizing Microbes (PSM): Biological tool to combat salinity stress in crops. *Symbiosis*, pp.1-18.

Thumm, M., Egner, R., Koch, B., Schlumpberger, M., Straub, M., Veenhuis, M. and Wolf, D.H., 1994. Isolation of autophagocytosis mutants of Saccharomyces cerevisiae. FEBS letters, 349(2), pp.275-280.

Tsukada, M. and Ohsumi, Y., 1993. Isolation and characterization of autophagy-defective mutants of Saccharomyces cerevisiae. FEBS letters, 333(1-2), pp.169-174.

Turkyilmaz, B., 2012. Effects of salicylic and gibberellic acids on wheat (Triticum aestivum L.) under salinity stress. *Bangladesh Journal of Botany*, *41*(1), pp.29-34.

Turan, M., Katkat, V. and Taban, S., 2007. Variations in proline, chlorophyll and mineral elements contents of wheat plants grown under salinity stress. *Journal of Agronomy*, *6*(1).

Truşcă, M., Gâdea, Ş., Vidican, R., Stoian, V., Vâtcă, A., Balint, C., Stoian, V.A., Horvat, M. and Vâtcă, S., 2023. Exploring the Research Challenges and Perspectives in Ecophysiology of Plants Affected by Salinity Stress. *Agriculture*, *13*(3), p.734.

Ullah, I., Toor, M.D., Basit, A., Mohamed, H.I., Gamal, M., Tanveer, N.A. and Shah, S.T., 2023. Nanotechnology: an Integrated Approach Towards Agriculture Production and Environmental Stress Tolerance in Plants. *Water, Air, & Soil Pollution*, *234*(11), p.666.

Virág, E., Kiniczky, M., Kutasy, B., Nagy, Á., Pallos, J.P., Laczkó, L., Freytag, C. and Hegedűs, G., 2023. Supplementation of the Plant Conditioner ELICE Vakcina® Product with β-Aminobutyric Acid and Salicylic Acid May Lead to Trans-Priming Signaling in Barley (Hordeum vulgare). *Plants*, *12*(12), p.2308.

Wang, L., Qin, L., Sun, X., Zhao, S., Yu, L., Chen, S. and Wang, M., 2023. Salt stress-induced changes in soil metabolites promote cadmium transport into wheat tissues. *Journal of Environmental Sciences*, *127*, pp.577-588.

Xie, Z. and Klionsky, D.J., 2007. Autophagosome formation: core machinery and adaptations. Nature cell biology, 9(10), pp.1102-1109.

Yan, S., Chong, P. and Zhao, M., 2022. Effect of salt stress on the photosynthetic characteristics and endogenous hormones, and: A comprehensive evaluation of salt tolerance in Reaumuria soongorica seedlings. *Plant Signaling & Behavior*, *17*(1), p.2031782.

Youssef, S.M., López-Orenes, A., Ferrer, M.A. and Calderón, A.A., 2023. Foliar Application of Salicylic Acid Enhances the Endogenous Antioxidant and Hormone Systems and Attenuates the Adverse Effects of Salt Stress on Growth and Yield of French Bean Plants. *Horticulturae*, *9*(1), p.75.

Zarbakhsh, S. and Shahsavar, A.R., 2023. Exogenous γ-aminobutyric acid improves the photosynthesis efficiency, soluble sugar contents, and mineral nutrients in pomegranate plants exposed to drought, salinity, and drought-salinity stresses. *BMC Plant Biology*, *23*(1), p.543.

Caryologia
International Journal of Cytology, Cytosystematics and Cytogenetics

Firenze University Press
https://riviste.fupress.net/index.php/caryologia

OPEN ACCESS

Citation: Sobhakumari, V.P., & Mohanraj, K. (2024). Genomic *in situ* hybridization (GISH) and performance analysis in intergeneric hybrids from five consecutive generations of *Erianthus* x *Saccharum*. *Caryologia* 77(3): 27-36. doi: 10.36253/caryologia-2727

Received: Apr 16, 2024

Accepted: Oct 16, 2024

Published: March 25, 2025

Data Availability Statement: All relevant data are within the paper and its Supporting Information files.

Competing Interests: The Author(s) declare(s) no conflict of interest.

ORCID
VPS: 0000-0003-4165-6826

Genomic *in situ* hybridization (GISH) and performance analysis in intergeneric hybrids from five consecutive generations of *Erianthus* x *Saccharum*

V. P. Sobhakumari*, K. Mohanraj

Crop Improvement Division, ICAR-Sugarcane Breeding institute, Coimbatore-641 007, Tamil Nadu, India
*Correspondeing author. E-mail: vpsobhakumari@rediffmail.com

Abstract. *Erianthus arundinaceus,* one of the species of '*Saccharum* complex' has a number of important agronomic traits including good ratooning ability, tolerance to both drought and waterlogging, disease resistance and vigor and is of interest as a potential source of parental germplasm to sugarcane breeders. We report here for the first time the chromosome composition, *Erianthus* chromosome transmission patten and agronomical trait evaluation of *Erianthus* addition lines in five consecutive generations of *E. arundinaceus* x *Saccharum*. The hybridity of randomly selected clones could confirm with *Erianthus* Specific Tandem Repeat (ESTR) sequences. The results of classical cytology revealed that the mode of transmission of gametes, except in the second generation, followed n+n pattern whereas in second generation (CYM 07-971) it was showing 2n+n with elimination of few chromosomes. Progressive elimination of *Erianthus* chromosomes is observed in consecutive generations where the F1 showed 30 *Erianthus* chromosomes and it was ranged from 0-2 in fifth generation. Agronomical trait analysis indicates that further backcrossing with commercial clones with high juice quality or intercrossing among the selected progenies would improve both juice quality and cane traits in *E. arundinaceus* x *Saccharum* hybrids.

Keywords: *Erianthus*, *Saccharum*, introgression, cytology, genomic *in situ* hybridization, intergeneric hybrid, sugarcane.

Sugarcane belongs to the genus *Saccharum* and it consists of six species namely *S. officinarum* L., *S. barberi* Jesw., *S. sinense* Roxb., *S. robustum* Brandes and Jesw. ex Grassl, *S. spontaneum* L. and *S. edule* Hassk. The cultivated sugarcane varieties are derivatives of interspecific hybridization between *S. officinarum* and *S. spontaneum*. Critical analysis of pedigree of the cultivated varieties revealed that, only a limited number of basic species clones have been contributed to the parental material in sugarcane breeding programmes (Roach, 1989; Hemaprabha et al., 2022). The cytoplasmic variability among major sugarcane varieties under cultivation are not much as only limited *S. officinarum* clones were used as female parent in early breed-

ing programmes (Hemaprabha et al., 2022). This may result in vulnerability to disease epidemics and abiotic stresses. In order to widen the cytoplasmic base of sugarcane cultivars, the wild related species with diverse chloroplast and mitochondrial genomes have been utilized in breeding programmes. The "*Saccharum* complex" includes the genera *Erianthus* Michx, *Miscanthus* Anderss., *Sclerostachya* (Hack.) A. Camus and *Narenga* Bor., besides the *Saccharum* species and constitute a closely related inter breeding group (Mukherjee 1957; Daniels *et al.* 1975).

The genus *Erianthus* has established by Michaux in 1803, based on the Greek word 'Erion' meaning wool

and 'anthos' meaning flower, referring to its woolly glumes. It is considered a primitive genus of 'Saccharum complex' (Mukherjee 1957). It is wide in distribution occurring in America (New World species), Mediterranean, India, China, South East Asia, New Guinea (Old World species). The Old-World species generally placed under section *Ripidium*, are only important in the evolution and improvement of sugarcane. Among the species of the genus *Erianthus* sect. *ripidium*, *E. arundinaceus* (Retz.) Jesw. (2n = 30, 40, 60) distributed in India, China, Indonesia and New Guinea and has many desirable agronomic traits for sugarcane breeding such as disease resistance, drought resistance, high biomass and broad adaptability. Efforts are under way in many research stations to introgress *Erianthus* germplasm into sugarcane to develop more productive and better adapted sugarcane varieties.

Fertile and sterile hybrids were reported from crosses involving *Saccharum* and *E. arundinaceus* (D' Hont *et al.* 1995, Besse *et al.* 1997, Piperidis *et al.* 2000, 2010, Cai *et al.* 2005, Wu *et al.* 2014, Huang *et al.* 2015) in which either *S. officinarum* or sugarcane variety used as female and was further back crossed with sugarcane. The major difficulty in transferring the desirable characters from *Erianthus* into sugarcane is the incompatibility among the genera which prevents further improvement through hybridization. When crosses between two species are not successful due to hybrid sterility and genome elimination bridge crosses were found to be effective in certain cases. The successful use of *S. spontaneum* as a bridge species for transferring characters from *Erianthus* to *Saccharum* was reported by Premachandran *et al.* 2011. In this case *Erianthus* has been used as female parent. The production and molecular cytogenetic characterization of intergeneric F1 progeny and back cross progenies has been reported earlier (Lekshmi *et al.* 2016, Premachanran *et al.* 2017). Later the backcross progenies were developed by crossing with sugarcane commercial varieties to develop near commercial sugarcane clones. Nuclear and cytoplasmic contribution from *Erianthus* was confirmed in second and third generation hybrids (Lekshmi *et al.* 2016).

Here we aimed to determine the somatic chromosome number of different backcross progenies of *Erianthus* x *Saccharum*. We also selected two different sets of BC1, BC2, BC3 and BC4 progenies and used GISH to clarify the pattern of *E. arundinaceus* chromosome transmission. The aim of the study was to find out the clone that contain 1-2 *Erianthus* chromosomes which can be further used for sequencing the *Erianthus* chromosomes and also to tag the trait specific *Erianthus* chromosomes by correlation studies. This work will provide a basis for subsequent genome research as well as trait specific breeding programmes in sugarcane.

MATERIALS AND METHODS

Plant material

The materials used for the study consist of two sets of progenies from BC2, BC3 and BC4 generations. In the first set, the BC 3 progeny, Co 15015, derived from a cross combination of CYM 08-903 and the Sugarcane cultivar Co 94008 (Lekshmi *et al.* 2016). BC4 progenies (GI 18-1, GI 18-2, GI 18-3, GI 18-4) were from a crossing combination between Co 15015 (female) and sugarcane cultivar, Co 11012 (male). In another set of clones used for the study BC2, BC3 and BC4 progenies were developed by a parallel set of hybridization process. A BC2 clone, CYM 08-922 was selected as female parent and BC3 progeny TWC 82, was derived from a cross combination CYM 08-922 x Sugarcane variety BO91. Four BC4 progenies were developed (FWC 28, FWC 29, FWC 39 and FWC 2) from a cross between TWC 82 x Sugarcane hybrid. The details of the clones used for the study are given in Table 1. To understand the flow of chromosome transmission pattern in successive generations of *Erianthus* x *Saccharum*, the clones from *Erianthus* (female parent), F1 and BC1 were also included in the study.

The somatic chromosome number in the F1 and back cross progenies was determined by root tip squash technique (Sobhakumari and Asmita Dutta, 2014). For GISH analysis the mitotic slide preparation was performed as per D'Hont *et al.* 1996 with minor modifications. Single budded cuttings from the hybrids were collected at 1.30pm. Excised root tips of about 1 cm were treated with 2mM 8-hydroxy quinolone at room temperature for 2h, washed in water and fixed in Ethanol: Acetic acid (3:1) for overnight at 4°C. The washed root tips were hydrolyzed in 0.25N HCl and digested at 37°C for 75min in the enzyme solution containing 2.0% cellulase

ONOZUKA R-10 (Himedia) and 20% pectinase (Himedia) in citrate buffer. After washing the meristematic tissues of the root tips were squashed in a drop of fixative. Cells can be separated by gentle pressing over the coverslip with filter paper. Slides were then freezed by dipping it in liquid nitrogen. After removing the coverslip, the frozen slide was immediately dehydrated in absolute ethanol and stored in moisture free slide box.

Genomic in situ *hybridization*

Total genomic DNA of the *Erianthus* clone, IK 76-62, was extracted from young leaves using CTAB method (Doyle and Doyle, 1990). Fragmentation (500bp – 1000bp) has been done by sonication. The fragmented DNA of *Erianthus* labeled with biotin 11-duTP using random primed labeling method as described by manufacturer (Thermo Scientific, USA) was used as probe. The 30µl hybridization mixture containing 5µlof labeled probe, 15µl deionized formamide, 6 µl 50% dextran sulphate, 2.25µl 20xSSC, 0.5 µl salmon sperm DNA and 1.25 µl double distilled water was denatured at 100°C for 10min, and then placed immediately in ice. Each chromosomal slide was denatured at 72°Cfor 2min in denaturation solution containing 70% deionized formamide and dehydrated in a series of precooled ethanol solutions (75%, 95%and 100%). After adding 30µl of hybridization solution to the slide it was incubated in a humid box with 2xSSC and at 37°C for overnight. Post hybridization washes in 2xSSC and 50% formamide at 42°C slides were dried. Biotin labeled probe was detected using avidin-FITC (Fluorescein iso thio cynate) (Vector laboratories, Burlingane, CA) by 1h incubation at 37°C. After washing and drying the chronosomes were counter stained with a vectasheild vibrance anti-fading medium with DAPI (4,6 diamino-2-phenylindole) (Vector laboratories, Burlingane, CA). GISH signals were captured using a ProgRes Capture Pro image capturing software attached to AxioScope A1fluorescent microscope (CarlZeiss, Gottingen, Germany). Images were processed using Adobe Photoshop.

Screening for drought tolerance and red rot resistance

The experimental trial was conducted at East Chithirai Chavadi farm of ICAR-Sugarcane breeding institute, Coimbatore, Tamil Nadu, India (110 N, 770E, 427 MSLaltitude) during 2021-22. The backcross hybrids involving Erianthus were planted in split plot desgn, treatments as main plots and genotypes as subplots. The drought treatment was insisted by withholding water during the formative phase of the crop (60-150 DAP). The yield and juice quality data were recorded at 10th month of crop.

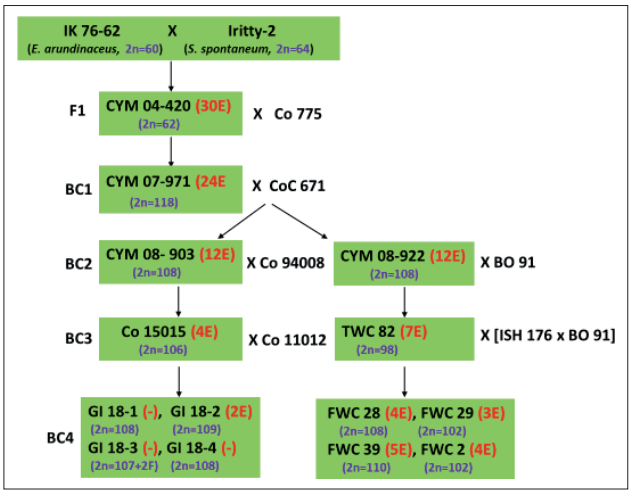

Figure 1. *Erianthus arundinaceus* introgression pattern in five generations of *Erianthus arundinaceus* x *Saccharum officinarum.*

The drought tolerance indices were calculated as follows:

Stress tolerance index (STI) STI = (Yp * Ys) / ($\bar{Y}$p)2

Yp and Ys are the average yield under normal and moisture stress conditions, respectively. $\bar{Y}$p is the average yield of all genotypes under normal moisture conditions, Screening for red rot resistance under controlled condition testing. The clones were screened for red rot resistance against the virulent inoculum of cf 671 (*Colletotricum falcatum*) under controlled condition testing (CCT) and the disease reaction was scored as per Mohanraj et al., (1997).

RESULTS AND DISCUSSION

Chromosome composition of the F1 hybrid

GISH analysis of the F1 hybrid CYM 04-420 from the cross between IK 76-78 (*Erianthus arundinaceus*, 2n=40) x Iritty-2 (*Saccharum spontaneum*, 2n= 64) revealed that a total of 62 chromosomes (Table 1) of which 30 were from *E. arundinaceus* and 32 were from *S. spontaneum* (Fig. 3a), as expected from a classical n+n chromosome transmission (Table. 1) (Lekshmi *et al.* 2016; Premachandran *et al.* 2017). The result was contradictory to the report of Wu *et al.* (2014) and Piperidis *et al.* (2000) where they have reported the presence of anueploids in F1 generation.

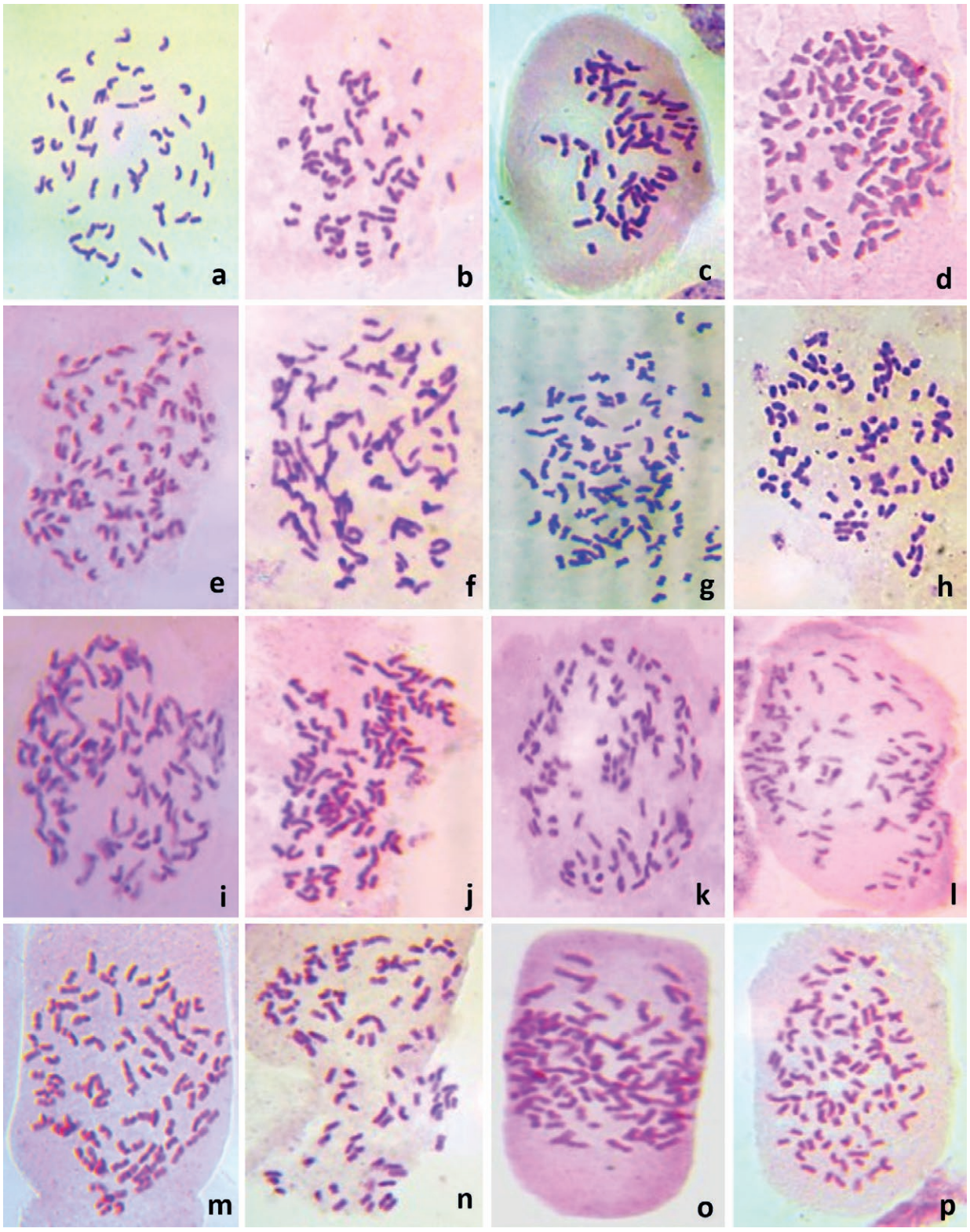

Figure 2. Somatic chromosome number of different clones in F1 to BC4 generations: a) IK 76-78 (2n=60), b) Iritty-2 (2n=64), c) CYM 04-420 (2n=62), d) CYM 07-971(2n= 118), e) CYM 08-903 (2n=108), f) CYM 08-922 (2n=108), g) Co 15015 (2n=106), h)TWC 82 (2n=98), i) GI 18-1(2n=108), j) GI 18-2 (2n=109), k)GI 18-3 (2n=107+2F), l) GI 18-4 (2n=108), m) FWC-2 (2n=102), n) FWC-28, (2n=108), o) FWC-29 (2n=102), p) FWC-39 (2n=110).

Table 1. Chromosome composition of parents and hybrids of different generations involving *Erianthus arundinaceus*.

S.No	Generation	Clone Name	Total 2n	From *Saccharum*	From *Erianthus*	Recombinant	No of cells observed
1	Female parent	IK76-62	60	-	60	0	10
2	Male parent	Iritty-2	64	-	-	0	10
3	F1	CYM 04-420	62	32	30	0	15
4	BC1	CYM 07-971	118	94	24	0	12
5	BC2	CYM 08-903	108	96	12	0	16
6	BC2	CYM 08-922	108	96	12	0	15
7	BC3	Co 15015	106	102	4	0	20
8	BC3	TWC 82	98	91	7	0	15
9	BC4	GI 18-1	108	108	-	0	10
10	BC4	GI 18-2	109	107	2	0	15
11	BC4	GI 18-3	108	108	-	0	10
12	BC4	GI 18-4	108	108	-	0	12
13	BC4	FWC-28	108	104	4	0	15
14	BC4	FWC-29	102	99	4	0	15
15	BC4	FWC-39	110	105	5	0	15
16	BC4	FWC-2	102	98	4	0	15

2n+ n chromosome transmission in BC1 progeny

Due to nonsynchronous flowering of the sugarcane hybrid the fundamental principles of backcross breeding are not appropriate in the case of this crop. During intergeneric hybridization in F1 the chromosome inherited from divergent parents of different genera are often unable to pair with each other during meiosis which leads to male sterility in F1 hybrid. In order to obtain BC1 generation the F1 hybrid (CYM 04-420) was used as a female parent and a commercial variety Co 775 was used as a male parent. From this cross many BC1 progeny were generated. We considered one BC1 progeny, CYM 07-971 for further analysis. The total chromosome compliment for this hybrid was 2n=118 of which 94 chromosomes were derived from *Saccharum* and 24 chromosomes were derived from *E. arundinaceus* (Table 1, Fig. 3b). These results indicated that the BC1 progeny was a product of 2n+n transmission. Piperidis *et al.* (2000), Piperidis *et al.* (2010) and Wu *et al.* (2014) were reported similar results. 2n gametes were originated from fusion of two megaspore (Megaspore Tetrad Cell Fusion) or due to chromosome doubling after second meiotic division (Post Meiotic Restitution) (Narayanaswami (1940), Bremer (1961).

n+n chromosome transmission in BC2 and BC3 progeny

GISH analysis of two BC2 (CYM 08-903 and CYM 08-922) revealed that these clones were with a total of chromosome compliment of 2n=118 of which 96 chromosomes were derived from *Saccharum* species and 12 chromosomes were from *E. arundinaceus* (Table 1, Fig. 3 c & d). It was found that the number of *E. arundinaceus* chromosomes in BC1 parent was 24 and in BC2 progeny it was reduced by half. This indicate that BC2 progeny (CYM 08-903 and CYM 08-922) were the product of n+n transmission. Parallel back crosses were conducted with these BC2 progenies. i. e., CYM 08-903 x Co 94008 and CYM 08-922 X Bo 91. A nearly commercial cane, Co 15015 with 2n=108 was generated as BC3 progeny from CYM 08-903 x Co 94008. GISH experiment revealed that 102 chromosomes were derived from *Saccharum* species and 4 from *E. arundinaceus*. Another BC3 progeny, TWC 82, from the cross CYM 08-922 X BO 91 was with 2n=98 of which 91 chromosomes were from *Saccharum* and 7 chromosomes were from *E. arundinaceus*. Our results indicate that the BC3 progeny were the product of n+n transmission. Piperidis *et al.* (2010, 2013) and Huang *et al.* (2014) reported that the similar transmission was in BC2 and Bc3 progeny between different species clones of *S. officinarum* and *E. arundinaceus*.

In this study, both the BC3 progeny, Co 15015 and TWC 82, were derived from BC2 clones CYM 08-903 and CYM 08-922 respectively. Both the BC2 parents were having 12 *E. arundinaceus* chromosomes. In TWC 82 is seven *Erianthus* chromosomes were observed. It is found that more than half of the *E. arundinaceus* chromosomes in CYM 08-922 was transmitted to TWC-82. Where as in the case of Co 15015 only four (less than half) *E. arundi-*

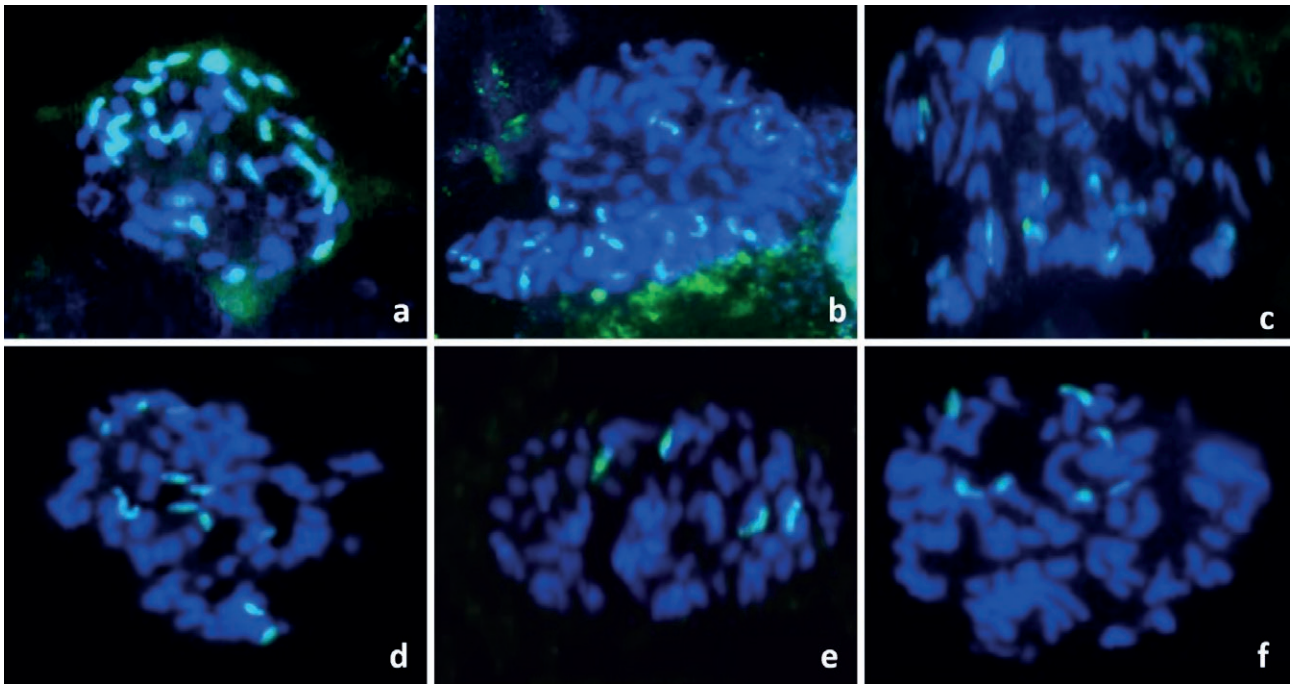

Figure 3. Genomic *in situ* hybridization with *E. arundinaceus* probe: a) *E. arundinaceus* x *S. spontaneum* hybrid, CYM 04-420, with 30 *E. arundinaceus* chromosomes, b) CYM 07-971 with 24 *E. arundinaceus* chromosomes, c) CYM 08-903 with 12 *E. arundinaceus* chromosomes, d) CYM 08-922 with 12 *E. arundinaceus* chromosomes, e) Co 15015 with four *E. arundinaceus* chromosomes, f) TWC- 82 with seven *E. arundinaceus* chromosomes.

naceus chromosomes from BC2 (CYM 08-903) was transmitted. Though there was difference in the number of *E. arundinaceus* chromosomes transmitted from female BC2 parents, the transmission pattern was n+n only with addition/deletion of few chromosomes.

During the nobilization of *S. officinarum* X *S. spontaneum* 2n+n chromosome segregation happened in the early generations like F1 and BC1. Whereas in the nobilization with *E. arundinaceus* 2n+n segregation happened during later stages and this slows down the progress of nobilization. In order to develop BC4 progenies the BC3 progeny, Co 15015, crossed with another improved Co cane, Co 11012. Cytological analysis of the four BC4 progeny revealed plants with a total chromosome compliment ranging from 107-109 chromosomes. GISH analysis revealed that out of these four BC4 progeny only one clone was having 2 *E. arundinaceus* chromosomes whereas three clones were not having any *Erianthus* chromosomes. In the parallel back crossing programme TWC 82 (BC3) crossed with an interspecific hybrid and four BC4 progeny were generated. The 2n chromosome number ranged from *Saccharum* spp. and 3-5 from *E. arundinaceus* respectively (Fig. 4).

Interspecific hybridization or intervarietal hybridization providing frequent utilization of limited number of parental clones resulted in the narrow genetic base of modern sugarcane cultivars and subsequently showing susceptibility to biotic and abiotic stresses. It has become necessary to include wild relatives of *Saccharum* in breeding programme to broaden the genetic diversity for increased productivity and better adaptability. As one of the most important wild relatives of sugarcane, *E. arundinaceus* has agronomically important genes for sugarcane breeding. At ICAR-Sugarcane breeding Institute we are regularly utilizing *E. arundinaceus* in breeding programmes and a series of genuine progeny have been developed in different back crossed generations.

Generally, the cytological methods and molecular markers are widely used to specifically detect the alien chromosomes and chromosome segments in the putative back cross progenies. It is found that Genomic *in situ* hybridization (GISH) is a powerful cytological tool for identifying the introgression pattern of alien chromosomes in sugarcane background. This study clearly indicates the number of back cross generations a breeder has to be developed to incorporate the alien chromosomes. In our study we found that in the BC4 progeny from a cross Co 15015 x Co 11012 only one hybrid was with two *Erianthus* chromosomes whereas the other progenies were without *E. arundinaceus* chromosomes. Hence

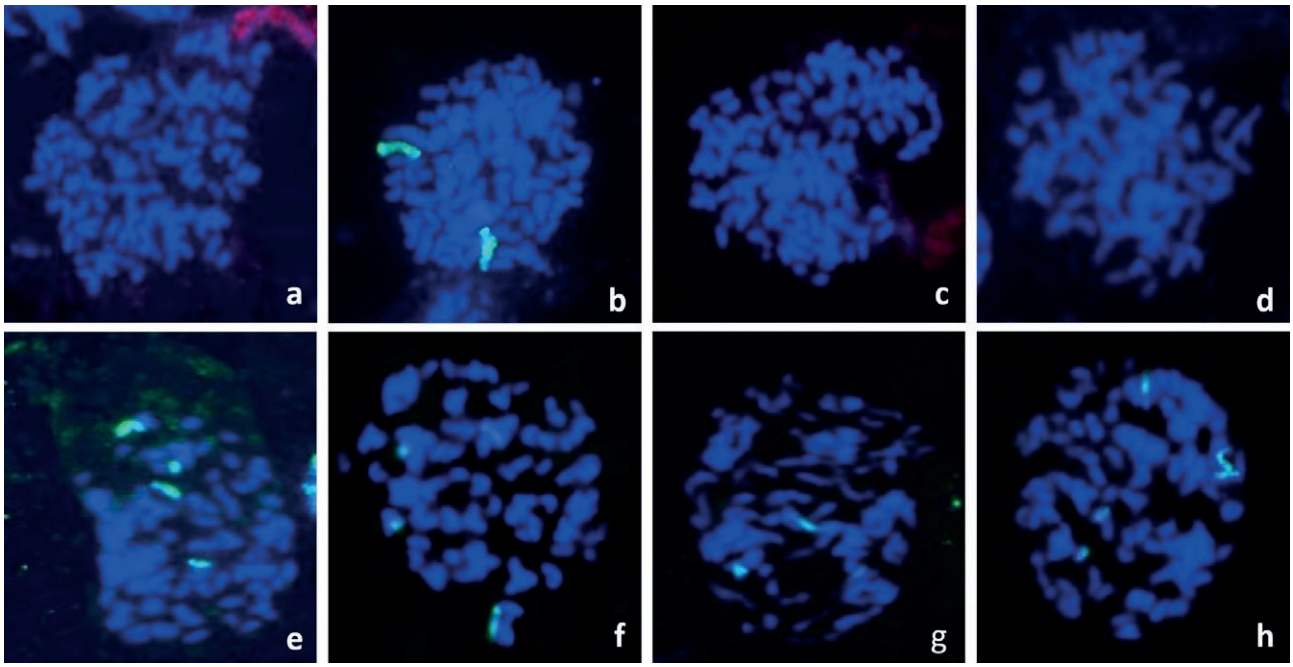

Figure 4. Genomic *in situ* hybridization with *E. arundinaceus* probe in 5th generation hybrids: a) GI 18-1 – Nil *E. arundinaceus*, b) GI 18-2 with two *E. arundinaceus* chromosomes c) GI 18-3 – Nil *E. arundinaceus*, d) GI-18-4 – Nil *E. arundinaceus*, e) FWC-2 with four *E. arundinaceus* chromosomes f) FWC-28 with *four E. arundinaceus* chromosomes g) FWC-29 with three *E. arundinaceus* chromosomes g) FWC-29 with three *E. arundinaceus* chromosomes.

this is the stage where the introgression breeding can be stopped as further transmission of *Erianthus* chromosomes is not possible in successive generations. Whereas in the parallel cross BC4 progenies from TWC 82 x ISH hybrid 3-5 *E. arundinaceus* chromosomes were there in which we can go for one more back crossing to get improved clone with minimum *Erianthus* chromosomes.

The agronomic performance of the backcross hybrids involving *Erianthus* for cane yield quality and red rot resistance is presented in the Table 2. Three hybrids recorded significantly higher cane height than the commercial hybrid Co 86032 (225.0 cm). The sucrose in juice ranged from 8.44% in TWC 82 to 19.98% in Co 15015. Three hybrids recorded significantly higher yield than the commercial check Co 86032 (121.8 t/ha). For red rot resistance, eight were moderately resistant and only one was susceptible. The clones were also screened for water stress during 2021-22. The results showed that the commercial check had a stress tolerance index of 0.761 and five clones recorded significantly higher STI (Table 3). The hybrid TWC 82 recorded the highest STI of 1.678 followed by FWC-2. The entry TWC combined both red rot resistance and water stress tolerance. The juice quality of the hybrids showed significantly lower than commercial check Co 86032 and only one Co 15015 had 19.98% of juice sucrose. Further backcrossing with commercial clones with high juice quality would further improve both juice quality and cane traits. Similarly, Nair et al. 2017 reported backcrossing of *E. procerus* hybrids with commercial varieties to obtain commercially acceptable levels of agronomic traits.

Intergeneric hybrid population between *Saccharum* spp. and *E. arundinaceus* often resulted in false hybrids due to selfing. In order to avoid this, it is highly encouraged to integrate efficient molecular markers with GISH or FISH. Deng *et al.* (2002) used isozyme markers because of similar banding pattern could not identify the genuine hybrids. Later 5Sr marker used to identify the true hybrid progeny with *Erianthus* specific 5SrDNA sequences. It was found that amplification was not obtained beyond BC2 generation. As 5Sr DNA had one locus per set of chromosomes it presents only on a few chromosomes in each genome. Due to unequal segregation of *Erianthus* chromosomes and also its elimination at different stages the advanced back cross progenies may not inherit the chromosomes that carry the 5SrDNA loci. Hence *Erianthus* specific 5Sr DNA sequences may not be reliable for the identification of true hybrid progeny. The *Erianthus* specific Tandem Repeat sequence (ESTR) reported by Yang *et al.* (2019) was used as a marker to confirm the hybridity of back cross progeny. In our study true intergeneric hybrids between *Saccha-*

Table 2. Performance of Backcross hybris involving *Erianthus* for cane yield, juice quality traits and red rot resistance.

	Clone Name	Cane Ht (cm)	Cane dia (cm)	SCW (Kgs)	Brix (%)	Pol (%)	Purity (%)	CCS %	NMC ('000/ha)	Cane yield (t/ha)	RR
1	CYM 07-971	210.00	2.61	1.09	14.72	12.06	81.93	8.03	89.00	96.71	MR
2	CYM 08-903	205.00	2.91	1.20	19.07	16.94	88.83	11.74	75.00	89.75	MR
3	CYM 08-922	255.00	2.75	1.38	14.89	12.09	81.20	8.01	101.50	140.07	MS
4	Co 15015	240.00	2.80	1.25	21.63	19.98	92.37	14.10	88.10	110.13	MR
5	TWC 82	265.00	2.95	1.68	11.88	8.44	71.04	5.16	98.30	165.14	MR
6	GI 18-1	220.00	2.46	0.82	19.67	17.60	89.48	12.24	85.00	69.98	MR
7	GI 18-2	235.00	2.57	1.15	15.61	13.17	84.37	8.90	89.00	102.35	MS
8	GI 18-3	235.00	2.71	1.22	19.41	17.11	88.15	11.82	91.50	111.63	MR
9	FWC-28	275.00	2.67	1.15	16.19	13.66	84.37	9.23	94.44	108.61	MS
10	FWC-29	205.00	2.83	1.23	15.47	13.28	85.84	9.05	86.11	105.92	MR
11	FWC-39	255.00	2.51	1.25	15.85	13.48	85.05	9.15	60.19	75.23	MR
12	FWC-2	235.00	2.65	1.45	13.51	10.51	77.79	6.80	100.00	145.00	S
	Co 86032	225.00	2.75	1.45	19.91	17.79	89.35	12.37	84.00	121.80	MS
	CD (P>0.05)	16.23	0.32	0.18	1.12	1.05	4.56	0.98	9.56	11.36	

Table 3. Stress tolerance Index (STI) of Backcross hybris involving Erianthus.

Sl.No.	Clone	Cane yield (t/ha)		STI
		Control	Stress	
1	CYM 07-971	96.71	72.3	0.558
2	CYM 08-903	89.75	68.5	0.490
3	CYM 08-922	140.07	115.5	1.290
4	Co 15015	110.13	75.34	0.662
5	TWC 82	165.14	127.35	1.678
6	GI 18-1	69.98	52.2	0.291
7	FWC-28	108.61	82.3	0.713
8	FWC-29	105.92	78.3	0.662
9	FWC-39	75.23	48.75	0.293
10	FWC-2	145.00	117.35	1.357
11	Co 86032	121.80	78.35	0.761
12	Co 06022	127.41	89.35	0.908
13	CoM 0265	126.00	86.54	0.870
14	Co 775	85.80	37.3	0.255
	Overall mean	111.97	80.67	0.771
	Treatments (P>0.05)	9.85		
	Clones (P>0.05)	16.34		0.34

rum spp. and *E. arundinaceus* could be rapidly identified using PCR with *Erianthus* Specific Tandem repeat primer pair (Fig. 5). It was found that PCR detection results highly coincides with GISH results.

Due to the genetic distance between the two genera the chromosome pairing and chiasma formation during meiosis is not taking place in intergeneric hybrids of *Saccharum* and *Erianthus*. From our study it has revealed that *E. arundinaceus* genome introgressed into *Saccharum* as whole chromosome by traditional breeding. The approaches like QTL mapping and marker assisted breeding in the advanced generations of back crosses (BC3 and BC4) will help to determine the agronomic value of individual *E. arundinaceus* chromosomes. Though *E. arundinaceus* clones are with many desirable agronomic traits for sugarcane genetic improvement. We have limited knowledge on the complex genome of this hexaploid species. Development and determination of *Saccharum – Erianthus* introgression lines with one or two *E. arundinaceus* chromosomes is a necessary step to simplify the genome analysis by dissecting out the alien chromosomes. In this study we identify a clone, GI 18-2, with two *Erianthus* chromosomes that can be segregated to much lower level in the next generation. In these population identifying genuine hybrid clones with 1-2 *E. arundinaceus* chromosomes without any recombination or translocation using GISH could be used for dissecting out and sequencing these alien chromosomes.

ACKNOWLEDGEMENTS

The authors are grateful to the Director, ICAR-Sugarcane Breeding Institute, Coimbatore, India, for the encouragement and providing facilities to conduct the study. The authors also acknowledge the funding support of the project (EEQ/2019/000124) awarded by the Science and Engineering Research Board (SERB), Department of Science and Technology, New Delhi. India.

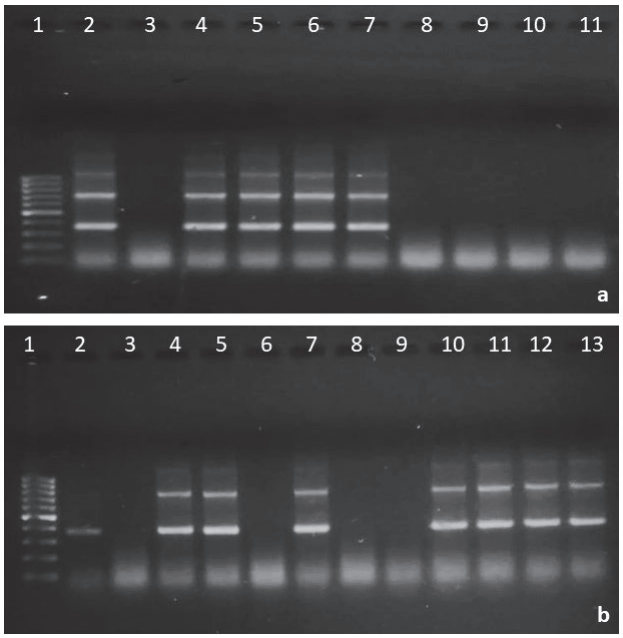

Figure 5. a) Electrophoretogram of F1, BC1 and BC2 progenies with their parents for amplification of ESTR primer in genomic DNA: 1) 100bp ladder, 2) IK 76-62 (Female parent). 3) Iritty-2 (Male parent), 4) CYM 04-420, 5) CYM 07-971, 6) CYM 08-903, 7) CYM 08-922, 8) Co 775, 9) CoC 671, 10) Co 94008, 11) Bo 91. b) Electrophoretogram of BC3 and BC4 progenies for amplification of ESTR primer in genomic DNA: 1) 100bp ladder, 2) IK 76-62 (Female parent). 3) Iritty-2 (Male parent), 4) TWC 82, 5) Co 15015, 6) GI 18-1, 7) GI 18-2, 80 GI 18-3, 9) GI 18-4, 10) FWC-2, 11) FWC-28, 12) FWC-29, 13) FWC-39

REFERENCES

Besse P, McIntyre CL, Burner DM, de Almeida CG. 1997. Using genomic slot blot hybridization to assess intergeneric *Saccharum* x *Erianthus* hybrids (*Andropogoneae—Saccharinae*). Genome 40 (4): 428–432. https://doi.org/10.1139/g97-057

Bremer G. 1961. Problems in breeding and cytology of sugar cane. Euphytica 1: 59-78.

Cai Q, Aitken KS, Fan FH, Piperidis G, Jackson P, McIntyre CL. 2005. A preliminary assessment of the genetic relationship between *Erianthus rockii* and the "*Saccharum* complex" using microsatellite (SSR) and AFLP markers. Plant. Sci. 169 (5): 976-984. https://doi.org/10.1016/j.plantsci.2005.07.002

D'Hont A, Rao P, Feldmann P, Grivet L, Islam-Faridi N, Taylor P, Glaszmann, JC. 1995. Identification and characterization of sugarcane intergeneric hybrids, *Saccharum officinarum* x *Erianthus arundinaceus*, with molecular markers and DNA *in situ* hybridization. Theor. Appl. Genet. 91 (2), 320–326. https://doi.org/10.1007/BF00220894

Daniels J, Smith P, Paton N, Williams CA. 1975. The origin of the genus *Saccharum*. *Sugarcane Breed. Newsl.* 36, 24–39.

Deng HH, Lia ZZ, Li QW, Lao FY, Fu C, Chen XW, Zhang CM, Liu SM, Yang YH. 2002. Breeding and isozyme marker assisted selection of F2 hybrids from *Saccharum* spp. x *Erianthus arundinaceus*. Sugarcane and Canesugar 1: 1–5.

Doyle JJ, Doyle JL. 1990. Isolation of plant DNA from fresh tissue. *Focus* 12, 13–15.

Hemaprabha G, Mohanraj K, Jackson P, Lakshmanan P, Ali GS, Li AM, Huang DL, Ram B. 2022. Sugarcane genetic diversity and major germplasm collections. Sugar Technol. , 24: 279– 29. https://doi.org/10.1007/s12355-021-01084-1

Huang Y, Wu J, Wang P, Lin Y, Fu C, Deng Z, Wang Q, Li Q, Chen R' Zhang M. 2015. Characterization of chromosome inheritance of the intergeneric BC2 and BC3 progeny between *Saccharum* spp. and *E. arundinaceus*. *PLoS ONE* 10: e0133722. https://doi.org/10.1371/journal.pone.0133722

Lekshmi M, Pazhany AS, Sobhakumari VP, Premachandran MN. 2017. Nuclear and cytoplasmic contributions from *Erianthus arundinaceus* (Retz.) Jeswiet in a sugarcane hybrid clone confirmed through genomic *in situ* hybridization and cytoplasmic DNA polymorphism. Genet. Resour. Crop EvoI. 64: 1553–1560. https://doi.org/10.1007/s10722-016-0453-5

Mohanraj D, Padmanaban P. Viswanathan R. Alexandar, KC. 1997. Sugarcane screening for red rot resistance. Sugar Cane 3: 18–23.

Mukherjee SK. 1957. Origin and distribution of *Saccharum*. Bot. Gaz. 119: 55–61.

Nair KN, Mohanraj K, Sundaravelpandian K, Suganya A, Selvi A, Appunu C. 2017. Characterization of an intergeneric hybrid of *Erianthus procerus* × *Saccharum officinarum* and its backcross progenies. Euphytica 213: https://doi.org/10.1007/s10681-017-2053-7

Narayanaswami S. 1940. Megasporogenesis and the origin of triploids in *Saccharum*. Indian J. Agric. Sci. 10: 534.

Piperidis G, Christopher MJ, Carroll BJ, Berding N. D'Hont. 2000. A. Molecular contribution to selection of intergeneric hybrids between sugarcane and the wild species *Erianthus arundinaceus*. *Genome* 43 (6): 1033–1037. https://doi.org/10.1139/gen-43-6-1033

Piperidis N, Chen J, Deng H, Wang L, Jackson P, Piperidis G. 2010. GISH characterization of *Erianthus arundinaceus* chromosomes in three generations of sugarcane intergeneric hybrids. *Genome* 53 (5): 331–336. https://doi.org/10.1139/g10-010

Premachandran MN, Sobhakumari VP, Lekshmi M, Raffee Viola V. 2017. Genome characterization of *in vitro*

induced amphiploids of an intergeneric hybrid *Erianthus arundinaceus* X *Saccharum spontaneum*. Sugar Tech. 19: 386–393. https://doi.org/10.1007/s12355-016-0482-6

Roach BT. 1989. Origin and improvement of the genetic base of sugarcane. In proceedings of the Australian Society of sugar cane technologists, Brisbane. 35-47.

Sobhakumari VP, Asmita, D. 2014. Cytogenetics and performance analysis of pre-breeding hybrids of *Saccharum officinarum* and S*accharum spontaneum*. J. Sugarcane Res. 4 (1), 33–39.

Wu J, Huang Y, Lin Y, Fu C, Liu S, Deng Z, Li Q, Huang Z, Chen R, Zhang R. 2014. Unexpected inheritance pattern of Erianthus arundinaceus chromosomes in the intergeneric progeny between *Saccharum* spp. and *Erianthus arundinaceus*. *PLoS ONE* 9, e110390. https://doi.org/10.1371/journal.pone.0110390

Caryologia
International Journal of Cytology, Cytosystematics and Cytogenetics

Firenze University Press
https://riviste.fupress.net/index.php/caryologia

OPEN ACCESS

Citation: Jha, T.B., Halder, M. & Bhowmick, B.K. (2024). Giemsa-based chromosome staining and comparative fluorescent banding pattern in five valuable Indian plant species. *Caryologia* 77(3): 37-45. doi: 10.36253/caryologia-3007

Received: Sep 26, 2024

Accepted: Sep 29, 2024

Published: March 25, 2025

Data Availability Statement: All relevant data are within the paper and its Supporting Information files.

Competing Interests: The Author(s) declare(s) no conflict of interest.

ORCID
TBJ: 0000-0003-0900-8167
MH: 0000-0002-8422-0814
BKB: 0000-0001-6029-1098

Giemsa-based chromosome staining and comparative fluorescent banding pattern in five valuable Indian plant species

Timir Baran Jha[1,*], Mihir Halder[2], Biplab Kumar Bhowmick[3]

[1] *Department of Botany, Maulana Azad College, Rafi Ahmed Kidwi Road, Kolkata-700013, West Bengal, India*
[2] *Department of Botany, Barasat Government College, 10 KNC Road, Barasat, Kolkata-700124, West Bengal, India*
[3] *Department of Botany, Scottish Church College, 1 & 3, Urquhart Square, Manicktala, Azad Hind Bag, Kolkata-700006, West Bengal, India*
*Corresponding author. E-mail: tbjha2000@yahoo.co.in

Abstract. This study presents repeatable enzymatic maceration and air drying (EMA)-based chromosome preparation methods in five valuable Indian plant species namely *Allium cepa*, *Allium sativum*, *Nigella sativa*, *Trigonella foenum-graecum*, and *Aloe vera*. Comparative fluorescent banding studies with two DNA base-specific fluorescent dyes have precisely unraveled the number, position, and patterns of secondary constriction of each species. Additionally, it has highlighted the fluorescent banding pattern of repetitive DNA sequences notably on two important constitutive heterochromatic sites like secondary and primary constrictions. The study has established that EMA-based fluorescent banding can provide valuable complementary information for modern genomics. The results are expected to enrich our knowledge of chromosome biology and crop genomics and inspire future academic and research endeavours.

Keywords: CMA-DAPI banding, Giemsa staining, *Allium cepa* and *Allium sativum, Aloe vera, Nigella sativa, Trigonella foenum-graecum*.

INTRODUCTION

Plants have been serving humanity for centuries. They rely on their species-specific chromosomes not just to carry genetic information, but also for their precise maintenance, management, and transmission (Flavell 2021). Therefore, analyzing and conserving genetic diversity to safeguard their adaptive potential is crucial for valuable populations of wild and domesticated species (Ainsworth 2022) in the era of climatic changes.

Classical cytogenetics has provided foundational information on plant chromosomes for many decades (Guerra 2008; Razumova et al. 2023) in a cost-effective manner. On the other hand, molecular cytogenetics has opened the door to unraveling genetic diversity not only on precise chromosomal morphology but also on the chromosomal DNA composition of

each population and species. Molecular cytogenetics has greatly benefited from the advancement of molecular biology, revealing that chromosomes contain low-copy regulatory gene sequences, while large chunks of DNA are composed of diverse repetitive DNA sequences throughout the length of the chromosomes (Liehr 2021). Some repetitive sequences are well conserved between species, while others define differences even between closely related species. In the 1970s, the introduction of the enzymatic maceration and air-drying (EMA) protocol for plant chromosome preparation (Kurata and Omura 1978), followed by Giemsa staining, and the subsequent application of DNA base-specific fluorochromes in plant chromosome research have helped in individual chromosome identification. These advancements have allowed a profound revision of the structure and function of repetitive DNA patterns in nucleolar organizing regions (NORs), centromeric, subtelomeric, and telomeric regions in many plant species (Fukui et al. 1996; Moscone et al. 1996; Hizume 2015; Jha and Halder 2016; Yamamoto et al. 2019; Jha et al. 2021; Jha and Halder 2023).

Keeping in mind the above-noted considerations the present studies have standardized the EMA-based protocol for chromosome preparation in some valuable Indian species and populations of *Allium cepa* L. (Amaryllidaceae), *Allium sativum* L. (Amaryllidaceae), *Nigella sativa* L. (Ranunculaceae), *Trigonella foenum-graecum* L. (Fabaceae), and *Aloe vera* (L.) Burm. f. (Asphodelaceae). All of these plant species are highly valued for both daily consumption and medicinal purposes. Detailed and comparative chromosomal analysis has been carried out using non-fluorescent Giemsa and two contrasting fluorochromes DAPI (4'-6-diamidino-2-phenylindole) and CMA (chromomycin A3 -CMA) staining. The standardized and repeatable protocol effectively produced numerous cytoplasm-free metaphases and subsequent staining with non-fluorescent and fluorescent dyes, precisely detailed their morphology, and number and positions of secondary constrictions. Additionally, it has highlighted the fluorescent banding pattern of repetitive DNA sequences notably on two important constitutive heterochromatic sites, secondary and primary constrictions. The results of this study are expected to instil interest in students, researchers, and breeders in their future academic and research endeavours, as well as conserve and explore the unique genetic diversity found in other family members of the studied materials.

MATERIAL AND METHODS

Plant materials

The bulbs of two commercially available *Allium* species, *Allium cepa* L. and *Allium sativum* L., were collected and grown in wet sand for 48 hours in the dark. The plants of *Aloe vera* (L.) Burm. f were obtained from a local nursery in Kolkata, West Bengal and grown in the medicinal garden of the Maulana Azad College. The healthy roots of *A. vera* were directly harvested from potted plants. Seeds of *Trigonella foenum-graecum* L. were obtained from the local market, while seeds of *Nigella sativa* L. were collected from a farmer's field in North 24 Parganas, West Bengal, and stored at 4°C. At least 20 seeds of each species were soaked overnight in water, then placed on moist filter paper and kept in the dark at temperatures between 16-22°C for germination. Experimental materials were used several times to harvest roots for chromosome analysis.

Chromosome preparation by enzymatic maceration and air-drying protocol

To standardize the chromosome preparation using the EMA protocol, a minimum of ten healthy root tips measuring 0.7-1 cm in length were collected from germinating seeds, bulbs, or potted plants. Root tips of *A. cepa, A. sativum* and *A. vera* were treated with a saturated solution of Para Dichlorobenzene (PDB), *Trigonella foenum-graecum* with PDB plus Aesculin and *Nigella sativa* with 0.5% Colchicine for 4-5 hours. Fixation was carried out with a 1:3 solution of acetic acid and methanol overnight and then stored at -20°C. The chromosome preparation was carried out following the EMA protocol established by Jha and Halder (2023), with some species-specific minor modifications.

Chromosome staining with Giemsa, DAPI and CMA

The air-dried slides of each species were stained with a phosphate buffer solution containing 2% Giemsa solution (Merck, Germany) for 10-15 minutes to achieve consistent, effective, and optimal staining. After staining, the slides were rinsed three to four times with distilled water air dried with a blower, and finally used for chromosome analysis under a Carl Zeiss compound microscope.

The best Giemsa-stained metaphase slides were destained in 70% methanol for 45 minutes, air-dried and subsequently re-stained with DAPI (0.1-0.2 μg mL^{-1} for 10-15 minutes) and CMA (0.1-0.8 mg mL^{-1} for 70-120 minutes), following Jha et al. (2021) with species-specific modifications.

Chromosome analysis, documentation, and ideogram preparation

A Carl Zeiss AxioLab A1 fluorescence microscope equipped with a CCD camera and computer software was used to examine, documentation, and karyotype analysis of cytoplasm-free metaphase chromosome preparations stained with Giemsa, DAPI, and CMA. Giemsa-stained slides were observed under bright field illumination, while DAPI- and CMA-stained slides were observed under a specific UV filter cassette using the Carl Zeiss Prog Res 2.3.3 software on a computer attached to the microscope. Images of metaphase chromosomes stained with Giemsa, DAPI, or CMA were captured with the help of a CCD camera for analysis.

More than 25 cytoplasm-free mitotic metaphases with well-spread chromosomes displaying distinct karyomorphometric features were chosen for each species. Documentation and measurement of karyomorphometric features such as the lengths of the long and short arms, the positions of the centromeres, the average chromosome length (ACL), the total chromatin length (TCL), and DAPI and CMA signals were performed using Axiovision L.E.4 software. At least five chromosome morphometric data for each species were considered for the calculation of ACL and TCL, and the data was expressed as the mean ± standard deviation (SD). Chromosome nomenclature was based on arm ratios (r = length of long arm/length of short arm) following Levan et al. (1964), and ideograms were prepared by evaluating morphometric data and organizing chromosome pairs in decreasing order of length.

RESULTS

The karyomorphological features of each plant species were determined from cytoplasm free well-spread mitotic metaphases and documented (Figures 1-4, and Table 1-2). Fluorescent staining with DAPI and CMA revealed distinct variability in banding patterns on the chromosomes (Figures 1, 3, Table 2). For the convenience of interpretation, based on the nature of the fluorescent banding pattern, chromosomes were categorized into eight types, namely, type A with CMA^{+ve} (positive) signal in the centromeric region, type B with $DAPI^{+ve}$ signal in the centromeric region, type C with CMA^{+ve} signal at two terminal regions of chromosome, type D with CMA^{+ve} signal at the secondary constriction region, type E with CMA^{+ve} signal at the satellite region and two terminal regions of chromosome, type F CMA^{0} (neutral) / $DAPI^{0}$ (neutral), type G with CMA^{+ve} signals at the centromeric region as well as at the secondary constriction region and type H with $DAPI^{+ve}$ signals at centromeric region and CMA^{+ve} signals in the secondary constriction region (Table 2). It was further confirmed that all CMA^{+ve} bands were $DAPI^{-ve}$ and the $DAPI^{+ve}$ bands were CMA^{-ve}. The unique karyotypes and fluorochrome banding patterns observed in each species are described as follows:

Allium cepa L. (Amaryllidaceae)

The karyotype in *Allium cepa* (2n=16), the age-old model plant material for chromosome studies, revealed the occurrence of five metacentric and three submetacentric pairs of long chromosomes (Fig. 1a-c, Fig. 2a,

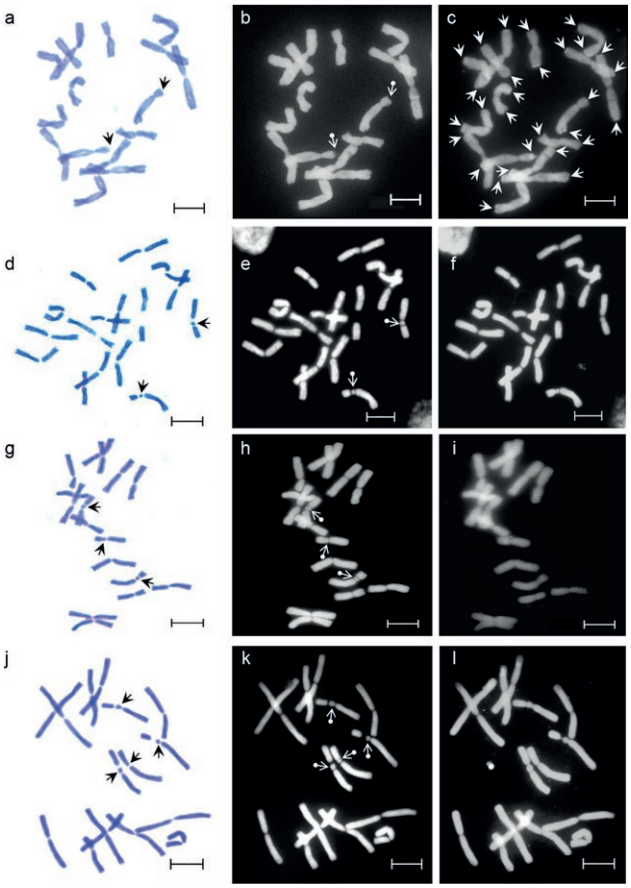

Figure 1. Somatic metaphase chromosomes of *Allium cepa* (2*n*=16) stained correspondingly with Giemsa **(a)**, DAPI **(b)** and CMA **(c)**; Somatic metaphase chromosomes of *Allium sativum* (2*n*=16) stained correspondingly with Giemsa **(d, g, j)**, DAPI **(e, h, k)** and CMA **(f, i, l)**. The positions of two (d-f), three (g-i) and four (j-l) secondary constrictions are indicated with black arrows in Giemsa-stained metaphases and corresponding DAPI negative signals are indicated with white arrows with round end in DAPI-stained metaphases. The positions of terminal CMA positive signals are indicated with white arrows in CMA-stained metaphases. Scale bars=10 μm.

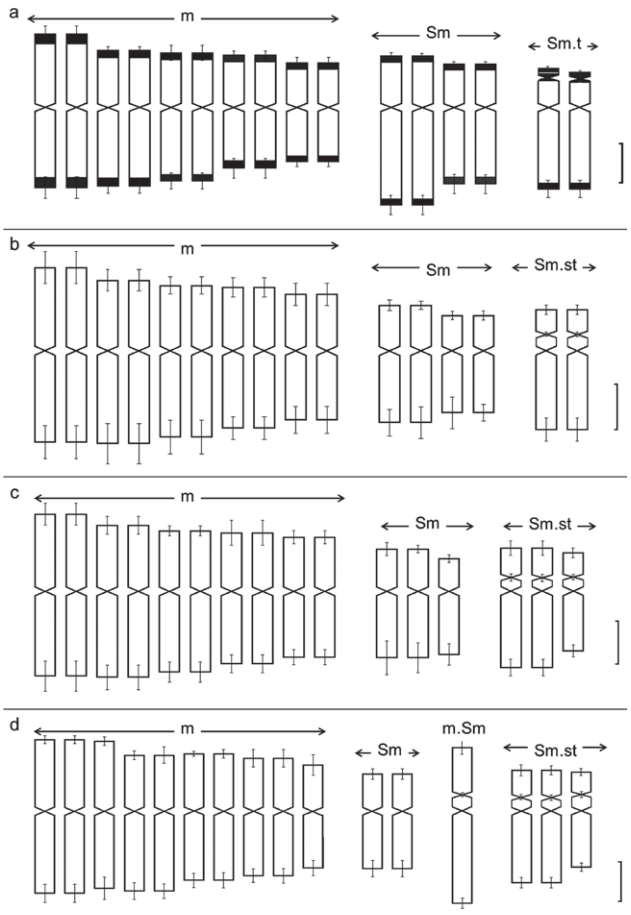

Figure 2. Somatic ideogram of *Allium cepa* (2*n*=16) with two secondary constriction-bearing chromosomes **(a)**; Somatic ideograms of *Allium sativum* (2*n*=16) with two **(b)**, three **(c)** and four **(d)** chromosomes with secondary constrictions. The positions of CMA-positive signals are indicated with black bands. Scale bars=5 μm.

Table 1). Out of three submetacentric pairs of chromosomes, the 6th pair of chromosomes bears the secondary constriction at terminal regions. Screening of over 25 metaphase plates stained with CMA fluorochrome confirmed bright CMA^{+ve} signals at the terminal regions of all chromosomes (Type C, Fig. 1c). Notably, CMA^{+ve} signal was also observed on the satellite of the 6th pair of chromosomes (Type E, Fig. 1c, 2a). Of the one pair of chromosomes with secondary constriction, one of the chromosomes showed a more intense CMA^{+ve} signal on the satellite than the other homologue (Fig. 1c), corresponding with the difference in the size of this satellite in Giemsa-stained chromosomes (Fig. 1a). On the other hand, no AT-specific $DAPI^{+ve}$ signal was observed in any of the chromosomes of this germplasm of *A. cepa* (Fig. 1b). The banding pattern of *A. cepa* thus remains 14C+ 2E with CMA^{+ve} and $DAPI^{-ve}$ signals (Table 2).

Allium sativum L. (Amaryllidaceae)

The studied germplasm of *Allium sativum* L. (Indian garlic) has 2*n* =16 chromosomes (Fig. 1d-l, Table 1), revealing three variant karyotypes with variable numbers (2-4) of chromosomes with secondary constrictions (Fig. 2b-d, Table 2). However, the position of secondary constriction was always interstitial (Fig. 1d-l). The modal karyotype of this species is 10m+4sm+2sm.st (Fig. 2b), with the 6th pair of submetacentric chromosomes exhibiting a secondary constriction region (Fig. 1d). In addition, we have noted three chromosomes with secondary constrictions, i.e. on the 6th pair of both homologous chromosomes plus one chromosome of the 8th pair (Fig. 2c) in some metaphases. Moreover, very few metaphase plates also showed four chromosomes with secondary

Table 1. Karyomorphometric data in the five valuable Indian plant species.

Species (Diploid chromosome number)	CSR in μm (mean±SD)	ACL in μm (Mean±SD)	TCL in μm (mean±SD)	Number of SAT chromosomes (pair number length-wise)	Position of satellite	Diploid Karyotype
Allium cepa (2*n*=16)	10.9±1.20-19.34±2.66	16.93±2.64	241.09±9.85	2 (6th)	T	10m+4sm+2sm.t
Allium sativum (2*n*=16)	8.46±0.71-19.67±2.93	13.54±1.81	224.18±5.85	2 (6th)	I	10m+4sm+2sm.st
				3 (6th, 8th)	I	10m+3sm+3sm.st
				4 (6th, 8th, 1st)	I	10m+2sm+3sm.st+1m.sm
Nigella sativa (2*n*=12)	7.29±0.65-16.64±2.09	13.54±1.81	159.0.9±18.06	6 (2nd, 3rd, 6th)	I	6m+4m.t+2t.sat
Trigonella foenum-graecum (2*n*=16)	8.85±0.76-12.21±1.25	10.34±1.17	165.52±18.42	4 (2nd, 4th)	I	2m+4sm+6st+2m.sm+2m.st
Aloe vera (2*n*=14)	8.52±0.60-30.75±1.08	21.13±10.12	295.86±10.72	4 (1st, 3rd)	T	4st+6sm+4sm.t

CSR: Chromosome size range (range of absolute length of shortest to longest chromosome), ACL: Average length of chromosomes, TCL: Total diploid chromosome length, SAT: Satellite bearing chromosomes, T: Terminal, and I: Interstitial.

constrictions, i.e. on the 6th pair of submedian homologous chromosomes, on one of the 8th pair of submedian chromosomes, and one on the 1st pair of metacentric chromosomes (Fig. 2d; Table 1). Detection of satellite in two heteromorphic and non-homologous chromosomes, i.e., one submedian and one metacentric chromosome, was another interesting finding in this germplasm (Fig. 2d). Interestingly, different karyotype variants were not detected in different metaphases of the same root tip; they were detected in different root tips.

In *A. sativum*, none of the 16 chromosomes showed any CMA^{+ve} or $DAPI^{+ve}$ signals even after repeated trials with varying concentrations of fluorochromes and varying incubation periods. The banding pattern of *A. sativum* thus remains 16F i.e. CMA^{0} / $DAPI^{0}$ (Fig. 1e, f, h, i, k, l, 2b-d, Table 2).

Nigella sativa L. (Ranunculaceae)

The karyotype of *N. sativa* (2n=12) was characterized by one pair of distinctly short telocentric chromosomes and five pairs of long metacentric chromosomes (Fig. 3a-c, Table 1). The secondary constrictions were located on terminal regions of one pair of short chromosomes (6th) and two pairs (2nd and 3rd) of long chromosomes (Fig. 3a, Table 1). The modal karyotype of *N. sativa* was determined as 6m+4m.t+2t.sat (Fig. 4a, Table 1).

CMA-DAPI staining was performed on the same Giemsa-stained metaphase plates to confirm the existence of secondary constrictions in three chromosome pairs (Fig. 3b-c). The staining revealed intense CMA^{+ve} signals at secondary constriction regions that corresponded with $DAPI^{-ve}$ signals (Fig. 3b-c). No additional distinct DAPI/CMA positive/negative signals were found on any chromosomes (Fig. 3b-c) and the fluorochrome banding pattern was determined as 6D+6F (Fig. 4a, Table 2).

Trigonella foenum-graecum L. (Fabaceae)

In *T. foenum-graecum* (2n=16), we have identified the presence of interstitial secondary constrictions at the submetacentric and subtelocentric positions of the 2nd and 4th pairs of chromosomes, respectively (Fig. 3d-f, 4b). The modal karyotype was determined as 6st+4sm+2m+2m.sm+2m.st (Fig. 4b, Table 1). Fluorescent staining revealed very distinct and intense CMA^{+ve} and $DAPI^{-ve}$ signals in all chromosomes at the centromeric regions (Fig. 3e-f). Additionally, the interstitial secondary constriction region of the 2nd and 4th pair of chromosomes also showed CMA^{+ve} and $DAPI^{-ve}$ signals

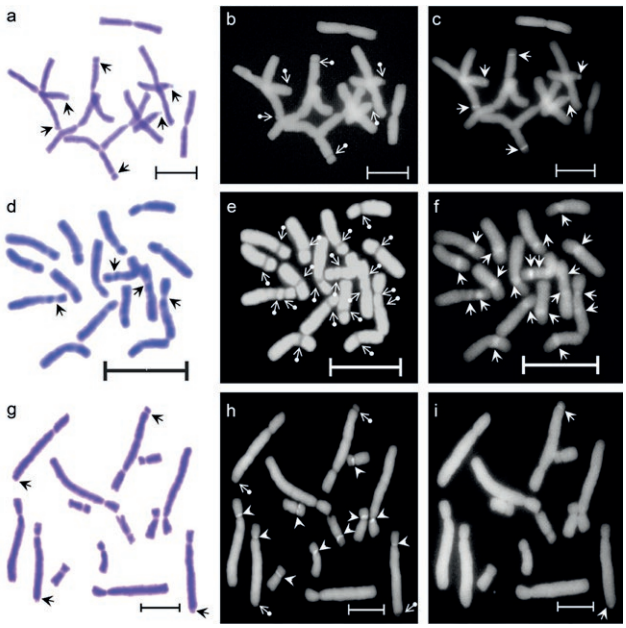

Figure 3. Somatic metaphase chromosomes of *Nigella sativa* (2*n*=12) stained correspondingly with Giemsa **(a)**, DAPI **(b)** and CMA **(c)**; Somatic metaphase chromosomes of *Trigonella foenum-graecum* (2*n*=16) stained correspondingly with Giemsa **(d)**, DAPI **(e)** and CMA **(f)**; Somatic metaphase chromosomes of *Aloe vera* (2*n*=14) stained correspondingly with Giemsa **(g)**, DAPI **(h)** and CMA **(i)**. The positions of secondary constrictions are indicated with black arrows in Giemsa-stained metaphases. DAPI-negative and centromeric DAPI-positive signals are indicated with white arrows with round end and white arrowheads, respectively in DAPI-stained metaphases. CMA-positive signals are indicated with white arrows in CMA-stained metaphases. Scale bars=10 μm.

(Fig. 3e, f, Table 2). The fluorescent banding pattern in *T. foenum-graecum* was 12A+4G (Fig. 4b, Table 2).

Aloe vera (L.) Burm. f. (Asphodelaceae)

The karyotype in *A. vera* (2n=14) consists of three pairs of small (8.52-11.30 μm) submetacentric chromosomes and four pairs of distinctly long (28.26-30.75 μm) chromosomes (Fig. 3g-i, Table 1). The primary constrictions of the long chromosomes were located at the submetacentric or subtelocentric positions, with secondary constrictions at the terminal region of the 1st and 3rd pairs of long chromosomes. (Fig. 3g-i, Table 1).

Fluorescence staining with different concentrations of DAPI and CMA enabled confirmation of chromosomes with secondary constrictions and additional heterochromatic bands in the karyotype. Very faint CMA^{+ve} signals could be seen in two to three chromosomes at their secondary constriction regions (Fig. 3i, Table 2),

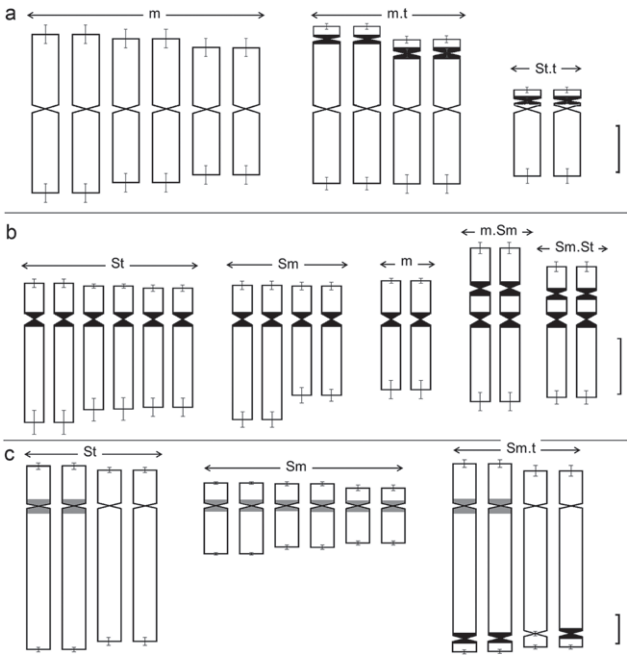

Figure 4. Somatic ideograms of (**a**) *Nigella sativa* (2*n*=12) with six secondary constriction-bearing chromosomes, (**b**) *Trigonella foenum-graecum* (2*n*=16) with four secondary constriction-bearing chromosomes, and (**c**) *Aloe vera* (2*n*=14) with four secondary constriction-bearing chromosomes. The positions of CMA-positive and DAPI-positive signals are indicated with black and grey bands, respectively. Scale bars=5 μm.

corresponding to DAPI^{-ve} signals (Fig. 3h). On the other hand, distinct and intense DAPI^{+ve} signals were scored in all six small chromosomes i.e. in the 5th, 6th and 7th pairs (Fig. 3h, Table 2) and four out of eight long chromosomes. Of these four long chromosomes, one pair had secondary constrictions, and the other was subtelocentric (Fig. 3h, 4c, Table 2). The distinctive CMA-DAPI banding pattern in *A. vera* was 8B+2H+3F+1D (Fig 4c, Table 2).

DISCUSSION

The current research has focused on standardizing chromosome processing using EMA-based preparation and a staining protocol that utilizes both fluorescent and non-fluorescent stains. The fluorescent banding in the species under study has revealed many new features, particularly in two important constitutive heterochromatic sites: secondary and primary constrictions. Both of these sites are considered to be evolutionarily conserved with diverse functions. There are very few comparative fluorescent banding studies available on seemingly common but highly valued plants.

In a standard karyotype of any plant species, the nucleolus organizer region (NOR) acts as a chromosomal marker for researchers and breeders. Guerra (2000) noted that secondary constriction regions are generally GC-rich and display CMA^{+ve} signals. The number and position of secondary constriction regions in the studied materials following the preparation of chromosomes through classical cytogenetics is still a topic of debate (Sato 1980, 1981; Agarwal 1983; Das et al. 2001; Ghosh and Dutta 2006; Das et al. 2011; Martin et al. 2011; Najafi et al. 2013; Shaker et al. 2017). The present investigation confirms the number and positions of secondary constrictions in all the studied species (Table

Table 2. Fluorescent banding patterns in the five valuable Indian plant species.

Species (diploid chromosome number)	Fluorescent banding patterns				Total number of fluorescent signals (CMA^{+ve} + DAPI^{-ve})	Banding pattern
	Chromosome number (p: pair/ s: single)	Position of the signals	Type of signals	Number of signals		
Allium cepa (2*n*=16)	1-8th (p)	Terminal region	CMA^{+}	32	34	14C+2E
	6th (p)	Satellite region	CMA^{+}	2		
Allium sativum (2*n*=16)	1st (s), 6th (p), 8th (s)	Secondary constriction region	CMA^{0} DAPI^{0}	Nil	Nil	16F
Nigella sativa (2*n*=12)	2nd, 3rd, 6th (p)	Secondary constriction region	CMA^{+}	6	6	6D+6F
Trigonella foenum-graecum (2*n*=16)	2nd, 4th (p)	Secondary constriction region	CMA^{+}	4	20	12A+4G
	1-8th (p)	Centromeric region	CMA^{+}	16		
Aloe vera (2*n*=14)	1st (p), 4-7th (p)	Centromeric region	DAPI^{+}	10	12-13	8B+2H+3F+1D
	1st (p), 3rd (s)	Secondary constriction region	faint CMA^{+}	2-3		

Fluorescent banding types- A: CMA-positive centromeric region, B: DAPI-positive centromeric region, C: CMA-positive terminal regions, D: CMA-positive secondary constriction region, E: CMA-positive terminal and secondary constriction regions, F: CMA- neutral and DAPI-neutral, G: CMA-positive centromeric and secondary constriction regions, H: DAPI-positive centromeric region and CMA-positive secondary constriction region.

1). In *Allium cepa* and *Allium sativum*, distinct differences in the number of chromosomes bearing secondary constrictions and fluorescent banding patterns were noted. In *A. cepa*, we scored 34 CMA^{+ve} signals including a pair of chromosomes with a CMA^{+ve} satellite region (Fig. 1b-c, Table 2). In this Indian germplasm, we report heteromorphy concerning $CMA^{+ve}/DAPI^{-ve}$ (GC-rich) band intensity or size in the 6th pair of chromosomes with satellite. Our results conform to Cortes et al. (1983) and Mancia et al. (2015) who have reported terminal bands in all the chromosomes of *A. cepa* through their C-banding and dual colour FISH studies, respectively.

The genus *Allium* has a history of possible chromosome rearrangements related to the distal and interstitial location of NORs in subgenera *Cepa* and *Allium*, respectively (Bhowmick et al. 2023). Numerical variations of secondary constrictions (2-6) have been reported in *A. sativum* (Sato et al. 1980; Cortes et al. 1983; Wajahatullah and Vahidy 1990). But for the first time, we report two to four interstitial secondary constrictions (Fig. 1d-l, Fig. 2b-d) in the Indian germplasm. In *A. sativum*, no CMA and DAPI-positive bands were observed in any chromosomes. It has been reported that chromosomal CMA bands are generally limited for *A. sativum* (Maragheh et al. 2019; Bacelar et al. 2021). However, C-bands were reported in some chromosome pairs of *A. sativum* (Cortes et al. 1983; Yuzbasioglu 2004). The atypical DNA banding pattern in general especially of the secondary constriction regions in *A. sativum* warrants further molecular analyses to unravel the structural complexity and uniqueness.

The use of EMA-based chromosome processing and differential staining has confirmed the presence of three pairs of secondary constrictions for the first time in *Nigella sativa*. Our findings are consistent with the 45S rDNA-loci analysis conducted by Orooji et al. (2022) in a different germplasm of *N. sativa*. However, the observed variation in CMA staining intensity in the NOR regions needs to be addressed in the future at the DNA sequence level. While, in *Trigonella foenum-graecum*, fluorescent banding studies confirmed the presence of two pairs of interstitial secondary constrictions on the 2nd and 4th chromosome pairs. Similar results have been observed in other germplasms through fluorescent banding and rDNA hybridization studies (Ahmad et al. 1999; Santra et al. 2023). Fluorescent banding studies in *Aloe vera* reveal secondary constrictions at the terminal region of 1st and 3rd pairs of long chromosomes (Table 2). However, $CMA^{+ve}/DAPI^{-ve}$ signals were obtained distinctly in one pair of secondary constricted chromosomes and the other pair remains indistinct and difficult to determine in many metaphases. Adams et al. (2000) reported variability in rDNA sites within the genus *Aloe* and reported three pairs of rDNA sites in *A. vera*.

In comparative studies of centromeric sites, three types of DNA sequence organization have been observed in the studied species: $CMA^{+ve}/DAPI^{-ve}$ (GC rich), $DAPI^{+ve}/CMA^{-ve}$ (AT-rich), and $CMA^{0}/DAPI^{0}$ (GC-AT neutral). CMA^{+ve} centromeric sites have not been reported in many plant species. Mondin et al. (2011) reported it in *Crotalaria juncea* (2n=16). Than et al. (2017) reported CMA^{+ve} centromeric sites in all the chromosomes of *Swertia nervosa* (2n=26), only in one pair in *S. chirayita* (2n=26), but not a single centromeric region of *S. bimaculata* (2n=26) chromosomes. In *Trigonella*, intense CMA^{+ve} signals have been found in the centromeric regions of all chromosomes in the present study. A similar report has been published by Santra et al. (2023) in *Trigonella*. Further fluorescent banding studies in different plant species are required to unravel DNA sequence patterns. Further fluorescent banding studies in *Trigonella* species and populations are equally necessary to confirm whether the CMA^{+ve} GC-rich centromeric nature is global or local in *Trigonella*.

On the other hand, a well-established bimodal karyotype in *Aloe vera* with eight long and six small chromosomes (2n=14) showing unique $DAPI^{+ve}/CMA^{-ve}$ fluorescent banding patterns in all six small and four long chromosomes is reported for the first time in this species. It is recognized that the centromere in every eukaryotic chromosome is a multifunctional dynamic complex. Despite mediating the evolutionarily conserved function of directing chromosome segregation, they show surprising diversity in their DNA sequence organisation (Tong et al. 2019; Barbosa et al. 2022). DNA sequence analysis in rice, maize, and *Arabidopsis* has shown that centromeres are composed of highly repetitive DNA sequences with considerable size variation and sequence divergence (Ma et al. 2007) but rarely has it been characterized as GC- or AT-rich or GC–AT neutral regions. On the other hand, the fluorescent banding patterns directly observed on the metaphases in highly conserved centromeric sites of *Trigonella, Aloe, Nigella* and *Allium* revealed their contrasting species and even chromosome-specific DNA divergence and necessitate further fluorescent banding and DNA sequencing studies in the future. We encourage further analysis of fluorescent banding in other plant species to gain a better understanding of the nature of DNA organization in secondary and centromeric regions. We hope that our findings will inspire researchers and scientists to come up with new ideas for studying chromosomes in plants.

CONCLUSION

The use of a repeatable EMA-based protocol for comparative fluorescent banding can be applied to any plant species with minor modifications. Recent studies on five common but valuable plant species have provided interesting and thought-provoking information on the nature of repetitive DNA sequences in two constitutive heterochromatin sites directly on the metaphase plates. The research has shown that EMA-based fluorescent banding can offer valuable complementary information for modern genomics. The results are expected to enhance our understanding of chromosome biology and crop genomics and to inspire future academic and research endeavours.

ACKNOWLEDGEMENTS

In honour of his mentor and teacher, the late Prof. A. K. Sharma, TBJ dedicates this paper to his birth centenary year. He would like to acknowledge Dr S. Dutta, the Principal, and Dr D. Mukhopadhya, the Head of the Department of Botany at Maulana Azad College, for providing basic facilities. MH expresses gratitude to the Principal of Barasat Government College, Kolkata, for his active support and encouragement in research activities. BKB is thankful to the Principal of Scottish Church College for encouraging research activities.

REFERENCES

Adams SP, Leitch IJ, Bennett MD, Chase MW, Leitch AR. 2000. Ribosomal DNA evolution and phylogeny in *Aloe* (Asphodelaceae). Ame J Bot. 87(11): 1578–1583.

Agarwal K. 1983. Cytological studies in the genus *Trigonella* Linn. Cytologia 48(4):771–779. https://doi.org/10.1508/cytologia.48.771

Ahmad F, Acharya SN, Mir Z, Mir PS. 1999. Localization and activity of rRNA genes on fenugreek (*Trigonella foenum-graecum* L.) chromosomes by fluorescent in situ hybridization and silver staining. Theor Appl Genet. 98:179–185. https://doi.org/10.1007/s001220051056

Ainsworth D. 2022. UN convention on biological diversity (COP 15) held in Montreal Canada.

Bacelar PAA, Feitoza LL, Valente SES, Gomes RLF, Martins LV, Almeida PM, Silva VB, Lopes ACA, Carvalh R, Peron AP. 2021. Variations in heterochromatin content reveal important polymorphisms for studies of genetic improvement in garlic (*Allium sativum* L.). Braz J Biol. 83: e243514. https://doi.org/10.1590/1519-6984.243514

Barbosa AC, Xu Z, Karari K, Williams W, Hauf S, Brown WR. 2022. Mutation and selection explain why many eukaryotic centromeric DNA sequences are often A+ T rich. Nu Acid Res. 50(1):579–596. https://doi.org/10.1093/nar/gkab1219

Bhowmick BK, Sarkar S, Roychowdhury D, Patil SD, Lekhak MM, Ohri D, Rao SR, Yadav SR, Verma RC, Dhar MK, Raina SN. 2023. *Allium* cytogenetics: a critical review on the Indian taxa. Comp Cytogenet. 17:129. 10.3897/CompCytogen.17.98903

Cortes F, Gonzalez-Gil G, Hazen MJ. 1983. C-banding and sister chromatid exchanges in three species of the genus *Allium* (*A. cepa*, *A. ascalonicum* and *A. sativum*). Caryologia 36(3):203–210. https://doi.org/10.1080/00087114.1983.10797661

Das A, Mukherjee P, Ghoroi A, Jha TB. 2011. Comparative karyomorphologycal analyses of *in vivo* and *in vitro* grown plants of *Aloe vera* l. Burm. F. Nucleus 53(3):89–94.

Das AB, Mohanty S, Das P. 2001. Cytophotometric estimation of 4C DNA content and karyotype analysis in ten cultivars of *Trigonella foenum-graecum*. Iran J Bot. 9(1):1–9

Flavell RB. 2021. Perspective: 50 years of plant chromosome biology. Plant Physiol. 185(3):731-53. https://doi.org/10.1093/plphys/kiaa108

Fukui K. 1996. Plant chromosomes at mitosis. In: Fukui K, Nakayama S, editors. Plant chromosomes: laboratory methods. Boca Raton (BR): CRC Press; p. 1–17.

Ghosh A, Datta AK. 2006. Karyotyping of *Nigella sativa* L. (black cumin) and *Nigella damascena* L. (love-in-a-mist) by image analyzing system. Cytologia 71(1):1–4.

Guerra M, Santos KGBD, Silva AEB, Ehrendorfer F. 2000. Heterochromatin banding patterns in Rutaceae-Aurantioideae– a case of parallel chromosomal evolution. Am J Bot. 87(5):735–747. https://doi.org/10.1159/000121083

Guerra M. 2008. Chromosome numbers in plant cytotaxonomy: concepts and implications. Cytogenet Genom Res. 120(3–4):339–350.

Hizume M. 2015. Fluorescent banding pattern in chromosomes of *Tsuga forrestii* and *T. Sieboldii* Pinaceae. Chromo Bot. 10(3):95–100. https://doi.org/10.3199/iscb.10.95

Jha TB, Bhowmick BK, Roy P. 2021. Analysis of CMA-DAPI bands and preparation of fluorescent karyotypes in thirty Indian cultivars of *Lens culinaris.* Caryologia 74(2):65–77.

Jha TB, Halder M. 2016. Searching chromosomal landmarks in Indian Lentils through EMA-based Giemsa staining method. Protoplasma 253:1223–1231.

Jha TB, Halder M. 2023. Evaluation of karyotype diversity in Indian traditional aromatic rice cultivars through EMA-based non-fluorescent Giemsa and fluorescent DAPI staining. Genet Resour Crop Evol. 1–22. https://doi.org/10.1007/s10722-023-01696-4

Kurata N, Omura T. 1978. Karyotype analysis in rice I. A new method for identifying all chromosome pairs. Jpn J Genet. 54:251–255. https://doi.org/10.1266/jjg.53.251

Levan A, Fredga K, Sandberg AA. 1964. Nomenclature for centromeric position on chromosomes. Hereditus. 52:210–220.

Liehr T. 2021. Molecular cytogenetics in the era of chromosomics and cytogenomic approaches. Front Genet. 12:720507.

Ma J, Wing RA, Bennetzen JL, Jackson SA. 2007. Plant centromere organization: a dynamic structure with conserved functions. Trends Genet 23(3):134-139.

Mancia FH, Sohn SH, Ahn YK, Kim DS, Kim JS, Kwon YS, Kim CW, Lee TH, Hwang YJ. 2015. Distribution of various types of repetitive DNAs in *Allium cepa* L. based on dual-colour FISH. Hortic Environ Biotechnol. 56(6):793–799. https://doi.org/10.1007/s13580-015-1100-3

Maragheh FP, Janus D, Senderowicz M, Haliloglu K, Kolano B. 2019. Karyotype analysis of eight cultivated *Allium* species. J Appl Genet. 60(1):1–11. https://doi.org/10.1007/s13353-018-0474-1

Martin E, Akan H. Ekici M, Aytac Z. 2011. Karyotype analyses of ten sections of *Trigonella* (Fabaceae). Comp Cytogenet. 5(2):105. 10.3897/compcytogen.v5i2.969

Mondin M, Aguiar-Perecin ML. 2011. Heterochromatin patterns and ribosomal DNA loci distribution in diploid and polyploid *Crotalaria* species (Leguminosae, Papilionoideae), and inferences on karyotype evolution. Genome 54:718–726. https://doi.org/10.1139/g11-034

Moscone EA, Lambrou M, Ehrendorfer F. 1996. Fluorescent chromosome banding in the cultivated species of *Capsicum* (Solanaceae). Plant Syst Evol. 202:37–63. https://doi.org/10.1007/BF00985817

Najafi S, Anakhatoon EZ, Birsin MA. 2013. Karyotype characterisation of reputed variety of fenugreek (*Trigonella foenum-graecum*) in West Azerbaijan-Iran. J Appl Biol Sci. 7(1):23–26.

Orooji F, Mirzaghaderi G, Kuo YT, Fuchs J. 2022. Variation in the number and position of rDNA loci contributes to the diversification and speciation in *Nigella* (Ranunculaceae). Front Plant Sci. 13:917310. https://doi.org/10.3389/fpls.2022.917310

Razumova OV, Alexandrov OS, Bone KD, Karlov GI, Divashuk MG. 2023. Sex chromosomes and sex determination in dioecious agricultural plants. Agron 13(2):540. https://doi.org/10.3390/agronomy13020540

Santra I, Biswas D, Ghosh B. 2023. Chromosomal characterization mediated by karyomorphological analysis and differential banding pattern in fenugreek (*Trigonella foenum-graecum* L.): a neglected legume. Caryologia 76(3):63–70. https://doi.org/10.36253/caryologia-2159

Sato S, Hizume M, Kawamura S. 1980. Relationship between secondary constrictions and nucleolus organizing regions in *Allium sativum* chromosomes. Protoplasma 105:77–85. https://doi.org/10.1007/BF01279851

Sato S. 1981. Cytological studies on the satellited chromosomes of *Allium cepa*. Caryologia 34(4):431–440. https://doi.org/10.1080/00087114.1981.10796911

Shaker SS, Mohammadi A, Shahli MK. 2017. Cytological studies on some ecotypes of *Nigella sativa* L. in Iran. Cytologia 82(2):123–126. https://doi.org/10.1508/cytologia.82.123

Than MMM, Samaddar T, Bhowmick BK, Jha S. 2017. Fluorescent chromosome banding and genome size estimation in three species of Swertia. Cytologia 82(5):513–520.

Tong P, Pidoux AL, Toda NR, Ard R, Berger H, Shukla M, Torres-Garcia J, Müller CA, Nieduszynski CA, Allshire RC. 2019. Interspecies conservation of organisation and function between nonhomologous regional centromeres. Nat Commun. 10(1):2343. https://doi.org/10.1038/s41467-019-09824-4

Wajahatullah MK, Vahidy AA. 1990. Karyotyping and localization of nucleolar organizer regions in Garlic, *Allium sativum* L. Cytologia. 55(3):501–504. https://doi.org/10.1508/cytologia.55.501

Yamamoto M, Takeuchi M, Nashima K, Yamamoto T. 2019. Enzyme maceration, fluorescent staining, and FISH of rDNA of Pineapple (*Ananas comosus* (L.) Merr.) chromosomes. J Hortic. 88(4):455–461.

Yuzbasioglu D. 2004. Karyotyping, C- and NOR banding of *Allium sativum* L. (Liliaceae) cultivated in Turkey. Pak J Bot. 36(2):343–349.

Caryologia
International Journal of Cytology, Cytosystematics and Cytogenetics

Firenze University Press
https://riviste.fupress.net/index.php/caryologia

OPEN ACCESS

Citation: Phimphan, S., Aiumsumang, S., Khoomsab, K., Tangsuwan, I. & Tanomtong, A. (2024). Karyomorphology and microsatellites characterization of *Limnonectes gyldenstolpei*: first report from Thailand. *Caryologia* 77(3): 47-52. doi: 10.36253/caryologia-2868

Received: Jul 14, 2024

Accepted: Sep 30, 2024

Published: March 25, 2025

Data Availability Statement: All relevant data are within the paper and its Supporting Information files.

Competing Interests: The Author(s) declare(s) no conflict of interest.

Karyomorphology and microsatellites characterization of *Limnonectes gyldenstolpei*: first report from Thailand

Sumalee Phimphan[1,*], Suracheat Aiumsumang[1], Kan Khoomsab[2], Itsara Tangsuwan[3], Alongklod Tanomtong[4]

[1] *Biology Program, Faculty of Science and Technology, Phetchabun Rajabhat University, Phetchabun 67000, Thailand*
[2] *Education Science Program, Faculty of Science and Technology, Phetchabun Rajabhat University, Phetchabun 67000, Thailand*
[3] *Natural Resources and Environmental Management Program, Faculty of Science and Technology, Phetchabun Rajabhat University, Phetchabun 67000, Thailand*
[4] *Department of Biology, Faculty of Science, Khon Kaen University, Khon Kaen 40002, Thailand*
*Corresponding author. E-mail: Sumalee.phi@pcru.ac.th, joodoof@gmail.com

Abstract. In the present investigation, karyotype and microsatellites pattern in the chromosome of Gyldenstolpe's Frog (*Limnonectes gyldenstolpei*) have been analyzed. The aspect of chromosome numbers, morphology, nucleolus organizer region (NOR) locations and microsatellites pattern [$d(CA)_{15}$, $d(CGG)_{10}$, $d(GC)_{15}$, $d(TA)_{15}$]. We provided the karyotype and idiogram of this species by conventional staining, Ag-NOR banding and Fluorescence *in situ* hybridization techniques. For the study, five male and female samples collected from northern Thailand, were used. The metaphase chromosome preparations were prepared from the bone marrows by the standard protocol. The result shows that *L. gyldenstolpei* had the diploid chromosome number ($2n$) was 26 and the fundamental number (NF) were 56 in both males and females. The karyotype is composed of 4 large metacentric, 4 large submetacentric, 2 medium metacentric, 14 small metacentric and 2 small submetacentric chromosomes. The NORs bearing chromosome were in close to the telomere region on chromosome pair 1. In addition, the microsatellite $d(CGG)_{10}$ and $(GC)_{15}$ hybridization results confirmed the NOR region. The *in situ* localization pattern of $d(CA)_{15}$ microsatellites was positive on all telomere chromosome, while microsatellites $d(TA)_{15}$ have no signal on chromosome. Here we provide a classical and some molecular genetics information for *L. gyldenstolpei* useful as a species specific marker.

Keywords: *Limnonectes gyldenstolpei*, karyotype, chromosome, microsatellites.

INTRODUCTION

Limnonectes gyldenstolpei is a species of frog in the Dicroglossidae family. It has been recorded throughout much of Thailand, northeastern Lao,

southwestern Cambodia, and central Vietnam. It has recently also been recorded from the Phong Nha-Kẻ Bàng National Park in central Vietnam (Luu et al., 2013). The members of the genus *Limnonectes* have a broad distribution in Asia from eastern and southern China, eastwards to Japan, throughout Indochina and southwards to Malaysia, Indonesia, Philippines, and New Guinea (Frost, 2016). *Limnonectes* is one of the most diverse groups amphibians with 69 currently species recognized and 15 of which have been described in the last ten years (Frost, 2016).

The gross chromosome numbers of 1,000 amphibian species were reported by Kuramoto (1990). But only 837 of the 3,521 anuran species have been analyzed chromosomally (King, 1991). The amphibian fauna in Thailand comprises of 176 species in 8 families and 3 orders (Khonsue and Thirakhupt, 2001). In the genus *Limnonectes* reported 11 species (Niyomwan, et al., 2019). The list shows chromosome number variation occurs in most of the seven families of anuran amphibians classified with 33 genera. The typical karyotype of the family Dicroglossidae is diploid chromosome number (2*n*)=22, 24 and 26. For the genus *Limnonectes*, there were some cytogenetic studies reported the diploid number was 2*n*=22-26, NF=44-52, including *L. kuhlii* and *L. blytthii* (Supaprom, 2003), *L. pileatus* (Supaprom, 2003; Supaprom and Baimai, 2004), *L. gruniens* and *L. modestus* (Nasaruddin, 2009), *L. blytthii* (Donsakul and Rangsiruji, 2005; Phimphan et al., 2020) and *L. taylori* (Phimphan and Aiumsumang, 2019). All previous knowledge demonstrated that there are several patterns of chromosomes (number, type, size).

This is the first report describing the molecular cytogenetic and karyotype study of chromosome size, standardized idiogram, karyotype formula and meiotic cell division of the *L. gyldenstolpei* species. The molecular data, microsatellite probes are used to detect if there is some specific hybridization pattern in *L. gyldenstolpei* has not been studied yet. The results obtain can be fulfilled to the basic knowledge. In addition, our knowledge advances cytogenetic information for further study on taxonomy relationship. Moreover, we provide useful basic information for the conservation and chromosome evolution study of this frog.

MATHERIAL AND METHODS

Field surveys were conducted in rainy season from northern (16.42°N 101.16°E), Thailand. Five males and five females of *L. gyldenstolpei* were mature obtained during. The frogs were transferred to the laboratory and were kept under standard conditions for 3 days before the experimentation. Experiments were performed in accordance with ethical protocols (Ref No. U1-04498-2559). The chromosomes were prepared *in vivo* with slight adaptations as follows (Sangpakdee et al., 2016). The colchicine was injected into the frogs' abdominal cavity. Then, the frogs were left in a box for eight hours and then killed. The bone marrow was collected by cutting the head and the end of femurs and tibias, and then a syringe was used to inject 0.075 M KCl into the marrow to drive out the bone marrow tissue or cells into the plate. We gently cut the tissue to pieces as small as possible. We transferred 8 mL of cell sediments to a centrifuge tube and incubated it for 30 min at 37 °C. After centrifugation at 1500 rpm for 8 min, the KCl was discarded. Cells were fixed in fresh cool fixative up to 8 mL by gradually adding it before being centrifuged again at 1500 rpm for 8 min. The fixation was repeated until the supernatant was clear, usually three times. Finally, the pellet was mixed with 1 mL fixative (depending on the amount of cell). The mixture was dropped onto a clean and cold slide by a micropipette, and then the air-dry technique was applied.

Conventional staining was done using 10% Giemsa's solution for 10 min (Phimphan and Aiumsumang, 2019). Ag-NOR banding was performed (Howell and Black, 1980) by applying two drops of 2% gelatin on the slides, followed with four drops of 50% silver nitrate. The slides were then covered with a cover slip and incubated at 60°C for 5 min or until the slide changed brownish. After that the slides were dipped in distilled water to remove the cover glass and air-dried on the slide. The microsatellites $(CA)_{15}$, $(CGG)_{10,}$ $(GC)_{15}$, and $(TA)_{15}$ were synthesized according to (Kubat etal., 2008; Supiwong et al., 2014). These sequences were directly labeled with Cy_3 at the 5'terminus during synthesis by Sigma (St. Louis, MO, USA).

Chromosome counting was performed on mitotic metaphase cells under a light microscope. Twenty clearly observable and well-spread chromosomes of each male and female were selected and photographed. The length of the short arm chromosome (Ls) and the length of the long arm chromosome (Ll) were measured, and the length of the total arm chromosome (LT, LT = Ls+Ll) calculated. The relative length (RL), the centromeric index (CI) and standard deviation (SD) of RL and CI were estimated. The CI (q/p+q) between 0.50–0.59, 0.60–0.69, 0.70–0.89 and 0.90–0.99 were described as metacentric, submetacentric, acrocentric and telocentric chromosomes, respectively (Levan, 1964). The fundamental number (number of chromosome arm, NF) was obtained by assigning a value of two to metacentric, submetacentric and acrocentric chromosomes and one to telocentric chromosome. All parameters were used in karyotyping and idiograming.

RESULTS AND DISCUSSION

The results showed *L. gyldenstolpei* had diploid chromosome number of 2*n*=26 and fundamental number (NF)=52, the karyotype comprised four large metacentric, four large submetacentric, two medium metacentric, 14 small metacentric and two small submetacentric chromosomes. The karyotype formula of *L. gyldenstolpei* is 2*n*(26)= L^m_4+L^{sm}_4+M^m_2+S^m_{14}+S^{sm}_2 in both males and female, while sex chromosomes were cytologically indistinguishable (Fig. 1A). The average lengths of each chromosome including short and long arm length, total length, relative length, and centromeric index were calculated and presented in Table 1. The previous relevant literatures have been reported that the numbers of diploid chromosome and fundamental number in *Limnonectes* studied herein are 2*n*=22-26 and NF=44-52 including, *L. kuhlii* and *L. blytthii* (Supaprom, 2003), *L. pileatus* (Supaprom, 2003; Supaprom and Baimai, 2004), *L. gruniens* and *L. modestus* (Nasaruddin, 2009), *L. blytthii* (Donsakul and Rangsiruji, 2005; Phimphan et al., 2020) and *L. taylori* (Phimphan and Aiumsumang, 2019). (Table 2). Comparison to closely related species, *L. gyldenstolpei* had diploid chromosome number similar to *L. gruniens* and *L. modestus* (2*n*=24), but is higher than that in *L. taylori* (2*n*=22) and lower than *L. kuhlii* and *L. pileatus* (2*n*=24). This result was the first report on *L. gyldenstolpei*. These characteristics are consistent with the theory that reorganization from the original karyotype resulted from Robertsonian fissions, fusions, or pericentric inversions (Gorman 1973; King 1978). Our results confirmed 2n for *L. gyldenstolpei* species but with differences in the diploid chromosome number. This incongruence reflects probably the number of the *Limnonectes* chromosomes, especially those of polyploids.

After Ag-NOR staining, these regions produce numerous gene expressions and contain more non-histone protein than others regions on the chromosome. Accordingly, the dark band (NOR-positive) is induced by the reduction of organic silver by these proteins that change from silver to dark (Sharma et al., 2002). If these regions were active during the interphase prior to mitosis, they can be detected by silver nitrate staining (Howell and Black 1980). The NOR could be detected to near telomeric region on long arm chromosome pairs 1 (Fig. 1B). We found one pair of Ag-NOR sites in all of the samples examined. However, the results were similar to the previous report on *L. kuhlii* and *L. blytthii* (Supaprom, 2003), *L. pileatus* (Supaprom, 2003; Supaprom and Baimai, 2004), *L. gruniens* and *L. modestus* (Nasaruddin, 2009), *L. blytthii* (Donsakul and Rangsiruji, 2005; Phimphan et al., 2020) and *L. taylori* (Phimphan and Aiumsumang, 2019). The most striking variation is seen in the morphology of the secondary constrictions. Generally, one major nucleolar organizer region is present per genome (n), which may vary in its position between species. However, closely related and often morphologically very similar species share the same type and location of their nucleolar organizer regions, which can therefore provide an effective taxonomic.

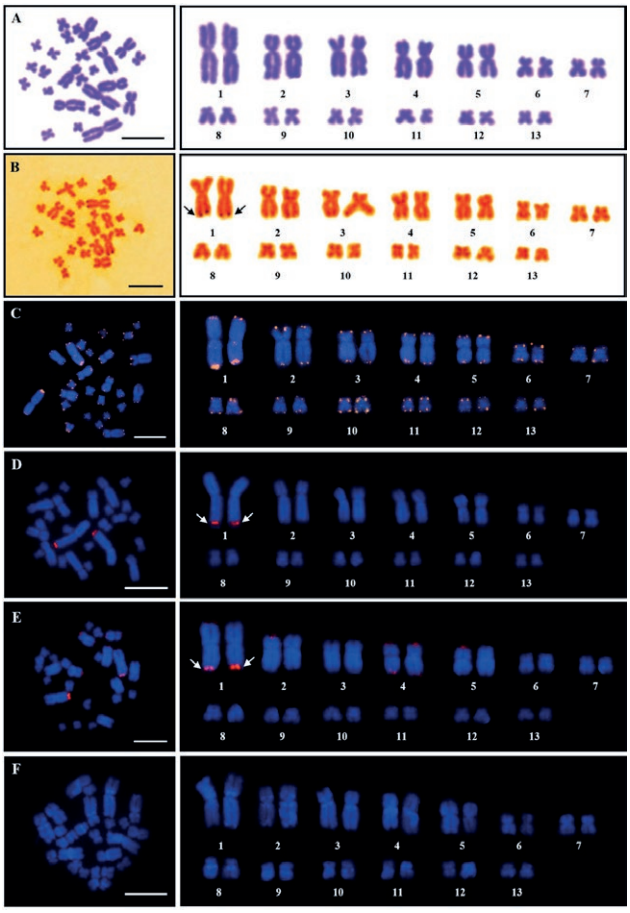

Figure 1. Metaphase chromosome plates and karyotypes of *Limnonectes gyldenstolpei*, 2*n*=26 by conventional staining [A.], Ag-NOR banding [B.], $d(CA)_{15}$ [C.], $d(CGG)_{10}$ [D.] $d(GC)_{15}$ [E.] and $d(TA)_{15}$ microsatellite probe [F.]. Note scale bars indicate 10 micrometers.

Here the first molecular cytogenetic study in metaphase chromosomes stained by FISH. The *in situ* hybridized localization of microsatellites $d(CA)_{15}$, $d(CGG)_{10,}$ $d(GC)_{15}$, and $d(TA)_{15}$. Microsatellites, also known as simple sequence repeats, consist of very short motifs (1-6 nucleotides in length) repeated in tandem arrays. Generally, they are located in the heterochromatic regions (telomeres, centromeres and in the sex chromosomes) of genomes, where a significant fraction of repetitive DNA is expected to be localized (Supiwong et al., 2013). The

Table 1. Mean length of short arm chromosome (Ls), length of long arm chromosome (Ll), length of total chromosomes (LT), relative length (RL), centromeric index (CI) and standart deviation (SD) from 20 metaphases of male and female *Limnonects gyldenstolpei*, 2*n* (diploid)=26.

Chromosome pairs	Ls	Ll	LT	CI±SD	RL±SD	Chromosome size	Chromosome type
1*	6.162	7.628	13.790	0.552±0.012	0.161±0.005	Large	metacentric
2	4.166	6.849	11.015	0.622±0.014	0.128±0.004	Large	submetacentric
3	3.469	5.991	9.460	0.633±0.019	0.110±0.004	Large	submetacentric
4	3.786	5.168	8.954	0.580±0.022	0.105±0.002	Large	metacentric
5	3.700	4.503	8.203	0.550±0.018	0.096±0.003	Medium	metacentric
6	2.179	2.966	5.145	0.577±0.014	0.060±0.002	Small	metacentric
7	1.866	2.892	4.758	0.606±0.032	0.056±0.002	Small	submetacentric
8	1.876	2.799	4.675	0.597±0.037	0.054±0.002	Small	metacentric
9	1.766	2.590	4.356	0.595±0.017	0.051±0.002	Small	metacentric
10	1.799	2.475	4.274	0.577±0.021	0.050±0.002	Small	metacentric
11	1.609	2.387	3.996	0.596±0.015	0.047±0.001	Small	metacentric
12	1.505	2.260	3.765	0.598±0.018	0.044±0.001	Small	metacentric
13	1.486	1.967	3.452	0.572±0.024	0.040±0.002	Small	metacentric

* NORs bearing chromosomes (satellite chromosome).

Table 2. Review of cytogenetic publications of family Dicroglossidae (genus *Limnonectes*).

Species	2*n*	Karyotype formula	NF	NORs	FISH	Reference
L. gruniens	24	24m	48	-	-	Nasaruddin et al. 2009
L. modestus	24	20m+4t	44	-	-	Nasaruddin et al. 2009
L. kuhlii	26	8m+14sm	52	2	-	Supaprom 2003
L. pileatus	26	16m+10sm	52	2	-	Supaprom 2003
	26	16m+10sm	52	2	-	Supaprom and Baimai 2004
L. taylori	22	16m+6sm	44	2	-	Phimphan and Aiumsumang 2019
	24	10m+12sm+2a	48	-	-	Donsakul and Rangsiruji 2005
L. blythii	24	20m+4sm	48	2	+	Phimphan et al. 2021a
L. gyldenstolpei	26	20m+6sm	52	2	+	Present study

2*n* diploid chromosome number, *NF*=fundamental number (number of chromosome arms), *m* metacentric, *sm* submetacentric, *a* acrocentric, *t* telocentric chromosome, *NORs* Ag-NOR banding, *FISH* Fluorescence in situ hybridization, + positive and - not available.

result of *L. gyldenstolpei* analyzed was being abundantly distributed on all telomere chromosomes such as, the accumulation of $(CA)_{15}$ in long arm chromosomal pair 1 (Fig 1C), while $(CGG)_{10}$ and $(GC)_{15}$ detected subtelomeric region on long arm chromosomal pair 1 (Fig. 1D, 1E) and $(TA)_{15}$ sequences are not present in the all chromosome (Fig. 1F). However, an intriguing feature exclusive for *L. gyldenstolpei* was the strong accumulation of all microsatellites at the regions of specific chromosomal pair, indicating that these microsatellites may be used as chromosomal markers in this frog species. In the frog genomes, microsatellites are usually abundant in the telomeric and centromeric regions, Otherwise, the dinucleotides $(CA)_{15}$, $(GC)_{15}$ and $(CGG)_{10}$ accumulated exclusively in telomeric and subcentromeric chromosomal regions, corroborating findings from other frog groups studied to date (Phimphan, et al. 2021a; 2021b). These molecular cytogenetics data could also be a substantial prerequisite for future frog genome projects. This study discovered that the cytogenetic maps of *L. gyldenstolpei* allowed us to map out the steps involved in this species' chromosomal rearrangement. This is the first report on the Fluorescence *in situ* hybridization (FISH) study of this species in Thailand.

The present study on the meiotic cell division of *L. gyldenstolpei* found that during interphase, nucleolus

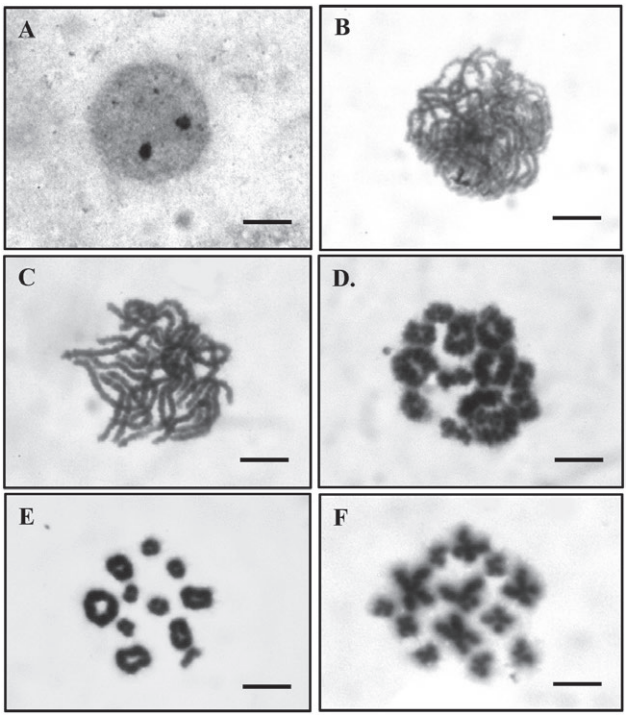

Figure 2. Meiosis cell division of the *Limnonectes gyldenstolpei*, 2*n*=26 on interphase (A.), leptotene (B.), pachytene (C.), diakinesis (D.), metaphase I (E.) and metaphase II (F.) by conventional staining technique. Scale bars indicate 10 micrometers.

could be clearly seen, while chromatins were absent. In prophase, metaphase I (meiosis I) the homologous chromosomes showed synapsis, which can be defined as the 13 bivalent and 13 haploid chromosomes at metaphase II as diploid species. It is confirmed for this species had 2n=26 in similar to previous reports. The largest metacentric chromosome pair 1 is the largest bivalent. We found that *L. gyldenstolpei* had the distinct character of the observable leptotene (initiation of chromosome shrinking), pachytene (completion of chromosome synapsis) and diakinesis (terminalization) according to Patawang (Patawang et al., 2013) (Fig. 2). In conclusion, this study provides the first chromosome, molecular cytological details and Ag-NOR marker for *L. gyldenstolpei* from Thailand. The results support the karyotype of genus *Limnonectes* are conserved among several other species. However, the chromosomal morphology may be slightly different depending on populations of *L. gyldenstolpei* present in different countries. Our results added new knowledge that can be used for karyological comparative analyses in *Limnonectes* species, on the basis of classical and banding approach within this taxon.

ACKNOWLEDGMENTS

This study was supported by the National Research Council of Thailand under the Phetchabun Rajabhat University (Grant No. TSRI2567/64).

REFERENCES

Donsakul T, Rangsiruji A. 2005. Liver karyotypes in *Limnonectes blythii*, *Rana erythraea*, *Rana leptoglossa*, *Occidozyga martensii* and *Glyphoglossus molossus* (Amphibia, Anura). Proceedings of 43rd Kasetsart University Annual Conference, Thammasart University, Bangkok.

Frost DR. 2016. Amphibian Species of the World:an online reference. Version 6.0. American Museum of Natural History, New York, USA.

Gorman GC. 1973. The chromosomes of the Reptilia, a cytotaxonomic interpretation. Cytotaxonomy and vertebrate evolution. New York: Academic Press, p. 349–424.

Howell WM, Black DA. 1980. Controlled silver-staining of nucleolus organizer regions with a protective colloidal developer: a 1-step method. Experientia. 36: 1014–5.

King M. 1978. A new chromosome form of *Hemidactylus frenatus* (Dumeril and Bibron). Herpetologica 34: 216–218.

Khonsue W, Thirakhupt K. 2001. A Checklist of the Amphibians in Thailand. Trop Nat Hist. 1: 69–82.

Kubat Z, Hobza R, Vyskot B, Kejnovsky E. 2008. Microsatellite accumulation in the Y chromosome of *Silene latifolia*. Genome. 51: 350–356.

Kuramoto M. 1980. Karyotype of several frogs from Korea, Taiwan and Philippines. Experientia. 36: 826–828.

Levan A, Fredga K, Sandberg AA. 1964. Nomenclature for centromeric position on chromosomes. *Hereditas*. 52: 201–220.

Luu, VQ, Truong QN, Cuong TP, Kien ND, Thanh NV, Sladjana M, Michael B, Thomas Z, 2013. No end in sight? Further new records of amphibians and reptiles from Phong Nha – Ke Bang National Park, Quang Binh Province, Vietnam". Biodiversity. 4(2): 285–300.

Nasaruddin, Suriana, Dwi Arinto Adi, Salamansyah. 2009. The Karyotype of Seven Species of Amphibians (Anuran Order) from South-east Sulawesi. Veteriner. 10: 77–76.

Niyomwan P, Priwan S, Pawangkanan P. 2019. Amphibians of Thailand. Bangkok. 487 pp.

Patawang I, Tanomtong A, Phimphan S, Chuaynkern Y, Chuaynkern C, Phaengphairee P, Khrueanet W, and Nithikulworawong N. 2013. The identification of sex-chromosomes and karyological analysis of rice frog, *Fejervarya limnocharis* (Anura, Ranidae) from Northeast Thailand. Cytologia. 79:141–150.

Phimphan S, Aiumsumang S. 2019. Chromosomal characteristics of Taolor's stream frog (*Limnonectes taylori*) (Amphibia, Anura) from Thailand. The Nucleus. 64(1): 129–133.

Phimphan S, Aiumsumang S, Tanomtong A, Jantarat S. 2021a. Karyomorphological delineation and linear differentiation of microsatellite patterns, and meiosis in giant Asian river frog (*Limnonectes blyhii*) from Thailand. The Nucleus 64(2): 249–254.

Phimphan S, Aiumsumang S, Tanomtong, A. 2021b. Charecterization of Chromosome and Repetitive elements in the Genome of Frog *Rana nigrovittata* (Anuran, Ranidae) from Thailand: Revealed by conventional, Ag-NOR banding, C-banding and FISH techniques. Cytology and Genetics. 55(6): 583–589.

Sangpakdee W, Phimphan S, Tengjaroenkul B, Pinthong K, Neeratanaphan L, Tanomtong, A. 2016. Cytogenetic Study of Three Microhylid Species (Anura, Microhylidae) from Thailand. Cytologia. 82: 67–74.

Sharma OP, Tripathi NK, Sharma KK. 2002. A review of chromosome banding in fishes. In: Sobti, RC (ed.). Some aspects of chromosome structure and functions. Narosa Publishing House, New Delhi.

Supaprom T. 2003. Cytogenetics of Amphibians in Thailand. Ph.D. Dissertation, Mahidol university.

Supaprom T, Baimai V. 2004. Karyotypes of ten species of ranid frogs (Anura: Ranidae) from Thailand. Amphibia-Reptilia. 25:104–111.

Supiwong W, Liehr T, Cioffi MB, Chaveerach A, Kosyakova A, Pinthong K, Tanee T, Tanomtong A. 2013. Karyotype and cytogenetic mapping of 9 classes of repetitive DNAs in the genome of the naked catfish Mystus bocourti (Siluriformes, Bagridae). Molecular Cytogenetics. 6:51

Supiwong W, Liehr L, Cioffi MB, Chaveerach A, Kosyakova N, Pinthong K, Tanee T, Tanomtong, A. 2014. Chromosomal evolution in naked catfishes (Bagridae, Siluriformes): A comparative chromosome mapping study. Zool. Anz. 253: 316–320.

Caryologia
International Journal of Cytology, Cytosystematics and Cytogenetics

Firenze University Press
https://riviste.fupress.net/index.php/caryologia

OPEN ACCESS

Citation: Morovati, Z., Karimzadeh, G., Naghavi, M.R. & Rashidi Monfared, S. (2024). Chromosome, ploidy analysis, and flow cytometric genome size estimation of *Datura stramonium* and *D. innoxia* medicinal plant. *Caryologia* 77(3):53-61. doi:10.36253/caryologia-2768

Received: May 17, 2024

Accepted: Oct 18, 2024

Published: March 25, 2025

Data Availability Statement: All relevant data are within the paper and its Supporting Information files.

Competing Interests: The Author(s) declare(s) no conflict of interest.

ORCID
ZM: 0009-0000-7291-706X
GK: 0000-0001-8209-3287
SRM: 0000-0001-5380-1387

Chromosome, ploidy analysis, and flow cytometric genome size estimation of *Datura stramonium* and *D. innoxia* medicinal plant

Zahra Morovati[1], Ghasem Karimzadeh[1,*], Mohammad Reza Naghavi[2], Sajad Rashidi Monfared[3]

[1] *Department of Plant Genetics and Breeding, College of Agriculture, Tarbiat Modares University, P. O. Box: 14115-336, Tehran, Iran*
[2] *Department of Agronomy and Plant Breeding, College of Agriculture, University of Tehran, Karaj, Iran*
[3] *Department of Agricultural Biotechnology, College of Agriculture, Tarbiat Modares University, P. O. Box: 14115-336, Tehran, Iran*
*Corresponding author: E-mail: karimzadeh_g@modares.ac.ir

Abstract. *Datura stramonium* and *D. innoxia* are among the important species of *Datura* genus. They have many uses in traditional and modern medicine. Since Iran is located in the origin area of *Datura*, it is expected that Iranian germplasms are factors of global genetic diversity of *Datura*. Ploidy level, chromosome number and length, and genome size estimation were studied on 15 populations of both *Datura* species mostly collected from different parts of Iran and a few from abroad. For chromosomal preparations, root tip was squashed and stained with 1% (w/v) aceto-orcein. For genome size estimation, flow cytometric analysis was conducted on fresh developed leaves of *Datura* samples along with those of internal standard reference (*Solanum lycopersicum* cv. Stupick, 2C = 1.96 pg DNA), using PI fluorochrome. All the studied populations were diploids ($2n = 2x = 24$). The mean chromosome length in *D. stramonium* and *D. innoxia* was determined as 1.97 µm and 2.39 µm, respectively; the latter had 21% larger chromosomes. The mean monoploid genome size was determined as 3.80 pg in *D. stramonium* (ranged 3.65 pg to 3.93 pg) and 3.91 pg in *D. innoxia* (ranged 3.68 pg to 4.30 pg). The present study provides completely new information about cytogenetics in *D. stramonium* and *D. innoxia* populations from Iran for the first time, which is useful for whole genome sequencing and the construction of genetic and physical maps in the future.

Keywords: chromosome, DNA C-value, monoploid genome size, *Datura,* Iran.

INTRODUCTION

Solanaceae is a large plant family that includes economically species and having still many members cytologically unexplored (Zhang *et al.*, 2023). The genus *Datura* from the Solanaceae family produces various secondary metabolites, for example tropane alkaloids, terpenoids, and glycoalkaloids

to defense against natural enemies such as herbivorous insects, pathogenic agents (bacteria, fungi, viruses) and different abiotic stresses (De-la-Cruz *et al.,* 2021). The classification of *Datura* species is organized into two primary groups. The first group, Ceratocauli, consists solely of the species *D. ceratocaula*. The second group encompasses a variety of other species and is further divided into two sections. The first section includes *D. arenicola*, *D. discolor*, *D. ferox*, *D. kymatocarpa*, *D. leichhardtii*, *D. quercifolia*, and *D. stramonium*, while the second section (termed polyphyletic) comprises *D. innoxia*, *D. lanosa*, *D. metel*, *D. reburra*, and *D. wrightii* (Bye and Sosa, 2013) which are native to North America (De-la-Cruz *et al*., 2021), distributed in subtropical regions of the world (Hassan and Amer, 2019; Papagrigoriou *et al.,* 2019). On the other hand, Karimi (2001) believed that the origin of *D. stramonium* are India and the western shores of the Caspian Sea. Hence, the two species *D. stramonium* and *D. innoxia* are found abundantly in Iran; *D. innoxia* is less distributed than *D. stramonium* in coastal areas, but it is more distributed in the outskirts of cities (Ghahraman, 1998; Muzafarian, 2000). Among the Iranian names of *Datura* weed, Tatore weed, Tatoleh, and Jozmash can be notified (Kirimi, 2001). In which, *D. stramonium* also known as the Thorn Apple, Jimson Weed, and Angel's Trumpet (Disel *et al.,* 2016). Both *D. stramonium* and *D. innoxia* are important species of *Datura* genus (Batool *et al.,* 2020; Al-Zharani *et al.,* 2021), having several traditional and modern medicinal uses (Mohammed *et al.,* 2021). Morovati *et al*. (2023) showed that the essential oil of the aerial parts of *D. stramonium* is rich in monoterpenoid derivatives such as camphor and borneol, which are widely used as therapeutic agents against the proliferation of cancer cells for the treatment of neurological and antiviral disorders (Salakhutdinov *et al.,* 2017).

Genome size, chromosome number and structure changes play an important role in speciation events, adaptation and the development of new genetic networks during evolution (Pellestor and Gatinois, 2020; Winterfeld *et al.,* 2020). Accordingly, analysis and chromosome observation and genome size estimates, elucidate phylogenetic relationships, structure, function, organization, and evolution (Amosova *et al.,* 2019). Such cytogenetic studies may be useful in establishing systematic and evolutionary relationships, resolving taxonomic ambiguities, and achieving a better understanding of the branching pattern of *Datura* genera (Dobigny *et al.,* 2004; Knight *et al.,* 2005; Bancheva and Greilhuber, 2006; Guerra, 2008; Bainard *et al.,* 2013). Hence, for those reasons, many studies are conducted to genome size estimates and chromosomes studies (Burchardt *et al.,* 2020).

Variation of chromosome number in the *Datura* genus can indicate intra- and inter-specific differences in genomic DNA quantities and also, variation of intra/interspecific genome size may reflect karyotypic differences, such as differences in the case of chromosome number and size (Bennett *et al.,* 2008). Previously, Blakeslee (1921) reported various chromosome number in *D. stramonium* as $2n$ = 12, 25, 26, 36, and 48 in the USA, but in recent years Hassan and Amer (2019) stated that the commonly chromosome number in this species was $2n$ = 24. Confirming the latter report, Badr *et al.* (1997) verified the chromosome base number in *D. innoxia* and *D. stramonium* as $n = x = 12$. Moreover, recently, Sadeghian and Hatami (2022) clarified that *D. innoxia* is diploid with $2n$ = 24. Monoploid genome size (1Cx-value) as the amount of DNA of one basic chromosome set (with chromosome base number x), regardless of the degree of generative polyploidy, aneuploidies, etc. (Greilhuber *et al.,* 2005; Karimzadeh *et al.,* 2011; Abedi *et al.,* 2015).

In previous study, the 2C DNA of *D. stramonium* was reported as 4.18 pg. (Kubešova *et al.,* 2010). Also, in the report of Bennett and Smith (1976) who evaluated the absolute amounts of nuclear DNA for 753 species of angiosperms, using Feulgen microdensitometry. The 2C DNA of *D. innoxia* was reported as 4.60 pg (Bennett and Smith, 1976). Due to shortcomings in some of the used cytogenetic techniques and lack of access to detailed information on DNA C value, karyology, and ploidy levels of *Datura* genus and since Iran is located in the center of the origin of diversity, so it is expected that Iranian *Datura* germplasm indicates much of the worldwide genetic diversity of *Datura*. On the other hand, there is no reliable report regarding the number of chromosomes and genome size regarding *Datura* genus in Iran. Thus, reliable conclusions cannot be drawn on the actual range of chromosomal variation in *Datura* without considering the Iranian germplasm. Hence, the current study, for the first time, was aimed to provide a detailed survey of chromosomal and genome size variation in the Iranian *D. stramonium* and *D. innoxia* by focusing on populations that were not studied before. For this purpose, several Iranian populations of *D. stramonium* and *D. innoxia* were investigated.

MATERIALS AND METHODS

Seed collection site

The seeds of 13 Iranian endemic populations of *Datura stramonium* (9 populations) and *D. innoxia* (4 populations) were collected from different sites of Iran

Table 1. Locality collection characteristics of *D. stramonium* and *D. innoxia.*

Altitude (m)	Latitude (N)	Longitude (E)	Local Collection locations	Population codes
1723	35°43'57"	53°37'49"	Semnan, Semnan, Iran	S1P1
1612	32°36'12"	51°26'01"	Isfahan, Isfahan, Iran	S1P2
120	39°29'18"	48°07'49"	Mughan plain, Ardabil, Iran	S1P3
1500	36°42'15"	48°21'31"	Zanjanrood, Zanjan, Iran	S1P4
1362	36°26'17"	45°56'43"	West Azerbaijan, Iran	S1P5
65	38°06'44"	41°07'33"	Saravan, Gilan, Iran	S1P6
30	33°95'04"	41°55'89"	Venous Rezvanshahr, Gilan, Iran	S1P7
1505	29°34'80"	52°35'26"	Shiraz, Fars, Iran	S1P8
1880	11°16'46"	51°49'27"	RuBland (RUS)	S1P9
1880	11°16'46"	51°49'27"	Brasitieh (BRA)	S1P10
1269	35°44'17"	51°10'23"	Tehran, Tehran, Iran	S1P11
1800	37°12'11"	44°52'21"	Turgor, Urmia, Iran	S2P1
1914	34°27'00"	46°80'76"	Mahidasht, Kermanshah, Iran	S2P2
981	34°35'17"	50°49'02"	Qom, Qom, Iran	S2P3
838	29°49'17"	51°33'48"	Kazerun, Fars, Iran	S2P4

S1: *Datura stramonium*, S2: *Datura innoxia.*

during the October and November of 2021, also, two populations (P9, P10) of *Datura stramonium* species were prepared from Leibniz Institute of Plant Genetics and Crop Plant Research (IPK), Germany. The species code and geographical descriptions, including latitude, longitude, and altitude are shown in Table 1 and Figure 1.

Figure 1. Location of the sampling sites of 13 Iranian endemic *Datura* populations on the map of Iran.

Plant material and growing conditions for genome size estimation

For study the genome size, the collected seeds were planted in grow bags with 10 kg soil (sandy loam) and placed for three months in greenhouse of agricultural faculty of Tarbiat Modares University in Tehran. Under greenhouse conditions, average air temperature was 25 °C. Finally, the developed leaves at the four-leaf stage were collected to determine their genome size.

Flow cytometric genome size estimation

The 2C-value of each *Datura* species was determined by flow cytometric analyses. FCM (Flow cytometric) analysis was carried out by PI (Propidium Iodide) staining technique and *Solanum lycopersicum* cv. Stupicke; 2C = 1.96 pg DNA (Doležel *et al.,* 1998) as an internal reference standard plant (Figure 2). About 2 cm^2 of healthy fresh young leaves of *Datura* and internal reference standard were co-chopped with a sharp razor blade in a glass petri dish, containing one ml of ice-cold WPB buffer (Woody Plant Buffer, Loureiro *et al.,* 2007). The crude nuclei suspension was filtered through a 30 µm green nylon mesh (Partec, Münster, Germany). Then RNase (Sigma-Aldrich Corporation, MO, USA) and propidium iodide (PI; ach 50 µg ml^{-1}) was added. For the resulting sample, the relative fluorescence intensity was calculated. After incubation for two min at RT, to determine the amount of genomic 2C DNA, the nuclei suspension was examined by BD FACSCantoTM-KE flow cytometer (BD Biosciences, Bedford, MA, USA), equipped with an

Figure 2. Two species of *Datura* in grow bags in greenhouse (a). *Datura innoxia*, (b) *D. stramonium* (c). *Solanum lycopersicum* cv. Stupicke (2C = 1.96 pg DNA) the internal reference standard plant (d).

argon ion laser (488 nm) via BD FACSDivaTM software. At least 5,000 nuclei were typically analyzed for each sample in three replications (Sayadi *et al.,* 2022; Zarabizadeh *et al.,* 2022). For create a histograms, the range of gating zone was calculated by using the Partec FloMax ver. 2.4e. (Partec, Münster, Germany). The measurements of relative fluorescence intensity of stained nuclei were performed on a linear scale. By calculating the values of the means of G1 peak, the absolute DNA amount of each sample was estimated (Doležel *et al.,* 2003, 2007; Greilhuber *et al.,* 2005; Karimzadeh *et al.,* 2011) as follows:

Sample 2Cx DNA (pg) = (Sample G1 peak mean/Standard G1 peak mean) × Standard 2C DNA (pg).

Value was calculated based on a conversion formula where 1 pg of DNA represents 978 Mbp (Doležel *et al.,* 2003).

Chromosome analysis

Initially, the scraped seeds were placed in Petri dishes with sandpaper and germinated on moist filter paper at 20 - 25 °C under light conditions in a growth chamber. For the cytological preparations, each root tip (0.5 - 1 cm long) was removed and pretreated with 0.002 M 8- hydroxyquinoline at 25 °C for 2.5 h in the dark to induce cell cycle delay in metaphase. The roots were washed by distilled H_2O in several times and fixed in 3:1 (v/v) of ethanol and glacial acetic acid (Carnoy solution) at 4 °C for 17 h. The fixed roots were washed in distilled H_2O, hydrolyzed in 1 M HC1 at 60 °C (11 min for *D. stramonium* and 13 min for *D. innoxia*) in a water bath, and washed in water, then stained by aceto-orcein 1% (w/v) at 25 °C (50 min for *D. stramonium* and 60 min for *D. innoxia*) in darkness (Reference). Finally, for microscopic studies, the five root tips from different individuals were squashed in a drop of 45% (v/v) acetic acid and analyzed per *Datura* populations. Slides were examined and High-resolution microscopic digital photographs (Super High Quality; SHQ; Tiff format images) were acquired, using an Olympus BX50 (Olympus Optical Co., Ltd., Tokyo, Japan) microscope equipped with an Olympus DP12 digital camera. It is reminded that each replicate is a cell from the meristem of the plant and five slides from the terminal meristem of five different plants were prepared from each population.

Statistical analysis

The karyotypic and flow cytometric data was analyzed according to analysis of variance based on a completely randomized design with five and three replications, using SAS Statistical Package Program version 9.0 and SPSS software version 20. The PROC UNIVARIATE within SAS was used to test the assumptions of *ANOVA*, and residuals were normally distributed. The means were compared through the least significant difference (LSD) posthoc test at the 5% probability level. Moreover, the standard errors of the means were calculated.

RESULTS

Chromosome counts and length and ploidy level

Figures 3 show the somatic complement karyotypes in the 15 *D. stramonium* and *D. innoxia* populations. All cells studied of the examined *Datura* populations consistently had ploidy levels and chromosome number of $2n = 2x = 24$ were with small chromosomes. Based on *ANOVA* results, among populations *D. stramonium* for Chromosome length (CL), were significant differences ($P < 0.05$; Table 2). The mean chromosome length (CL) was determined as 1.966 µm, varied from 1.627 µm (S1P2) to 2.286 µm (S1P8, Table 3). On the other hand, the ANOVA results, among populations *D. innoxia* verified significant differences ($P < 0.01$; Table 2) in Chromosome length (CL). The highest and the least values of Chromosome length (CL) in S2P1 (2.819 µm) and S2P2 (1.967

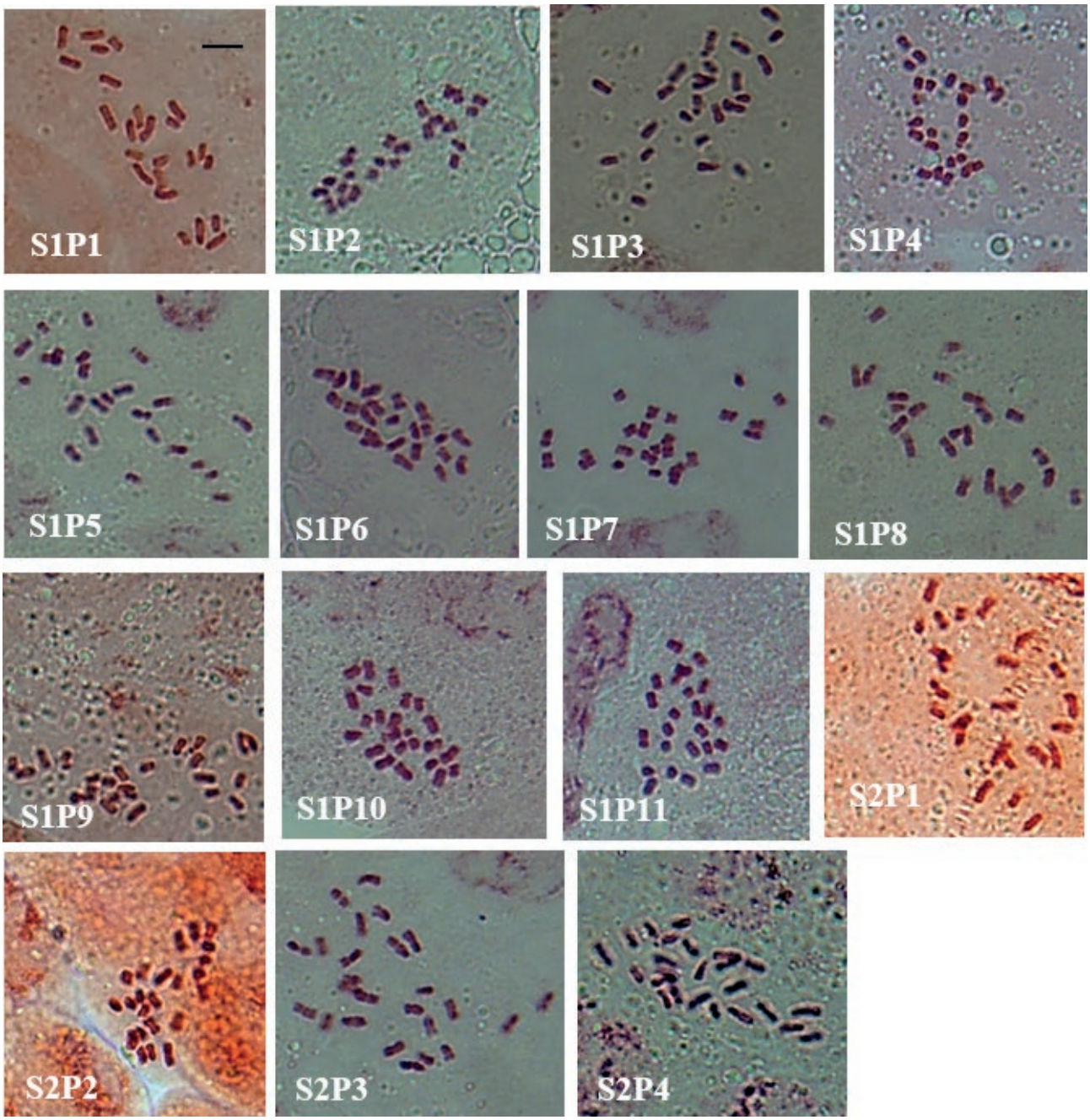

Figure 3. Somatic chromosomes ($2n = 2x = 24$) of 11 *Datura stramonium* populations and four *D. innoxia* populations. Scale bar = 5 μm.

μm), respectively and the mean Chromosome length in this species was 2.388 μm (Table 3).

Flow cytometric analysis of monoploid genome size

The nuclear DNA values of 15 populations of two species of *Datura* genus were estimated by flow cytometry. In the process of estimating the DNA content of the nuclei in the leaf tissue, two peaks were observed in the obtained histograms. In all populations under study, the left peak corresponds to the *Solanum lycopersicum* cv. Stupicke (2C value = 1.96 pg DNA) internal reference standard plant, and the right peaks refer to the *Datura* populations (Figures 4). Based on the *ANOVA* results (Table 4), no significant difference in the comparison

Table 2. *ANOVA* of chromosome length (µm) of *Datura stramonium* and *D. innoxia* populations.

S.O.V.	*D. stramonium*		*D. innoxia*	
	df	MS	df	MS
Population	10	0.17039*	3	0.6176**
Error	44	0.06506	8	0.1081
Total	54		11	
CV%		12.97		13.77

*Significant (P<0.05); **Significant (P<0.01).

Table 4. *ANOVA* of monoploid genome size (2Cx DNA, pg) of *Datura stramonium* and *D. innoxia* populations.

S.O.V.	*D. stramonium*		*D. innoxia*	
	df	MS	df	MS
Population	10	0.03099ns	3	0.25142*
Error	44	0.05217	8	0.04042
Total	54		11	
CV%		6.0		5.12

ns non-significant (P>0.05); * Significant (P<0.05)..

Table 3. Means (±SE) and the range comparisons of chromosome length (µm) of *Datura stramonium* and *D. innoxia* populations.

Population codes	CL (µm) *D. stramonium*	Population codes	CL (µm) *D. innoxia*
S1P1	2.032 ± 0.212abc	S2P1	2.819 ± 0.076a
S1P2	1.627 ± 0.071d	S2P2	1.967 ± 0.142b
S1P3	2.133 ± 0.132ab	S2P3	2.323 ± 0.119ab
S1P4	1.757 ± 0.061cd	S2P4	2.441 ± 0.216ab
S1P5	1.883 ± 0.086bcd	---	---
S1P6	2.006 ± 0.100abc	---	---
S1P7	2.005 ± 0.092abc	---	---
S1P8	2.286 ± 0.119a	---	---
S1P9	1.985 ± 0.068abc	---	---
S1P10	2.092 ± 0.160ab	---	---
S1P11	1.820 ± 0.040bcd	---	---
Mean	1.966		2.3876
Range	1.627-2.286		1.967-2.819
$LSD_{5\%}$	0.325		0.607

CL: chromosome length (µm), S1: *Datura stramonium*, S2: *D. innoxia.*

Table 5. Means (±SE) and the range monoploid genome size (DNA 2Cx value, pg) of *D. innoxia* populations.

Population codes	2Cx genome size (pg)	1Cx genome size (pg)	1Cx genome size (Mbp)
S2P1	4.305 ± 0.032a	2.152	2104.66
S2P2	3.682 ± 0.122b	1.841	1800.50
S2P3	3.708 ± 0.119b	1.854	1813.21
S2P4	3.963 ± 0.155ab	1.982	1938.40
Mean	3.914	1.957	1914.19
Range	3.682-4.305	1.841-2.152	1800.50-2104.66
$LSD_{5\%}$	0.377		

of genome size among populations *D. stramonium* was observed. However, the mean monoploid genome size was determined as 3.8 pg, varied from 3.650 pg (S1P5) to 3.934 pg (S1P4). Also, the *ANOVA* results, between four populations *D. innoxia* verified significant differences in genome size (Table 4). The mean genome size (Table 5) was determined as 3.91 pg, varied from 3.682 pg (S2P2) to 4.305 pg (S2P1).

DISCUSSION

Fifteen *Datura* populations we studied, among which nine populations of *Datura stramonium* and four populations of *D. innoxia* were of Iranian endemic origin. The results of the current study, which were used to examine karyotype diversity and estimate genome size from the new and unworked populations of *Datura* plant, are being reported for the first time in the world. Our results provide basic cytogenetic information for these two species, which are helpful for the whole-genome sequencing and the construction of genetic and physical maps in the future. Cytogenetic investigations carried out on the populations of *Datura stramonium* and *D. innoxia* showed that all the studied populations were diploid with chromosome number of 24, which was completely consistent with the results of previous reports (Badr *et al.,* 1997; Hassan and Amer, 2019; Sadeghian and Hatami, 2022). Because of short chromosomes' lengths, the locations of the centromeres could not be identified clearly, hence chromosome length (CL) parameter was measured, as reported for different species by researchers (e.g. Morales Valverde, 1986; Karimzadeh *et al*., 2010; Abbasi-Karin *et al*., 2022; Rasekh and Karimzadeh, 2023, Yari *et al*., 2024). According to the results of the current study, the mean chromosome length (CL) in *D. stramonium* and *D. innoxia* populations was 1.97 µm and 2.39 µm, respectively. In other words, *D. innoxia* populations had 21% larger chromosomes. Moreover, in the present study, the leaf materials were used for the estimation of genome size, using

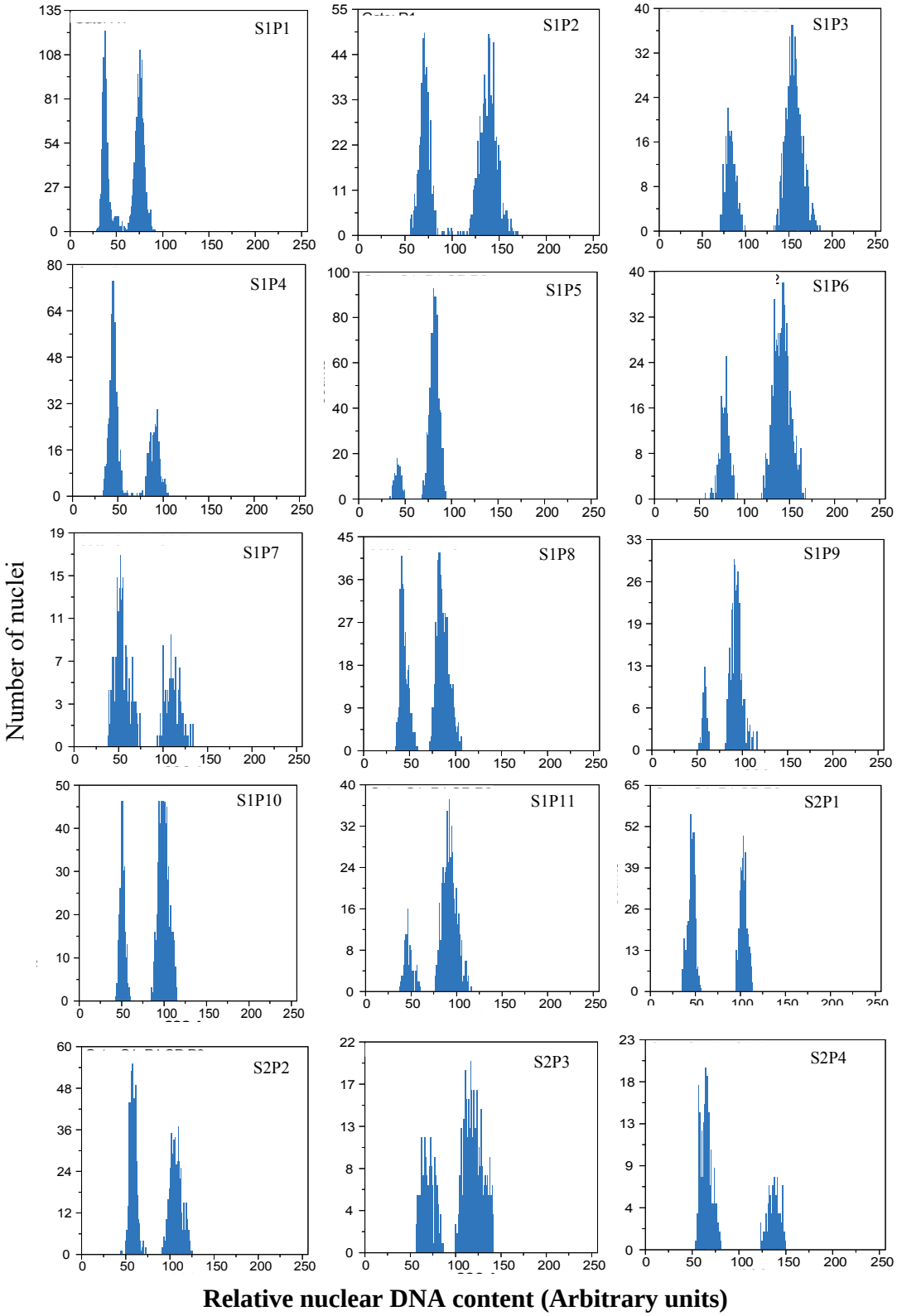

Figure 4. Histograms of monoploid genome size (2Cx DNA content) of *Datura stramonium* and *D. innoxia* populations. The left peaks refer to the G1 peaks of *Solanum lycopersicum* cv. Stupicke (2C = 1.96 pg DNA) as an internal reference standard plant and the right peaks refer to the G1 peaks of the samples.

flow cytometric analysis (Mohammadpour *et al.,* 2022; Rasekh and Karimzadeh, 2023; Yari *et al.,* 2024). The mean monoploid genome size in *D. stramonium* and *D. innoxia* populations was 3.799 pg and 3.914 pg, respectively. The cytogenetic information obtained from this research is more than the mean chromosome length and the mean genome size reported in the previous studies (Bennett and Smith *et al.,* 1976; Badr *et al.,* 1997). The reason for this is unknown, but this difference could be related to the cell cycle, the rate of cell division, ecological behavior in plant communities and life forms, and differences between the methods of nuclear DNA content analysis (Bennett *et al.,* 2000). On the other hand, previous studies have only been conducted on one population. In general, it can be concluded that the average chromosome length and average monoploid genome size in *D. innoxia* species are 0.40 and 0.11 times higher than those in *D. stramonium* species, respectively.

ACKNOWLEDGMENT

Authors acknowledge the Tarbiat Modares University (TMU) and Iran National Science Foundation (Grant Number: 4014886) for financial supporting of this research work. The authors would also like to acknowledge the financial support of Modares Science and Technology Park for this project.

REFERENCES

Abbasi-Karin Sh, Karimzadeh G, and Mohammadi-Bazargani M. 2022. Interspecific chromosomal and genome size variations in *in vitro* propagated willow herb (*Epilobium* spp.) medicinal plant. Cytologia 87(2): 129-135.

Abedi R, Babaei A, and Karimzadeh G. 2015. Karyological and flow cytometric studies of Tulipa (Liliaceae) species from Iran. Plant Syst. Evol. l301: 1473-1484.

Al-Zharani M, Nasr FA, Alqahtani AS, Cordero MAW, Alotaibi AA, Bepari A, Alarifi S, Daoud A, Barnawi IO, and Daradka HM. 2021. *In vitro* cytotoxic evaluation and apoptotic effects of *Datura innoxia* grown in Saudi Arabia and phytochemical analysis. Appl. Sci. 11(6): 2864.

Amosova AV, Zoshchuk SA, Rodionov AV, Ghukasyan L, Samatadze TE, Punina EO, Loskutov IG, Yurkevich OY, and Muravenko OV. 2019. Molecular cytogenetics of valuable Arctic and sub-Arctic pasture grass species from the Aveneae/Poeae tribe complex (Poaceae). BMC Genetic 20(1): 1-16.

Badr A, Khalifa SF, Aboel-Atta AI, and Abou-ElEnain MM. 1997: Chromosomal criteria and taxonomic relationships in the Solanaceae. Cytologia 62(2): 103-113.

Bainard JD, Forrest LL, Goffinet B, and Newmaster SG. 2013. Nuclear DNA content variation and evolution in liverworts. Mol. Phylogenet. Evol. 68: 619-627.

Blakeslee AF. 1921. Types of mutations and their possible significance in evolution. Am Nat. 55: 254-267.

Bancheva S and Greilhuber J. 2006. Genome size in Bulgarian Centaurea s.l. (Asteraceae). Plant Syst. Evol. 257: 95-117.

Batool A, Batool Z, Qureshi R, and Raja NI. 2020. Phytochemicals, pharmacological properties and biotechnological aspects of a highly medicinal plant: *Datura stramonium*. J. Plant Sci., 8(2): 29-40.

Bennett MD, Bhandol P, and Leitch I J. 2000. Nuclear DNA amounts in angiosperms and their modern uses- 807 new estimates. Ann. Bot. 86: 859-909.

Bennett MD and Smith JB. 1976. Nuclear DNA amounts in angiosperms. Philosophical Transactions of the Royal Society B-Biological Sciences 274: Issue 933.

Bennett MD, Price HJ, and Johnston JS. 2008. Anthocyanin inhibits propidium iodide DNA fluorescence in Euphorbia pulcherrima: implications for genome size variation and flow cytometry. Ann. Bot. 101: 777-790.

Burchardt P, Buddenhagen CE, Gaeta ML, Souza MD, Marques A, and Vanzela ALL. 2020. Holocentric karyotype evolution in *Rhynchospora* is marked by intense numerical, structural, and genome size changes. Front. Plant Sci. 11: 1390.

Bye R, and Sosa V. 2013. Molecular phylogeny of the jimsonweed genus *Datura* (Solanaceae). Systematic Botany, 38(3): 818-829.

De-la-Cruz IM, Hallab A, Olivares-Pinto U, Tapia-López R, Velázquez-Márquez S, Piñero D, Oyama K, Usadel B, and Núñez-Farfán J. 2021. Genomic signatures of the evolution of defense against its natural enemies in the poisonous and medicinal plant *Datura stramonium* (Solanaceae). Sci. Rep. 11(1): 1-19.

Disel NR, Yılmaz M, Kekec Z, and Karanlık M. 2016. Poisoned after diner: Dolma with *Datura stramonium*. Turkish Journal of Emergency Medicine, 15(1): 51-55.

Dobigny G, Ducroz JF, Robinson TJ, and Volobouev V. 2004. Cytogenetics and cladistics. Syst. Biol., 53: 470-484.

Doležel J, Bartos J, Voglmayr H, and Greilhuber J. 2003. Nuclear DNA content and genome size of trout and human. Cytometry 51: 127-128.

Doležel J, Greilhuber J, Lucretti S, Meister A, Lysak M. A, Nardi L, and Obermayer R. 1998. Plant genome size

estimation by flow cytometry: Inter-laboratory comparison. Ann. Bot., 82(Suppl. A): 17-26.

Doležel J, Greilhuber J, Suda J. 2007. Estimation of nuclear DNA content in plants using flow cytometry. Nat. Protoc., 2: 2233-2244.

Ghahraman A. 1998. Flora of Iran. Research Institute of Forests Rangelands. Tehran, Iran, pp. 17. (In Persian)

Greilhuber J, Doležel J, Lysák MA, and Bennett MD. 2005. The origin, evolution and proposed stabilization of the terms 'genome size'and 'C-value'to describe nuclear DNA contents. Ann. Bot. 95: 255-260.

Guerra M. 2008. Chromosome numbers in plant cytotaxonomy: concepts and implications. Cytogenet. Genome. Res. 120: 339-350.

Hassan RA and Amer WM. 2019. Biosystematic study of the Egyptian *Datura stramonium* (Solanaceae). Phytotaxa 408(3): 178-194.

Karimi H. 2008. Weeds of Iran. Iran University Press, Tehran, Iran, 419 p. (In Persian).

Karimzadeh G, Danesh-Gilevaei M, and Aghaalikhani M. 2011. Karyotypic and nuclear DNA variations in *Lathyrus sativus* (Fabaceae). Caryologia 64: 42-54.

Karimzadeh G, Mousavi SH., Jafarkhani-Kermani M, and Jalali-Javaran M. 2010. Karyological and nuclear DNA variation in Iranian endemic muskmelon (*Cucumis melo* var. Inodorus). Cytologia 75: 451-461.

Knight CA, Molinari NA, and Petrov DA. 2005. The large genome constraint hypothesis: evolution, ecology and phenotype. Ann. Bot. 95: 177-190.

Kubešova M, Moravcova L, Suda J, Jarošik V, and Pyšek P. 2010. Naturalized plants have smaller genomes than their non-invading relatives: a flow cytometric analysis of the Czech alien flora. Preslia 82(1): 81-96.

Loureiro J, Rodriguez E, Doležel J, and Santos C. 2007. Two new nuclear isolation buffers for plant DNA flow cytometry: a test with 37 species. Ann. Bot. 100: 875-888.

Mohammadpour S, Karimzadeh G, and Ghaffari SM. 2022. Karyomorphology, genome size, and variation of antioxidant in twelve berry species from Iran. Caryologia 75(4): 133-148.

Mohammed FS, Kına E, Sevindik M, Dogan M, and Pehlivan M. 2021. *Datura stramonium* (Solanaceae): Antioxidant and antimicrobial potentials. Turk. J. Agric. Food Sci. Technol. 9(4): 818-821.

Morales Valverde R. 1986. Taxonomía De Los Géneros *Thymus* (Excluida De La Sección Serpyllum) Y Thymbra En La Península Ibérica). CSIC - Real Jardín Botánico (RJB), Ruizia. Monografias del Jardín Botánico 3: 324 p.

Muzafarian V. 2000. Plant Classification. Amirkabir Publications, Tehran, Iran, pp. 393 (In Persian).

Papagrigoriou G, Papazoglou D, Lazari D, Zorić L, and Tsialtas J. 2019. Hybridization effects on seed traits of annual *Datura* accessions focusing on oil concentration and composition. Ind. Crops Prod. 132: 69-75.

Pellestor F and Gatinois V. 2020. Chromoanagenesis: A piece of the macroevolution scenario. Mol. Cytogenet. 13: 3.

Rasekh SZ and Karimzadeh G. 2023. Chromosomal and genome size variations in opium poppy (*Papaver somniferum* L.) from Afghanistan. Caryologia 76(4): 15-22.

Sadeghian S and Hatami A. 2022. Chromosome number reports and karyotype analysis of seven species from the flora of Iran. Iran. J. Bot. 28(2): 165-169.

Salakhutdinov NF, Volcho KP, and Yarovaya OI. 2017. Monoterpenes as a renewable source of biologically active compounds. Pure. Appl. Chem. 89(8): 1105-1117.

Sayadi V, Karimzadeh G, Naghavi MR, and Rashidi Monfared S. 2022. Interspecific genome size variation of Iranian endemic *Allium* species (Amaryllidaceae). Cytologia 87(4): 335-338.

Winterfeld G, Ley A, Hoffmann MH, Paule J, and Röser M. 2020. Dysploidy and polyploidy trigger strong variation of chromosome numbers in the prayer-plant family (Marantaceae). Plant Syst. Evol. 306: 36.

Zarabizadeh H, Karimzadeh G, Rashidi Monfared S, and Tarkesh Esfahani S. 2022. Karyomorphology, ploidy analysis, and flow cytometric genome size estimation of *Medicago monantha* populations. Turk. J. Bot. 46: 50-61.

Zhang Y, Guo W, Yuan Z, Song Z, Wang Z, Gao J, Fu W, and Zhang G. 2023. Chromosome-level genome assembly and annotation of the prickly nightshade *Solanum rostratum* Dunal. Sci. Data 10: 341.

Yari A, Karimzadeh G, Rashidi Monfared S, and Sayadi S. 2024. Mixed-ploidy in Iranian endemic *Cymbopogon olivieri* (Boiss.) Bor: A chromosomal and holoploid genome size study. Cytologia 89(2): 1-5.

Caryologia
International Journal of Cytology, Cytosystematics and Cytogenetics

Firenze University Press
https://riviste.fupress.net/index.php/caryologia

OPEN ACCESS

Citation: Singh, S. & Kumar, G. (2024). Report of genomic doubling in *Cyamopsis tetragonoloba* (L.) Taub. (Fabaceae): salient features and effects. *Caryologia* 77(3): 63-71. doi: 10.36253/caryologia-2478

Received: Mar 14, 2024

Accepted: Sep 28, 2024

Published: March 25, 2025

Data Availability Statement: All relevant data are within the paper and its Supporting Information files.

Competing Interests: The Author(s) declare(s) no conflict of interest.

ORCID
SS: 0000-0001-9670-7286

Report of genomic doubling in *Cyamopsis tetragonoloba* (L.) Taub. (Fabaceae): salient features and effects

Shefali Singh[1,*], Girjesh Kumar[2]

[1] *Department of Botany at K. N. Govt. P.G. College, Gyanpur, Bhadohi, India*
[2] *Plant Genetics Laboratory, Department of Botany, University of Allahabad, India*
*Corresponding author. E-mail: shefalisingh.910@gmail.com

Abstract. Leguminous plants have always been highly valued to meet the nutritional necessities of human. An attempt to for genome multiplication in a legume crop is present in this study. Induced polyploidy as a technique has opened immense future prospects for the agriculture world. In this regard, *in-vivo* autopolyploidization experiment was planned on Cluster bean (*Cyamopsis tetragonoloba* (L.) Taub.). Present study is the successful documentation of the artificial induction of genome doubling by the application of colchicine i.e.C_1 and is the first report of its successful establishment in the next generation (C_2). Colchicine treatment was given to the young seedlings in two different concentrations of 0.2 and 0.4% for three different time durations. Results deciphered that chromosomal complement in case of diploid control plant is 2n=2x=14, whereas in the true polyploids it went on to be 2n=4x=28. Among the total of 148 seedlings that were treated with colchicine solution, 44 putative polyploid plants were monitored based on their distinctive morphological variations. Efficiency of 0.2% concentrations was found to be more than 0.4% concentrations. Palynological and anatomical evidences were also used for ascertaining polyploid organization to the putative plants with increment in size of stomata and pollen grains in the successful autotetraploids. Stomatal size is also an important determinant of ploidy where larger stomata with increase in chloroplast number was a typical feature among tetraploids. Cluster bean is a self-pollinated crop with narrow genetic base, but ploidy manipulation experiment might augment in broadening the genetic diversity. Procurement of large sized flower and seeds is a promising benchmark considering its improved aesthetic value. Autopolyploidization *via* colchicine has bestowed with the splendiferous act that offers prudent significance for diverse fields.

Keywords: Colchicine, chromosome, induced polyploidy, legume, meiosis.

INTRODUCTION

The seemingly proficient pace of morphological up-gradation required several editing at genetic level to augment a more robust genome constitution. One such passage was attained *via* accomplishment of polyploidy has been suggested as a major driving force of plant evolution (Soltis and Soltis

2009). There is ample source of evidence in this relation since many sequenced genomes display the signature of polyploid ancestry (Comai 2005; Yu et al. 2005). Classic studies estimated that 30–50% of angiosperms are polyploids (Stebbins 1950). It is proposed to be the most predominant mechanisms of sympatric speciation in plants (Sattler et al. 2016). The first example of a natural plant polyploid was the gigas mutant of *Oenothera lamarkiana* catalogued by De Vries (Lutz 1907). Lateron, Winkler (1916) recorded first artificial polyploid in *Solanum via* callus regeneration from the surfaces of stem explants and coined the term 'polyploidy' for these types of plant.

Several anti-mitotic agents are known to engineer polyploids artificially such as oryzalin, trifluralin and colchicine. However, in the present study colchicine has been selected. Colchicine is an alkaloid extracted from meadow saffron (*Colchicum autumnale* L.) which binds tubulin dimers *in vitro* and results in the formation of a tubulin–colchicine complex acting primarily to prevent microtubule (MT) assembly (Panda et al. 1995). It has been successfully used to modify the chromosome numbers in diverse plants species including ornamentals, medicinal and cereals.

Cluster bean or Guar (*Cyamopsis tetragonoloba* is a chief leguminous vegetable crop of semi-arid regions of the Indian sub-continent. It is an economically important gum yielding plant and a wonderful green manure crop with magnificient soil replenishing properties. The sterols of guar seeds include campesterol, avenasterol, stigmasterol, sitosterol and traces of Delta-7-avenasterol, stigmast-7-enol, brassicasterol and cholesterol (Mukhtar et al. 2006). The plant contains many important nutrients and phytochemicals such as saponin and flavonoids and is well-known traditional plant used in folklore medicine (Mukhtar et al. 2006; Wang and Morris 2007). Considerable levels of saponin help in normalizing cholestrol levels in body.

Gum yielded from seeds is natural polysaccharide galactomannan rich constituents found effective in osteoarthritis, transdermal drug delivery systems (Murthy et al. 2004). These pharmacological properties and immense economic importance are the compelling forces to enhance the productivity of clusterbean. Attempts to elevate endogenous phytochemical constituents as well as protein content of this excellent nutraceutical plant shall have excellent contribution. This has been the foundation for conceptualising autopolyploidization experiment on cluster bean. Three crucial parameters including cytogenetical, morphological and anatomical were explored for granting confirmatory elucidation regarding successful polyploid induction.

MATERIAL AND METHODS

Plant material

Accessions of seeds of *Cyamopsis tetragonoloba* were procured from regional station of National Bureau of Plant Genetics Resources i.e. Central Arid Zone Research Institute, Jodhpur Rajasthan and among these RGC- 1038 was selected for experimental work.

Agroclimatic conditions of the experimental site

This study was conducted in an experimental cage in Roxburgh Botanical Garden, Department of Botany, University of Allahabad, Prayagraj, UP, India during kharif season (July to November). The geographical location is 25°27'43.01''N, 81°51'10.42''E. Prayagraj lies in sub-tropical climatic zone and receives an annual rainfall of 1027mm where relative humidity is 59%.

Colchicine treatment

Previous literature mentioning standardised protocols for colchicine treatment were referred. Fresh seeds of cluster bean were sown in triplicates in pots. After the emergence of two-cotyledonary stage of seedlings, colchicine treatment ($C_{22}H_{25}NO_6$) was applied on their apical meristem. For this, good quality of sterilized absorbent cotton was utilised for making small spherical balls. Cotton balls dipped in colchicine solution at two different concentrations viz. 0.2% and 0.4%, were placed in between cotyledons carefully for three different time duration of 12 hours (1 day), 24 hours (2 consecutive days) and 36 hours (3 consecutive days), respectively. The plants were covered with earthen pots to prevent evaporation of colchicine solution from the cotton balls. For 24 hours and 36 hours, the treatment was repeated for second and third day also. After completion of each treatment, cotton balls were removed and the growing apical tips were washed thoroughly with distilled water. Plants were carefully monitored in their developing stage in normal field condition.

Morphological studies and anatomical studies

Recording of the various morphological characteristics in the diploid and tetraploids was an important purview of this work. Henceforth, parameters such as plant height, Days to 50% flowering, Days to 50% maturity, leaf length, leaf breadth, cluster per plant, pods per cluster and seed weight were calculated for C_1 and C_2 gen-

Table 1. Colchicine treatment on the apical meristems of seedlings of *Cyamopsis tetragonoloba.*

Concentration	Durations of treatment (hrs)	Number of seedlings	Plants survived	Expected polyploids	Reverted polyploids	Confirmed	
						Number	%
	12	24	23	-	-	-	0
0.2%	24	24	21	8	6	2	8.33%
	36	24	18	15	12	3	12.50
	12	24	17	9	9	-	-
0.4%	24	24	15	10	9	1	4.16
	36	24	12	-	-	-	-

eration. With respect to the control (diploid), morphologically distinct features such as leathery texture and excessive hairy outgrowth were marked, based on this several plants were suspected to be of polyploid organization. The epidermal layer from the abaxial surface of fully expanded leaves was stripped with a razor blade for stomatal study. Stomata of these leaves were observed under microscope by preparing temporary glycerine mounts. Differences in the size of suspected polyploid and diploid plants were taken into account by measuring three parameters i.e. stomatal index, stomatal length and stomatal breadth on micrometer scale in Dewinter Bio-wizard software at 40X resolution. For length and breadth measurement, data from 20 microscopic views were recorded from each slide for diploid and polyploid leaf samples for C_1 and C_2 generation.

Meiotic study

With the arrival of blooming season**,** young floral buds were fixed in Carnoy's fixative (Glacial Acetic Acid and Absolute alcohol in proportion of 1:3, v/v) which were transferred to pure alcohol next day for preservation at 4ºC. These buds were utilised for performing microsporogenic studies where anthers were teased in 2% acetocarmine stain with traces of Iron acetate. Slides were observed under Olympus CH20i at 40X resolution and photography was done using Pinnacle software under Nikon phase contrast microscope. Chromosome counting, as prescribed to be the usual method for ploidy determination (Maluszynska 2003), was performed in the meiocytes of suspected polyploids and diploids was done. Pollen fertility was also calculated as assessment of viability is imperative in relation to the reproductive success of plants. Adequately stained globose pollen grains were marked as fertile against those pollens which appear to be pale yellow with shrunken cytoplasm.

Statistical analysis

Statistical calibration was done using SPSS 16.0 version of software. The means were compared at $p \leq 0.5$ applying Post hoc and Duncan Multiple Range Test (DMRT).

RESULTS

With the help of detailed study, six successful polyploids were isolated on the basis of morphological, cytogenetical and anatomical studies.

Morphological observations

After treatment, an instant retardation in growth was discernible in the seedlings unlike that of the of control set. Emergence of the third leaf was delayed by a week in the treated sets, while in case of control it appeared normally within a span of three to four days after seedling emergence. Survivability was also affected, especially at 0.4% concentration, as some of the seedlings collapsed plausibly because apical meristem was damaged due to cellular necrosis. After initial hindrances, these plants got acclimatized and normalized towards growth and development. However, their rate of growth was still slower than that of the diploid ones which had attained normal plant height and were profusely developed. An array of variations were visible in leaves and this is demonstrated in Figure 1. Leaves were highly deformed and appeared to be invariably concentrated in a whorl at the first node. Leaves were peculiarly leathery, thickened and of fairly large sized as compare to the diploid ones. Large number of trichomes were present on the leaf surface which imparted glabrous texture to the stem and leaf surface, as shown in Figure 1. There were certain plants which initially displayed morphological variations and were prudently examined, however they reverted later on.

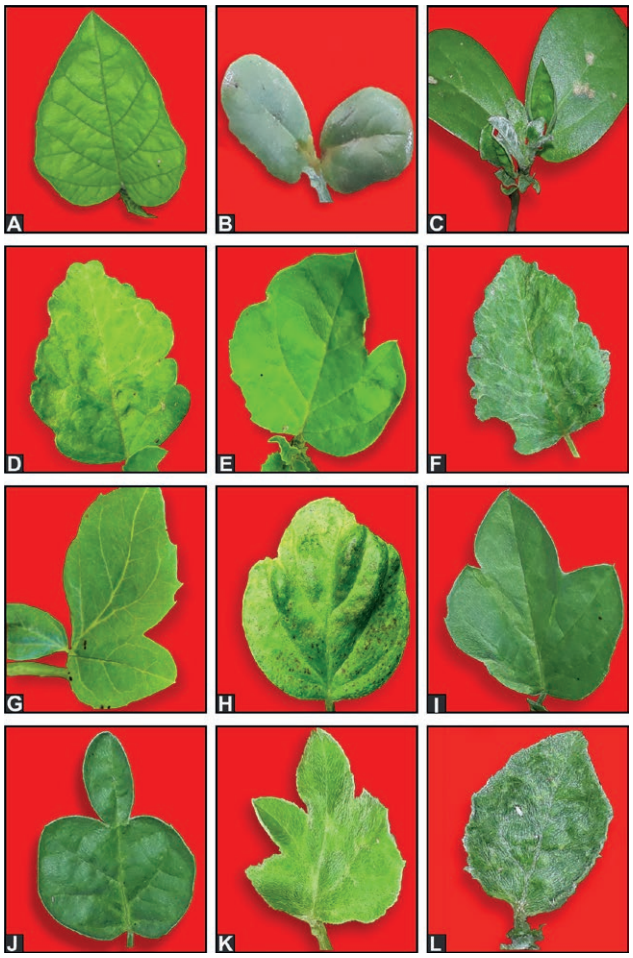

Figure 1. Mutants/variants in leaf shape A: Control; B: Waxy thickened seedling; C: Stunted growth at seedling stage; D: Leathery sinuous leaf; E: Surface extension from one side of leaf; F: Sinulate leaf; G: Leaf fusion among two leaflets of trifoliar leaf; H**:** Leathery coated leaf; I:Triapiculated leaf; J**:** Elliptical leaf protrusion from leaf midrib; K**:** Glabrous assymetrical leaf; L: Tomentosa leaf.

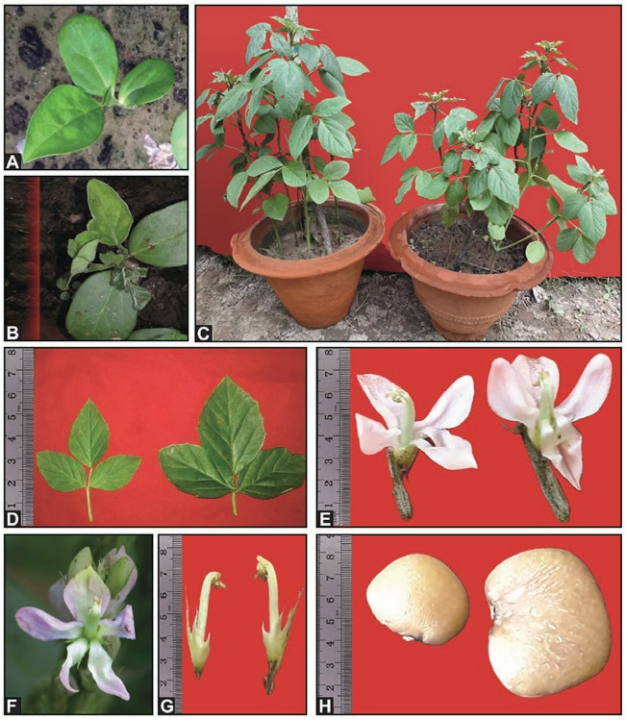

Figure 2. Morphological traits in diploid and autotetraploid plants of Cluster bean [*Cyamopsis tetragonoloba* (L.) Taub.]. A: Seedling of diploid (2n=14); B: Dark green thick texture of putative polyploid seedling; C: Comparative trend of diploid and polyploid plants; D: Leaves of diploid and tetraploid plants; E: Flowers from diploid and tetraploid plants; F: Flower with splitting of petals; G: Reproductive unit of diploid and polyploids; H: Diploid and tetraploid seeds.

With the onset of flowering, several notifiable differences in the reproductive stages were also observed and monitored. Flowers are usually present in clusters but the number of flowers in the cluster was quite less in these putative polyploids; however the size of the flowers (Figure 2E) alongwith the reproductive organs (Figure 2G) was distinctively and conspicuously enlarged with respect to the diploid ones. This behaviour is perceived in relation to the 'gigas' effects of polyploidy. A unique flower with splitting of the two fused petals was spotted (Figure 2F). Days to 50% flowering was recorded, data of which implicits delay in flowering in case of tetraploid plants as mentioned in Table 2. Days to 50% maturity was also delayed by significant margin in tetraploids as compared to the diploids. Seed setting was affected in the polyploids; however the size of seed was enlarged as shown in Figure 2H.

Anatomical observations

Compared to stomata of control plants, stomatal apparatus of several suspected polyploid plants were encountered to be larger, that were surrounded by jumbo sized accessory cells (Figure 3). Number of chloroplast per stomata was also increased. Both stomatal length (22.18±0.38 micrometer) and stomatal breadth (13.45±0.65 micrometer) were remarkably increased in polyploid plants as compare to diploids where calculated stomatal length was 15.93±0.28 micrometer and stomatal breadth was 10.54±0.15 micrometer (Figure 3A and 3B). Data of these parameters is mentioned in Table 2.

Cytogenetical and palynological observations

Previous cytogenetical illustration at mitotic stages has proved that chromosomal complement in *Cyamop-*

Table 2. A comparative analysis of various morphological parameters in diploid and autotetraploid plants of *Cyamopsis tetragonoloba* (L.) Taub. in C_1 and C_2 generation.

Characteristics	Diploid plants (2n=14) (Mean ± SE)	Autotetraploid plants C_1 generation (2n=4x=28) (Mean ± SE)	Autotetraploid plants C_2 generation (2n=4x=28) (Mean ± SE)
Plant height (cm)	86.33±1.91	45.66±1.56	51.70±2.07
Days to 50% flowering	48.66±0.88	65.66±1.45	57.33±1.76
Days to 50% maturity	87.66±1.20	117.33±1.40	113.33±3.84
Leaf length (cm)	7.37±0.52	9.77±0.78	9.60±0.85
Leaf breadth (cm)	4.43±0.26	5.50±0.28	5.87±0.64
Length of Stomatal guard cells (micrometer)	15.93±0.28	22.18±0.38	20.71±0.72
Breadth of Stomatal guard cells (micrometer)	10.54±0.15	13.45±0.65	12.89±0.56
Size of Pollen Mother Cells (micrometer)	16.18±0.74	27.97±1.15	28.08±1.18
Size of Pollen grains (micrometer)	18.93±0.57	33.01±0.83	33.68±0.87
Pollen fertility	97.66±0.88	61.66±0.88	64.33±2.40
Cluster per plant	12.33±1.20	6.33±0.66	6.66±0.33
Pods per cluster	10.00±0.57	4.33 ± 0.88	5.67±0.66
Seed weight (gm)	1.57±0.11	2.37±0.15	2.18±0.14

S.E. = Standard Error.

Table 3. Metaphase I configuration of all induced autotetraploids in *Cyamopsis tetragonoloba* (L.) Taub.

Chromosomal Associations	Percent frequency (Mean ± SE)
8II+2IV+1III+1I	2.97±0.21
7II +3IV+ 2I	2.19±0.1
7II+1IV+1VIII+2I	1.55±0.09
5II+3IV+1VI	0.92±0.24
4II+2IV+1III+1VIII+1I	1.55±0.09
4II+2IV+3III+31	1.25±0.16
3II+2IV+2III +1VII+1I	1.08±0.11
3II+1VIII+1VI+1V+1III	0.77±0.16
3II+1X+1V+1IV+1III	0.95±0.29
3II+2IV+1III+2V+1I	1.25±0.16
2II+2VI+1V+1IV+1III	0.93±0.04
1II+1VI+3IV+1VIII	0.96±0.31
1II+1X+2IV+1V+1III	0.63±0.18
1II+2VI+2V+1IV	0.46 ± 0.02

sis tetragonoloba is 2n=14. Haploid or the base chromosome number of this plant is n=x=7. Figure 4 is the cytological plate which denotes various stages of meiosis in Pollen mother cells of diploid as well as in polyploid cells. Size of PMC was enlarged in case of polyploid cells as it was measured to be 27.97±1.15 micrometer against the diploid cells 16.18±0.74 micrometer. Figure 4A is metaphase I and Figure 4B is anaphase I in case of control. Microsporogenic studies in the suspected polyploids were performed, where diakinesis and metaphase I (Figure 4C) stages revealed that number of chromosomes bivalents was 14. Chromosomal counting was also done at anaphase I where 14:14 poleward separation was recorded (as mentioned in Figure 4D) against the diploid chromosome segregation of 7:7. This provides affirmation to the chromosomal doubling. Several prominent multivalents configurations were recorded, data of which is documented in Table 3. Figure 4E to 4J is the illustrations of multivalent configurations. Laggards (Figure 4N) at anaphase I and unequal separation at anaphase were also recorded. Figure 4M shows 12:16 unequal separation of chromosomes at anaphase I towards opposite poles.

Palynological study was executed to assess viability of pollens in the diploids and polyploids. A noteworthy increment in pollen size was registered in the pollen grains of polyploids. Pollen size of diploid pollen grains was 18.93±0.57 micrometer whereas in polyploids, it was measured to be 33.01±0.83 micrometer. Figure 3C and 3D is diploid and polyploid pollens. Pollen fertility was considerably reduced in polyploids as it declined to a very low percentage of 61.66±0.88 compared to 97.66 ± 0.88% of control.

C_2 generation observations

The plants of C_2 generation were comparatively stronger, resistant, healthier and larger than those of C_1 generation. The morphological traits such as plant

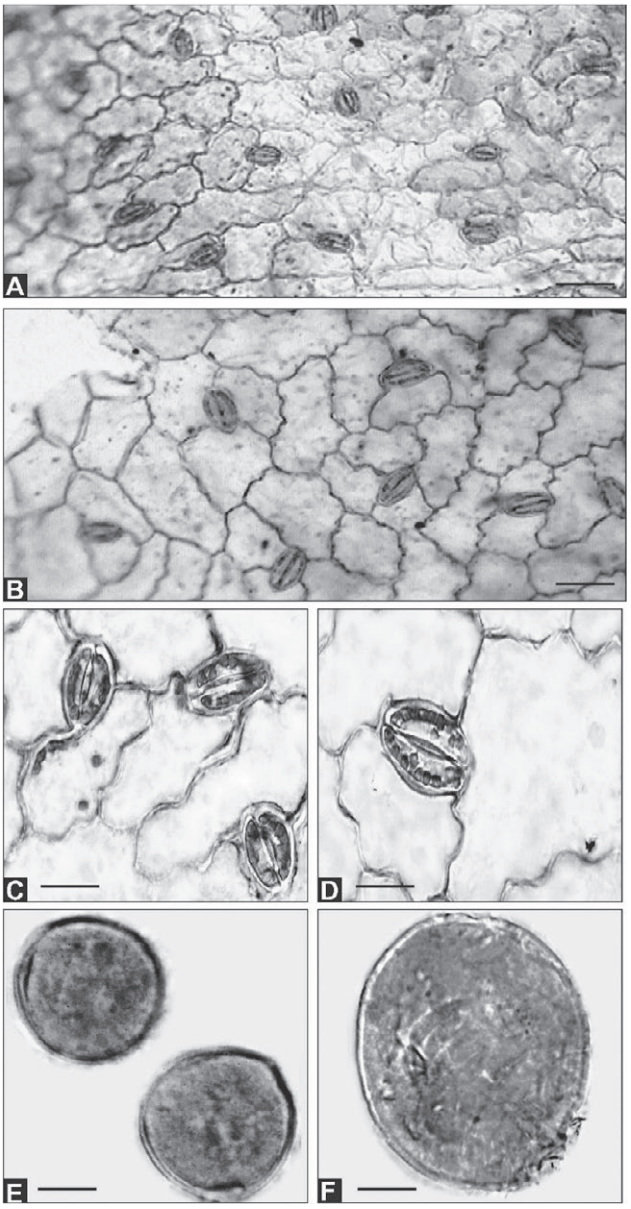

Figure 3. Stomatal and pollen morphology in diploids and autotetraploids of Clusterbean. A: Stomata (diploid) at 10X; B: Stomata (autotetraploid); C**:** Stomata (diploid) at 40X; D: Stomata (autotetraploid at 40X; E: Diploid pollen; F: Tetraploid pollen (40X).

height, length displayed a slight increment while leaf breadth, stomatal guard cell length and breadth displayed a slight decrement in C_2 generation as compared to C_1 generation (Table 2). The morphological parameters such as days to 50% flowering and days to maturity of C_2 generation of colchicine induced autotetraploids were registered as 57.33 and 113.33 days which was considerably earlier than C_1 generation.

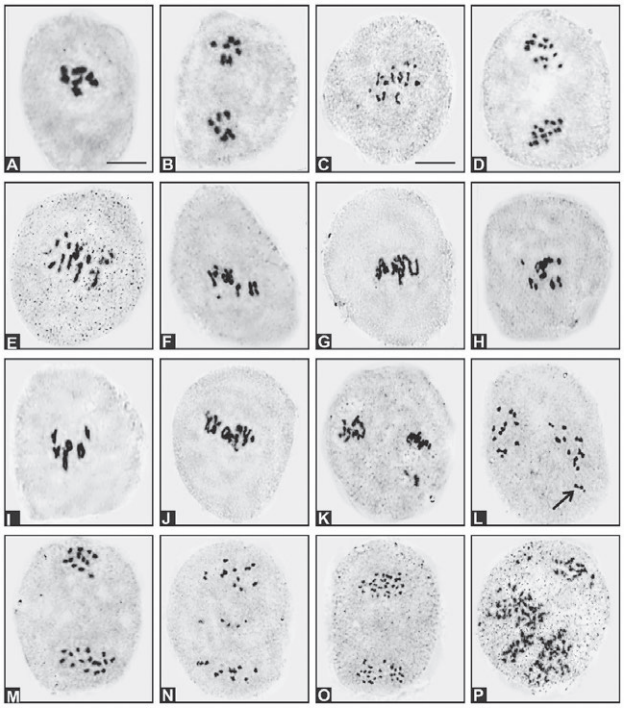

Figure 4. Chromosomal complement in diploids and polyploidy plants. a and b are PMCs of diploid plants- A: Normal metaphase I (seven bivalents); B: Normal anaphase I (7:7 separations), C-P are stages of autotetraploid PMCs- C: Metaphase I with 14 bivalents; D: Anaphase I with 14:14 separations; E-J are multivalents- E: 2II+6I+3III+1IV+1V; F: 4II+2IV+1III+1VIII+1I; G: 1II+1VI+3IV+1VIII; H: 3II+ 2IV+2III+1VII+1I; I: 1X+ 2III+3IV; J: 3II+2IV +1III+ 2V +1I; K: Precocious movement with stickiness at one side at Metaphase II; L: Two precocious at Metaphase II; M: Unequal separation at Anaphase I where 12:16 chromosomes at opposite poles; N: 4 Laggards at Anaphase I; O: Asynchronous division; P: unoriented Anaphase II. Scale bar – diploid cell (16.18 micrometer), polyploid (27.15 micrometer).

DISCUSSION

Polyploidization, in a simple sense, is the heritable condition of possessing more than two complete sets of chromosomes (Comai 2005) which is regarded as an important speciation mechanism for all eukaryotes and has a profound impact on biodiversity dynamics and ecosystem functioning (Ainouche and Jenczewski 2010). Dewey (1980) highlights that each crop species responds differently to polyploidization, depending on their original ploidy level, genome structure, reproduction mode, perenniality and the plant organ for which the crop is cultivated.

Induced tetraploids were conspicuously identifiable among the other diploid population owing to their distinctive morphological features such as vigorousity

in growth, robust nature with thick waxy coated large sized dark green leaves and flowers, excessive trichomes and hairs on stem and leaf surface. This robust nature is explained by the larger number of gene copies which compound into 'gigas' effect to the polyploid (Sattler et al. 2016) which also complements with a higher tolerance to environmental stress (Kermani et al. 2003; Tossi et al. 2022). It appears that there are environmental drivers for coordinated variation in cell size and that changes in genome size can facilitate generic changes in cell size (Jordan et al. 2015). However, gigas effect is not a universal feature of all autopolyploids.

Plants survivability was highly affected due to colchicine and it consistently decreased with the increasing colchicine concentration. Colchicine brings mitotic arrest (Bakar-ates et al. 2018) by inhibiting mitosis by preventing the polymerization of tubulin. This results in a failure of spindle formation, thus, preventing normal chromosomal movement and replication (Kamath et al. 2008). The slower growth rate could be attributed to the lower rate of metabolic activities in the colchitetraploids (Joshi and Verma 2004). Also, rate of cell division was reduced since larger genomes require longer time in cell division, particularly in the S phase (Doyle and Coate 2019).

Stomatal length assessment is regarded to be a reliable and convenient method comparing diploids and polyploids (Jeloudar et al. 2019). Stoma size is associated with CO_2 gain and water discharge in plant photosynthetic and transpiration processes and can be an indicator of ploidy levels (Moghbel et al. 2015). Compare to control, polyploids had enlarged stomatal apertures than those of diploid plants. However there was a reduction in the stomatal density in the tetraploids. Anatomical studies imply that reduction in stoma is a measure to check transpiration discharge. The tetraploid plants had significantly larger stomata and higher chlorophyll content indices, suggesting that the tetraploid plants may have higher photosynthetic and transpiration capacities (Zhang et al. 2018). These adaptive features of a polyploid genome explain their natural invasiveness to extreme environmental conditions and the reason for their greater stabilisation over diploid genome. Number of chloroplast in the stomatal guard cells was also increased in the tetraploids. Polyploid leaves are of dark green texture which might be due to the increase in chloroplast number with quantitative increase in DNA content in tetraploids (Butterfass 1983).

Significance of genomic doubling can be easily realized since several ancient polyploidization events existed at the base of evolution and several of these events gave rise to species-rich groups (Otto 2007). There are several salient features of a genome multiplication which established superlinear advancement of polyploids over their diploid counterparts. For instance, gene redundancy is a very peculiar characteristic of a polyploid cell where redundant copies of the genes have a possible chance for functional diversification (Comai 2005). These redundant set of genes posses the ability of shielding the polyploids from deleterious effects of recessive mutations (Joshi and Verma 2004; te Beest et al. 2012) by providing "buffering actions" in which extra copies of wild-type alleles masks the expression of harmful recessive counterparts. Polysomic inheritance confers higher level of heterozygosity to the polyploid individuals as compare to the diploids (Osborn et al. 2003). Heterozygosity is intimately associated to enhanced vigour.

Transition of vegetative stage into reproductive is associated with activation of floral meristem identity genes. Delay in flowering in polyploids might be related to late triggering of floral responsive genes. Slower growth rates at initial stages results in delay in flowering. Apparently, this delay may also cause reproductive isolation of the neopolyploid. Polyploids are recognised with longer petals, deeper corolla tubes, fewer flowers per inflorescence as found in present work; therefore, attract different assemblages of pollinators compared with diploids. Large sized flowers enhance the aesthetic properties and it may increase pollinator visitation frequencies (Kennedy et al. 2006). This may in turn provide opportunities for diversification in both plant and insect taxa (Nuismer and Thompson 2001). Polyploids also escape pathogenic attack compared to the diploids. Changes in disease resistance genes between polyploids and diploids also point towards altered pathogen resistance (Innes et al. 2008).

The plausible causes of the chromosomal abnormalities encountered in polyploids complement is perhaps the struggle among the doubled chromosome number in the neo-polyploid. Diploid PMCs oblige seven bivalents of the cell perfectly but the tetraploid PMCs have to accommodate more bivalents. This chromosomal doubling setsup an inter-repulsive hindrance among the chromosomes which reciprocates into aberrant meiosis. Occurrence of multivalents particularly quadrivalents was conspicuous in varying frequencies in the present tetraploids, since the latter are derived from a single genome resulting in four homologous sets of chromosomes in tetraploids (Stace 1980). These multivalents create abnormal patterns during anaphase such as '3:1' or '2:1 plus one laggard (Comai 2005). Such type of improper segregation results in formation of abnormal gametes with unbalanced ploidy that lead to aneuploids and sterility.

A noteworthy feature recorded during palynological assessment was the increment in pollen grain diameter

among the polyploids. However, there was a substantial deceleration in pollen viability in the tetraploids, as also reported in *Pinellia ternata* (Thunb.) (Liu et al. 2012). Parthasarathy and Rajan (1953) have advocated that chromosome doubling in the tetraploid may upset the balance of polygenes or modifying genes which may probably control the sterility. As a consequence of chromosomal aberrations, some sort of sterility takes place resulting to lower seed yield which is a barrier for the inheritance of polyploid (Kumar and Dwivedi 2017). Reduction in seed yield is also an after-effect of the pollen sterility; since reproductive success largely relies on the viability of gametes. However, the seed size and weight were increased.

Change in ploidy may also have substantial effect in altering quantity and quality of secondary metabolites. Polyploidization can be artificially induced to increase the production and/or improve the quality of important medicinal compounds, such as pharmaceuticals and aroma chemicals (Dhawan and Lavania 1996). Medicinal aromatic polyploids *viz. Carum carvi* L. (Dijkstra and Speckman 1980), *Ocimum kilimandscharicum* Gürke (Bose and Choundhury 1962) had increased terpene levels and elevated essential oil concentration. These changes in phytochemical composition might be associated with difference in triggering of metabolic cascade in the polyploid cell.

Science of polyploidization has been adopted by researchers and plant breeders for attaining superior genotypes. Natural autopolyploidization is well proven to be proximal drivers in specie diversification and differentiation whereas inception of *in vivo* polyploidization bears the potential to revolutionize the face of agricultural and pharmaceutical areas. Leguminous crops such as cluster bean has narrow genetic base, but ploidy manipulation experiment might augment in broadening the genetic diversity. Genomic doubling opens a new passage for neo-polyploids to evolve and diversify, but there is a need to further the level of knowledge on the mechanism behind this as it is still not very clearly understood. Gigas effect and robust nature of established polyploids are important characteristics that might confer environmental tolerance to the neo-polyploid. Shorter plant height, as observed in the present documentation, can act as a boon for plants with lodging issues. Increased flower size is also significant attribute that elevates the aesthetic properties which is of profound interest in floriculture. These traits had played pivotal role in past and may also have crucial influence in future on plant diversification and invasion to hostile realms.

ACKNOWLEDGEMENT

Authors express gratitude towards the lab members of Plant Genetics Laboratory for their guidance and support. One of the author who is Assistant Professor at KN Govt. PG College also acknowledges her Department members for their cooperation.

AUTHOR'S CONTRIBUTION

Prof. Girjesh Kumar gave expert guidance and also did editing and corrections in the manuscript. Dr. Shefali Singh designed the experiment, conducted it and wrote the manuscript.

REFERENCES

Ainouche ML, Jenczewski E. 2010. Focus on polyploidy. The New Phytologist. 186:1-4.

Bakar-Ateş F, Özmen N, Kaya-Sezginer E, Kurt EE. 2018. Effects of colchicine on cell cycle arrest and MMP-2 mRNA expression in MCF-7 breast adenocarcinoma cells. Turk Hij Den Biyol Derg. 75:239-244.

Bose RB, Choudhury JK.1962. A comparative study of the cytotaxonomy, palynology and physiology of diploid and polyploid plants from *Ocimum kilimandscharicum* Guerke and their yield of raw material and volatile contents. Caryologia 15:435–453.

Butterfass TH.1983.A nucleotypic control of chloroplast reproduction. Protoplasma. 118:71-74

Comai L. 2005. The advantages and disadvantages of being polyploid. Nature Review Genetics. 6:836-846.

Dewey DR. 1980. Some applications and misapplications of induced polyploidy to plant breeding. In: Lewis WH (ed) Polyploidy: biological relevance. Plenum Press, New York, pp: 445–470.

Dhawan OP, Lavania UC. 1996. Enhancing the productivity of secondary metabolites via induced polyploidy: a review. Euphytica. 87:81-89.

Dijkstra H, Speckman GJ. 1980. Autotetraploidy in caraway (*Carum carvi* L.) for the increase of the aetheric oil content of the seed. Euphytica.29:89–96.

Doyle JJ, Coate JE. 2019. Polyploidy, the nucleotype, and novelty: the impact of genome doubling on the biology of the cell. Int J Plant Sci. 180:1–52.

Innes RW, Ameline-Torregrosa C, Ashfield T, Cannon E, Cannon SB, Chacko B, Chen NW, Couloux A, Dalwani A, Denny R, et al. 2008. Differential accumulation of retroelements and diversification of NBLRR disease resistance genes in duplicated regions fol-

lowing polyploidy in the ancestor of soybean. Plant Physiol.148:1740–1759.

Jeloudar NI, Chamani E, Shokouhian AA, Zakaria RA. 2019. Induction and identification of polyploidy by colchicine treatment in *Lilium regale*. Cytologia.84:271-276.

Jordan GJ, Carpenter RJ, Koutoulis A, Price A, Brodribb TJ. 2015. Environmental adaptation in stomatal size independent of the effects of genome size. New Phytol. 205: 608-617.

Joshi P, Verma RC. 2004. High frequency production of colchicine induced autotetraploids in faba bean *(Vicia faba L.)*. Cytologia. 69:141-147.

Kamath A, Mehal W, Jain D. 2008). Colchicine-associated ring mitosis in liver biopsy and their clinical implications. J Clin Gastroenterol. 42:1060.

Kennedy B, Sabara HA, Haydon D, Husband BC. 2006. Pollinator-mediated assortative mating in mixed ploidy populations of *Chamerion angustifolium* (Onagraceae). Oecologia. 150:398-408.

Kermani MJ, Sarsan V, Roberts AV, et al, (2003) Oryzalin induced chromosome doubling in *Rosa* and its effect on plant morphology and pollen viability. Theor Appl Genet. 107:1195–1200.

Kumar G, Dwivedi H. 2017. Induced Autotetraploidy in *Trachyspermum ammi* (L.) Sprague (Apiaceae). Cytol Genet.51:391–400.

Liu Y, Hui RK, Deng RN, Wang JJ, Wang M, Li ZY. 2012. Abnormal male meiosis explains pollen sterility in the polyploid medicinal plant *Pinellia ternata* (Araceae). Genet Mol Res. 11:112-120.

Lutz AM. 1907. A preliminary note on the chromosomes of *Oenothera lamarkiana* and one of its mutants, *O. gigas*. Science. 26:151–152.

Maluszynska J. 2003. Cytogenetic tests for ploidy level analyses – chromosome counting. In: Doubled Haploid Production in Crop Plants: A Manual, Maluszynski, M., Kasha, K.J., B.P. Forster and I. Szarejko, pp. 391-395, Kluwer Academic Publishers, ISBN 1- 4020-1544-5, Dordrecht.

Moghbel N, Borujeni MK, Bernard F. 2015. Colchicine effect on the DNA content and stomata size of *Glycyrrhiza glabra* var. glandulifera and *Carthamus tinctorius* L. cultured *in vitro.* J Genet Eng Biotechnol. 13:1–6.

Mukhtar, HM, Ansari SH, Bhat ZA, Naved T. 2006. Anti-hyperglycemic activity of *Cyamopsis tetragonoloba* Beans on blood glucose levels in alloxan-induced diabetic rats. Pharm Biol. 44:10-13.

Murthy SN, Hiremath SRR, Paranjothy KLK. 2004. Evaluation of carboxymethyl cluster bean films for the formulation of transdermal therapeutic systems. Int J Pharm. 272: 11-18.

Nuismer SL, Thompson JN. 2001. Plant polyploidy and non-uniform effects on insect herbivores. Proc Royal Soc B 268:1937–1940.

Osborn TC, Pires JC, Birchler JA, et al. 2003. Understanding mechanisms of novel gene expression in polyploids. Trends Genet.19: 141–147.

Otto S. 2007. The Evolutionary Consequences of Polyploidy. Cell. 131: 452-462.

Panda D, Goode BL, Feinstein SC, Wilson L. 1995. Kinetic stabilization of microtubule dynamics at steady state by tau and microtubule-binding domains of tau. Biochemistry (Washington). 34: 11117–11127.

Parthasarathy N, Rajan SS 1953. Studies on the fertility of autotetraploid of *Brassica campestris* var. toria. Euphytica. 2: 25-32.

Sattler MC, Carvalho CR, Clarindo WR. 2016. The polyploidy and its key role in plant breeding. Planta. 243: 281–296.

Shyale S, Chowdary K, Krishnaiah Y, Bhat NK. 2006. Pharmacokinetic evaluation and studies on the clinical efficacy of cluster bean gum-based oral drug delivery systems of albendazole and albendazole-β-cyclodextrin for colon targeting in human volunteers. Drug Development Res. 67: 154-165.

Soltis P, Soltis D. 2009. The role of hybridization in plant speciation. Ann Rev Plant Biol. 60: 561–588.

Stace CA. 1980. Plant Taxonomy and Biosystematics. Edward Arnold, London.

Stebbins GL. 1950. Variation and evolution in plants. New York, NY Columbia University Press.

te Beest, M, Le Roux JJ, Richardson DM, Brysting AK, Suda J, Kubesova M, Pysek P. 2012. The more the better? The role of polyploidy in facilitating plant invasions. Ann Bot. 109: 19–45.

Thompson JN, Merg KF. 2008. Evolution of polyploidy and the diversification of plant–pollinator interactions. Ecology. 89: 2197–2206.

Tossi VE, Martínez Tosar LJ, Laino LE, Iannicelli J, Regalado JJ, Escandón AS, Baroli I, Causin HF, Pitta-Álvarez SI. 2022. Impact of polyploidy on plant tolerance to abiotic and biotic stresses. Front Plant Sci. 13 869423.

Wang ML, Morris JB. 2007. Flavonoid content in seeds of guar germplasm using HPLC. Plant Genet Resour: Characterization Util. 5: 96.

Winkler H. 1916. Uber die experimentelle erzeugung von pflanzen mit abweichenden chromosomenzahlen. Zeits Bot 8: 417–531.

Yu J *et al.* 2005. The Genomes of *Oryza sativa*: a history of duplications. PLoS Biol. 3: 266-281.

Zhang H, An S, Hu J, Lin Z, Liu X, Bao H, Chen R. 2018). Induction, identification and characterization of polyploidy in *Stevia rebaudiana* Bertoni. Plant Biotechnol J. 35: 81-86.

Finito di stampare da
Logo s.r.l. – Borgoricco (PD) – Italia

OPEN ACCESS POLICY

Caryologia provides immediate open access to its content. Our publisher, Firenze University Press at the University of Florence, complies with the Budapest Open Access Initiative definition of Open Access: By "open access" , we mean the free availability on the public internet, the permission for all users to read, download, copy, distribute, print, search, or link to the full text of the articles, crawl them for indexing, pass them as data to software, or use them for any other lawful purpose, without financial, legal, or technical barriers other than those inseparable from gaining access to the internet itself. The only constraint on reproduction and distribution, and the only role for copyright in this domain is to guarantee the original authors with control over the integrity of their work and the right to be properly acknowledged and cited. We support a greater global exchange of knowledge by making the research published in our journal open to the public and reusable under the terms of a Creative Commons Attribution 4.0 International Public License (CC-BY-4.0). Furthermore, we encourage authors to post their pre-publication manuscript in institutional repositories or on their websites prior to and during the submission process and to post the Publisher's final formatted PDF version after publication without embargo. These practices benefit authors with productive exchanges as well as earlier and greater citation of published work.

PUBLICATION FREQUENCY

Papers will be published online as soon as they are accepted, and tagged with a DOI code. The final full bibliographic record for each article (initial-final page) will be released with the hard copies of *Caryologia*. Manuscripts are accepted at any time through the online submission system.

COPYRIGHT NOTICE

Authors who publish with *Caryologia* agree to the following terms:

- Authors retain the copyright and grant the journal right of first publication with the work simultaneously licensed under a Creative Commons Attribution 4.0 International Public License (CC-BY-4.0) that allows others to share the work with an acknowledgment of the work's authorship and initial publication in Caryologia.
- Authors are able to enter into separate, additional contractual arrangements for the non-exclusive distribution of the journal's published version of the work (e.g., post it to an institutional repository or publish it in a book), with an acknowledgment of its initial publication in this journal.
- Authors are permitted and encouraged to post their work online (e.g., in institutional repositories or on their website) prior to and during the submission process, as it can lead to productive exchanges, as well as earlier and greater citation of published work (See The Effect of Open Access).

PUBLICATION FEES

Open access publishing is not without costs. *Caryologia* therefore levies an article-processing charge of € 150.00 for each article accepted for publication, plus VAT or local taxes where applicable.

We routinely waive charges for authors from low-income countries. For other countries, article-processing charge waivers or discounts are granted on a case-by-case basis to authors with insufficient funds. Authors can request a waiver or discount during the submission process.

PUBLICATION ETHICS

Responsibilities of *Caryologia*'s editors, reviewers, and authors concerning publication ethics and publication malpractice are described in *Caryologia*'s Guidelines on Publication Ethics.

CORRECTIONS AND RETRACTIONS

In accordance with the generally accepted standards of scholarly publishing, *Caryologia* does not alter articles after publication: "Articles that have been published should remain extant, exact and unaltered to the maximum extent possible".

In cases of serious errors or (suspected) misconduct *Caryologia* publishes corrections and retractions (expressions of concern).

Corrections

In cases of serious errors that affect or significantly impair the reader's understanding or evaluation of the article, *Caryologia* publishes a correction note that is linked to the published article. The published article will be left unchanged.

Retractions

In accordance with the "Retraction Guidelines" by the Committee on Publication Ethics (COPE) *Caryologia* will retract a published article if:

- there is clear evidence that the findings are unreliable, either as a result of misconduct (e.g. data fabrication) or honest error (e.g. miscalculation)
- the findings have previously been published elsewhere without proper crossreferencing, permission or justification (i.e. cases of redundant publication)
- it turns out to be an act of plagiarism
- it reports unethical research.

An article is retracted by publishing a retraction notice that is linked to or replaces the retracted article. *Caryologia* will make any effort to clearly identify a retracted article as such.

If an investigation is underway that might result in the retraction of an article *Caryologia* may choose to alert readers by publishing an expression of concern.

COMPLYNG WITH ETHICS OF EXPERIMENTATION

Please ensure that all research reported in submitted papers has been conducted in an ethical and responsible manner, and is in full compliance with all relevant codes of experimentation and legislation. All papers which report in vivo experiments or clinical trials on humans or animals must include a written statement in the Methods section. This should explain that all work was conducted with the formal approval of the local human subject or animal care committees (institutional and national), and that clinical trials have been registered as legislation requires. Authors who do not have formal ethics review committees should include a statement that their study follows the principles of the Declaration of Helsinki

ARCHIVING

Caryologia and Firenze University Press are experimenting a National legal deposition and long-term digital preservation service.

ARTICLE PROCESSING CHARGES

All articles published in *Caryologia* are open access and freely available online, immediately upon publication. This is made possible by an article-processing charge (APC) that covers the range of publishing services we provide. This includes provision of online tools for editors and authors, article production and hosting, liaison with abstracting and indexing services, and customer services. The APC, payable when your manuscript is editorially accepted and before publication, is charged to either you, or your funder, institution or employer.

Open access publishing is not without costs. *Caryologia* therefore levies an article-processing charge of € 150.00 for each article accepted for publication, plus VAT or local taxes where applicable.

FREQUENTLY-ASKED QUESTIONS (FAQ)

Who is responsible for making or arranging the payment?

As the corresponding author of the manuscript you are responsible for making or arranging the payment (for instance, via your institution) upon editorial acceptance of the manuscript.

At which stage is the amount I will need to pay fixed?

The APC payable for an article is agreed as part of the manuscript submission process. The agreed charge will not change, regardless of any change to the journal's APC.

When and how do I pay?

Upon editorial acceptance of an article, the corresponding author (you) will be notified that payment is due.

We advise prompt payment as we are unable to publish accepted articles until payment has been received. Payment can be made by Invoice. Payment is due within 30 days of the manuscript receiving editorial acceptance. Receipts are available on request.

No taxes are included in this charge. If you are resident in any European Union country you have to add Value-Added Tax (VAT) at the rate applicable in the respective country. Institutions that are not based in the EU and are paying your fee on your behalf can have the VAT charge recorded under the EU reverse charge method, this means VAT does not need to be added to the invoice. Such institutions are required to supply us with their VAT registration number. If you are resident in Japan you have to add Japanese Consumption Tax (JCT) at the rate set by the Japanese government.

Can charges be waived if I lack funds?

We consider individual waiver requests for articles in Caryologia on a case-by-case basis and they may be granted in cases of lack of funds. To apply for a waiver please request one during the submission process. A decision on the waiver will normally be made within two working days. Requests made during the review process or after acceptance will not be considered.

I am from a low-income country, do I have to pay an APC?

We will provide a waiver or discount if you are based in a country which is classified by the World Bank as a low-income or a lower-middle-income economy with a gross domestic product (GDP) of less than $200bn. Please request this waiver of discount during submission.

What funding sources are available?

Many funding agencies allow the use of grants to cover APCs. An increasing number of funders and agencies strongly encourage open access publication. For more detailed information and to learn about our support service for authors.

APC waivers for substantial critiques of articles published in OA journals

Where authors are submitting a manuscript that represents a substantial critique of an article previously published in the same fully open access journal, they may apply for a waiver of the article processing charge (APC).

In order to apply for an APC waiver on these grounds, please contact the journal editorial team at the point of submission. Requests will not be considered until a manuscript has been submitted, and will be awarded at the discretion of the editor. Contact details for the journal editorial offices may be found on the journal website.

What is your APC refund policy?

Firenze University Press will refund an article processing charge (APC) if an error on our part has resulted in a failure to publish an article under the open access terms selected by the authors. This may include the failure to make an article openly available on the journal platform, or publication of an article under a different Creative Commons licence from that selected by the author(s). A refund will only be offered if these errors have not been corrected within 30 days of publication.

2024
Vol. 77 – n. 3

Caryologia

International Journal of Cytology, Cytosystematics and Cytogenetics

Table of contents